Review

Non-Noble Metal Aromatic Oxidation Catalysis: From Metalloenzymes to Synthetic Complexes

Eduard Masferrer-Rius and Robertus J. M. Klein Gebbink *

Organic Chemistry & Catalysis, Institute for Sustainable and Circular Chemistry, Faculty of Science, Utrecht University, Universiteitsweg 99, 3584 CG Utrecht, The Netherlands
* Correspondence: r.j.m.kleingebbink@uu.nl

Abstract: The development of selective aromatic oxidation catalysts based on non-noble metals has emerged over the last decades, mainly due to the importance of phenol products as intermediates for the generation of pharmaceuticals or functional polymers. In nature, metalloenzymes can perform a wide variety of oxidative processes using molecular oxygen, including arene oxidations. However, the implementation of such enzymes in the chemical industry remains challenging. In this context, chemists have tried to mimic nature and design synthetic non-noble metal catalysts inspired by these enzymes. This review aims at providing a general overview of aromatic oxidation reactions catalyzed by metalloenzymes as well as synthetic first-row transition-metal complexes as homogeneous catalysts. The enzymes and complexes discussed in this review have been classified based on the transition-metal ion present in their active site, i.e., iron, copper, nickel, and manganese. The main points of discussion focus on enzyme structure and function, catalyst design, mechanisms of operation in terms of oxidant activation and substrate oxidation, and substrate scope.

1. Overview of Arene Oxidations

1.1. Relevance and Challenges

Oxidations of organic compounds are essential reactions that are widely studied in academia as well as in the chemical industry [1,2]. The interest in these reactions is based on the fact that oxygenated organic molecules can be used as intermediates to produce different classes of chemicals and end products. Since the last decade, improvements have been made in the development of different catalytic oxidation systems, however, in most cases, the selective oxidation of the organic substrate represents a critical challenge. Of more recent interest are C–H oxidations that can be applied for late-stage functionalization, in which C–H bonds are basically considered functional groups [3–7].

A particular area of interest has been the direct oxygenation of aromatic compounds to the corresponding phenol products (Figure 1), which has been a challenging class of reactions for decades. Indeed, the direct hydroxylation of benzene to phenol using molecular oxygen as a benign oxidant has been known as one of the "10 challenges for catalysis" [8,9]. Phenols are essential intermediates in the generation of a broad range of products, such as pharmaceuticals or functional polymers, which makes them highly desired [6,10–12]. However, the direct transformation of an aromatic C–H bond into a hydroxyl functionality, such as in benzene oxidation, is difficult because of poor substrate reactivity (an aromatic C–H bond has a high bond dissociation energy of about 112 kcal·mol^{-1}) [13]. To overcome this challenge, the generation of highly reactive and selective oxygen species is necessary. However, often phenol products are more easily oxidized than non-oxidized aromatic compounds, causing a chemoselectivity issue. Generally, the oxidation of phenols to the corresponding catechols, hydroquinones, or benzoquinones is well documented, particularly in oxidations catalyzed by metalloporphyrins (Figure 1) [14–18]. Additionally, a lack

of discrimination between different oxidation sites produces a regioselectivity issue. This is particularly evident when alkylbenzenes are used, as oxidation at the weaker and activated (benzylic) aliphatic C(sp^3)–H bonds is thermodynamically preferred over oxidation at the aromatic ring.
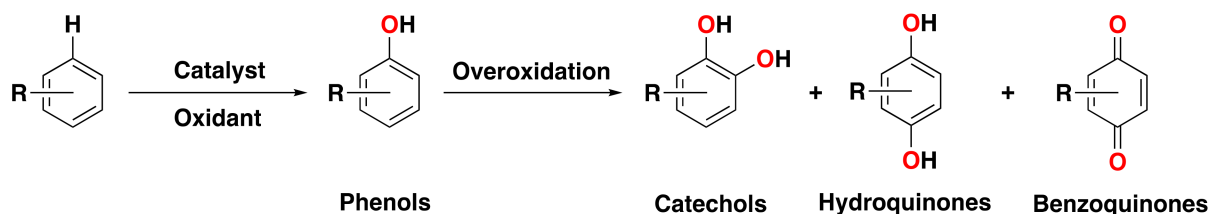
Figure 1. Direct hydroxylation of aromatic substrates to the corresponding phenol products and overoxidation to catechols, hydroquinones, or benzoquinones products.
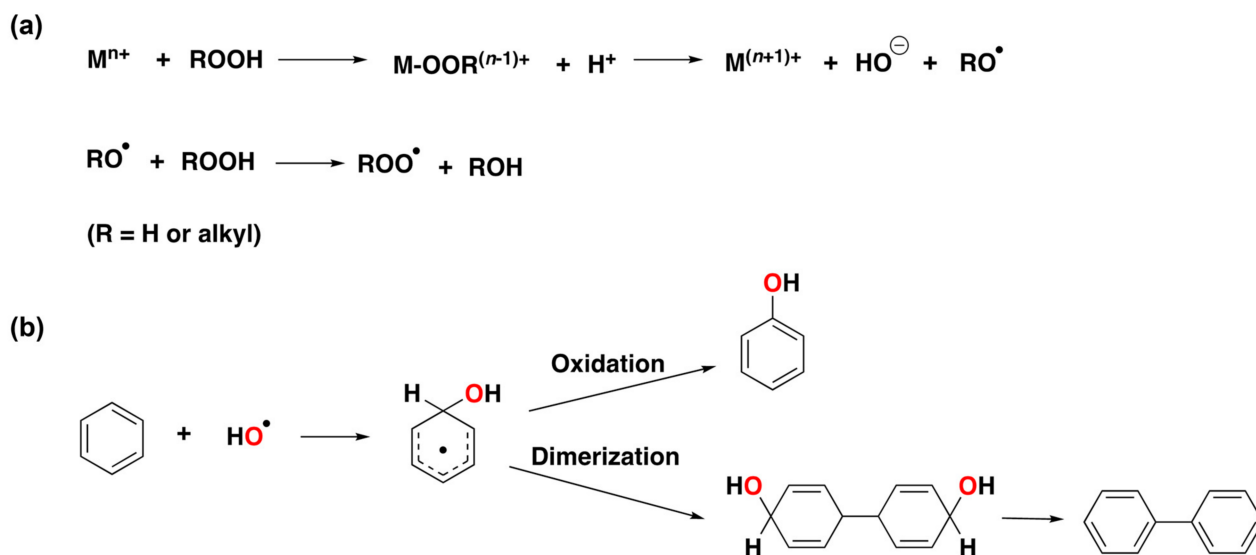
Generally, the field of homogeneous catalysis has been dominated by noble metal complexes, which are based on elements that are generally considered toxic for humans and the environment and are associated with high costs due to their low availability in the Earth's crust [19]. In this context, non-noble metal complexes have appeared as attractive catalysts, particularly in oxidation catalysis. Within this field, chemists have typically looked to nature for inspiration. A widely applied approach has been the development of synthetic catalytic systems that can mimic the active site and functionality of metalloenzymes to carry out oxidative processes. A well-known inspiration example is iron-containing metalloenzymes that can activate molecular oxygen [20–26]. However, other kinds of metalloenzymes containing copper, nickel, or manganese have also been investigated in this field [22,25,27–32]. Generally, the active site is the only area of the enzyme that is being mimicked in such bioinspired complexes. A downside of this design strategy is that these synthetic complexes generally display poor selectivities, whereas their natural counterparts show outstanding selectivities due to their highly elaborated structure, including the second coordination sphere around the active site [22,33]. Thus, a lot of efforts have been devoted to understanding the geometric and electronic structure/function correlations between the synthetic and their enzyme "molds" [34,35].

In this review, we provide a non-comprehensive overview of homogeneous, non-noble metal catalysis for aromatic oxidation reactions. Several reviews can be found in the literature regarding heterogeneous catalytic systems for oxidation chemistry, also detailing arene oxidation reactivity [36–38]. Of note, a review on heterogeneous catalysts for the direct hydroxylation of benzene to phenol, with a special focus on mesoporous transition metal-based catalysts, was recently published [39]. The present overview of homogeneous catalyst systems specifically targets catalytic systems capable of performing the direct hydroxylation of an aromatic substrate using a metal-based oxidant and avoiding the use of unselective hydroxyl radicals generated via Fenton-type processes. We have classified this review based on the transition metals that are used in catalysis, i.e., iron, copper, nickel, and manganese, and provided typical examples that have been developed in the field. First, we introduce the most important families of metalloenzymes capable of catalyzing aromatic oxidation reactions, followed by a description of the development of synthetic bioinspired transition-metal complexes for arene oxidation. Special attention is given to complexes based on aminopyridine ligands, which have been extensively used and investigated in general in the field of homogeneous oxidation chemistry [40]. Initially, we will review enzymes and complexes based on iron and copper, since these are the two metals that chemists have employed most in the field of oxidation chemistry, in particular for aromatic oxidation. In the second part, nickel- and manganese-based complexes will be covered. Although fewer examples of arene oxidation using these metals are known, several publications show the recent interest in the development of arene oxidation catalysts based on these metals. At this point, it is important to mention that complexes containing other first-row transition metals, such as cobalt or vanadium, have also been proven to

be active for aromatic oxidation. For further information on these complexes and their catalytic activity, the reader is referred to several selected examples [41–46]. This review is part of the Ph.D. thesis of Eduard Masferrer-Rius [47] and, as such, covers examples up until the beginning of 2022. A complementary and excellent review on homogeneous aromatic oxidation catalysis has since been published by Sankaralingam et al. [48]. This particular review focuses on the use of the complete series of first-row transition metals in catalysis and does not include a thorough description of naturally occurring metallo-enzymes capable of catalyzing aromatic oxidation reactions nor their comparison to synthetic systems.

1.2. Hydroxyl Radicals vs. Metal-Based Oxidants

Fenton-type chemistry has been known and studied in detail for quite some time [49–51]. Overall, this chemistry consists of the reaction between an iron(II) salt and H_2O_2 to generate an oxidized iron(III) species and hydroxyl radicals [52–54]. The oxidation of aromatic substrates, such as benzene and benzene derivatives, by Fenton-type chemistry using H_2O_2 as an oxidant has been investigated and is well understood, and studies have shown that hydroxyl radicals are added rapidly to the aromatic ring [55–58]. After the addition of the hydroxyl radical to the benzene ring, the reaction can proceed either by dimerization of the hydroxycyclohexadienyl radical and dehydration to form biphenyl or alternatively by oxidation to generate phenol (Figure 2). Other oxidants, such as *tert*-butylhydroperoxide (TBHP), can also engage in a Fenton-type process, generating free-diffusing *tert*-butoxy and *tert*-butylperoxy radicals that can engage in hydrogen abstraction reactions with aliphatic C–H bonds [59–61]. However, TBHP activation does not produce hydroxyl radicals, and *tert*-butoxy radicals, unlike hydroxyl radicals, do not add to aromatic rings [62]. For this reason, the effectiveness of using TBHP in arene hydroxylation reactions has been used as evidence against the involvement of hydroxyl radicals and consequently in favor of the involvement of metal-based oxidants.

(a)

$$M^{n+} + ROOH \longrightarrow M\text{-}OOR^{(n-1)+} + H^+ \longrightarrow M^{(n+1)+} + HO^{\ominus} + RO^{\bullet}$$

$$RO^{\bullet} + ROOH \longrightarrow ROO^{\bullet} + ROH$$

(R = H or alkyl)

(b)

Figure 2. (**a**) Generation of free diffusing oxygen-centered radicals via the initial Fenton reaction. (**b**) Hydroxylation of benzene by addition of hydroxyl radicals to generate phenol and biphenyl.

In 1954, another process involving hydroxyl radicals was reported, known as the Udenfriend system [63–65]. This consists of a mixture of an iron(II) salt with EDTA (EDTA = ethylenediaminetetraacetic acid) and ascorbic acid under an oxygen atmosphere, which can generate hydroxyl radicals that can attack aromatic substrates in the same way as described for Fenton-type chemistry. A system using iron(II) salts and tetrahydropterins as reducing agents has also been reported to be efficient for the hydroxylation of aromatic compounds using dioxygen as an oxidant. In this particular case, hydroxylation of electron-rich arenes, such as anisole, phenetole, toluene, and ethylbenzene, is possible, favoring *meta*-

hydroxylation in all cases [66]. Overall, free-diffusing oxygen-centered radicals are known to provide low catalytic efficiencies and selectivities, leading to side products through lateral site chain oxidation for alkylbenzene substrates [57,58,67,68]. For this reason, over the past years, research efforts have focused on the development of catalytic systems that make use of metal-based oxidants rather than hydroxyl radicals so that higher selectivities and efficiencies for aromatic oxidations can be achieved.

2. Iron in Biological and Synthetic Systems

2.1. Iron-Containing Metalloenzymes

Iron is one of the most often found transition metals in the active sites of metalloenzymes. Numerous iron-containing enzymes are known to be able to activate oxygen to perform oxidative processes. Among these enzymes, we can distinguish two groups based on the active site structure: heme- and non-heme-containing enzymes (Figure 3). The first group has been well investigated, and their chemistry is well understood.
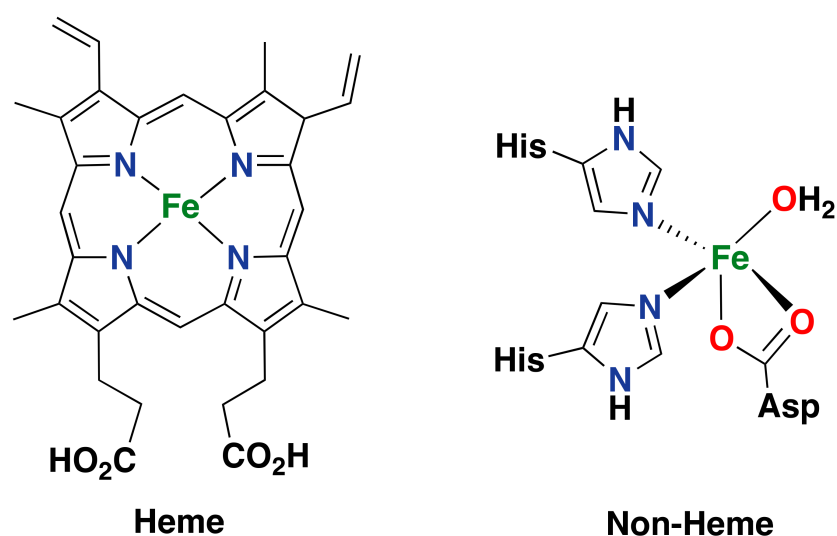
Figure 3. Schematic diagram of the typical heme prosthetic group (iron protoporphyrin IX) found in the active site of heme enzymes (**left**) [69,70] and of the 2-His-1-carboxylate facial triad active site found in the mononuclear non-heme enzyme naphthalene dioxygenase (NDO; **right**) [26,34,71,72].

The main feature of this group of enzymes is the prosthetic heme group that bears the iron center in their active site [26,69,70,73–75]. Within this group, we can distinguish heme-containing enzymes such as cytochrome P450's, peroxidases, nitric oxide synthases, chloroperoxidases, heme oxygenases, indoleamine 2,3-dioxygenases, and tryptophan 2,3-dioxygenases. Non-heme enzymes, on the other hand, can be classified as mononuclear or dinuclear depending on the number of iron atoms in their active site [23,34,76]. Within the former type, different types of mononuclear active sites have been identified. One very common active site features an iron center bound to two histidine ligands and one carboxylate ligand in a facial manner; this structural feature is known as the "2-His-1-carboxylate facial triad" [23,25,37,71,77–81]. One remarkable example of this last family of enzymes is Rieske oxygenases, which can perform the *syn*-dihydroxylation of aromatic substrates, among other substrate oxidations, with high levels of regio- and stereospecificity [24,82,83]. In the following sections, some of the most important iron-containing metalloenzymes able to perform aromatic oxidation reactions are discussed in terms of the structure of their active site and their catalytic oxidation capabilities.

2.1.1. Cytochrome P450

Cytochromes (CYP) are ubiquitous in all life forms, from bacteria to humans. Within this family, cytochrome P450 is one of the most important classes of iron enzymes found in nature that metabolize atmospheric dioxygen in an oxygenase catalytic cycle, and a lot of

details on the mechanism of dioxygen activation for this enzyme family are known. Overall, this class of iron enzymes takes part in several processes, ranging from the detoxification of xenobiotic compounds to drug metabolism and the biosynthesis of steroids [69,84–87].

Among the different oxidative processes, cytochrome P450 is best known for its monooxygenation capability, i.e., the insertion of an oxygen atom from molecular oxygen into an organic compound. Aromatic oxidations, arene and alkene epoxidations, and the oxygenation of heteroatoms are all examples of these reactions. Due to the catalytic capabilities of cytochrome P450 enzymes, a lot of research efforts have been devoted to the investigation of cytochrome P450 variants as catalysts for site-selective and enantioselective C–H hydroxylation reactions in the past decades [88–91]. Several studies have shown the coordination chemistry of the active site of cytochrome P450's in detail, which nowadays has been well established based on several X-ray crystal structures [69,92–97]. It is based on a ferric iron center coordinated to four nitrogen atoms (protoporphyrin IX) and a cysteinate sulfur atom; this last residue occupies an axial position at the metal center, whereas the other axial position contains a hydroxide ligand or a water molecule [73,98,99]. The mechanism of cytochrome P450's operation starts with the ferric compound accepting an electron to form the respective ferrous state of the enzyme. Next, reaction with molecular oxygen produces an Fe(III)-OOH species that undergoes O–O bond cleavage to generate the real active oxidant, which is a high-valent Fe(IV)-oxo porphyrin π radical cation complex, also known as Compound I (CpdI) (Figure 4a) [14,85,100–103]. For the oxidation of aliphatic C–H bonds, this last species transfers the oxo group to the substrate following a two-step process known as the "oxygen rebound" mechanism [87,104,105]. First, a hydrogen atom abstraction takes place from the substrate to the oxo group, and secondly, a fast rebound to the substrate carbon radical by the hydroxyl group occurs.
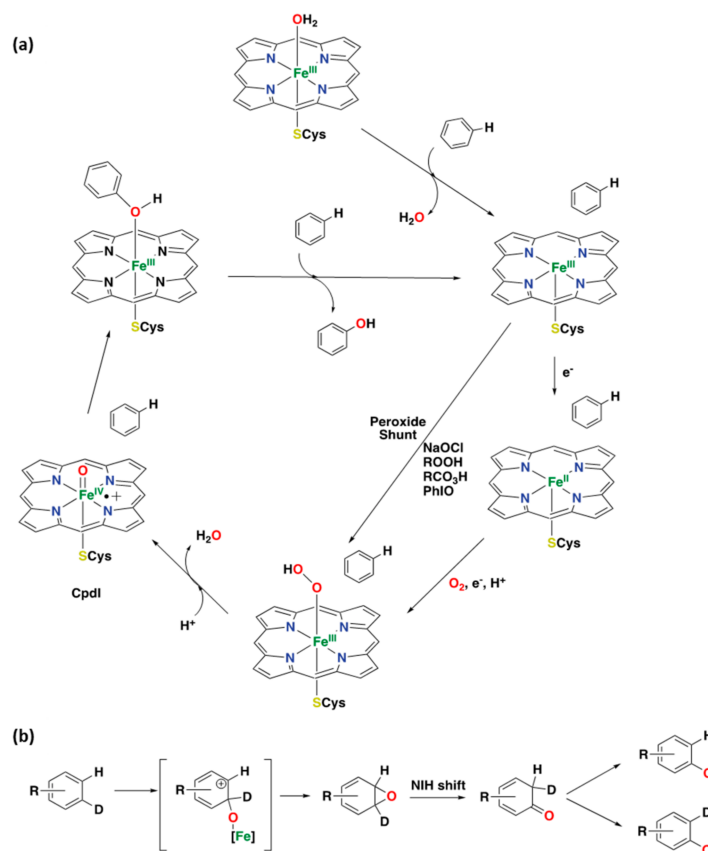

Figure 4. (**a**) Established catalytic cycle for arene oxidation is catalyzed by cytochrome P450 [73,94,106–108]. (**b**) Oxidation of deuterated aromatic compounds catalyzed by cytochrome P450, illustrating the "NIH shift" process [106,109].

In contrast, the oxidation of aromatic substrates with CpdI proceeds via the oxidation of a π-bond, generating arene oxides that transform into an unstable ketone intermediate via heterolytic cleavage of the epoxide followed by migration of a hydride ion (known as the "NIH shift") [106,109,110]. The last step is the tautomerization of the ketone compound to generate the final phenol product (Figure 4b) [106,107]. Worth mentioning is the use of hydro- and alkylperoxides, sodium hypochlorite, iodosobenzene, or peracids, which allow the conversion of the resting state directly to the high-valent iron-oxo species; this cycle is known as the "peroxide shunt" [73].

2.1.2. Rieske Oxygenases

Rieske oxygenases are a family of bacterial enzymes based on a non-heme iron center, with the metal facially coordinated to two histidine residues and one carboxylate residue (Figure 5b) [79]. This class of enzymes has been well studied, and they are effective in several oxidative reactions, such as selective C–H hydroxylations and stereoselective *syn*-dihydroxylations of arenes and alkenes [82,111,112]. The reactions performed by this class of enzymes are involved in the biodegradation of aromatic compounds [24,71,82,83]. Rieske oxygenases are based on a reductase and an oxygenase component [113]. The first one is a Rieske-type dinuclear iron cluster that mediates the electron transfer from NAD(P)H to the oxygenase component. The latter is characterized by an octahedral mononuclear non-heme iron(II) that can perform the activation of dioxygen to oxidize a hydrocarbon substrate [114,115].
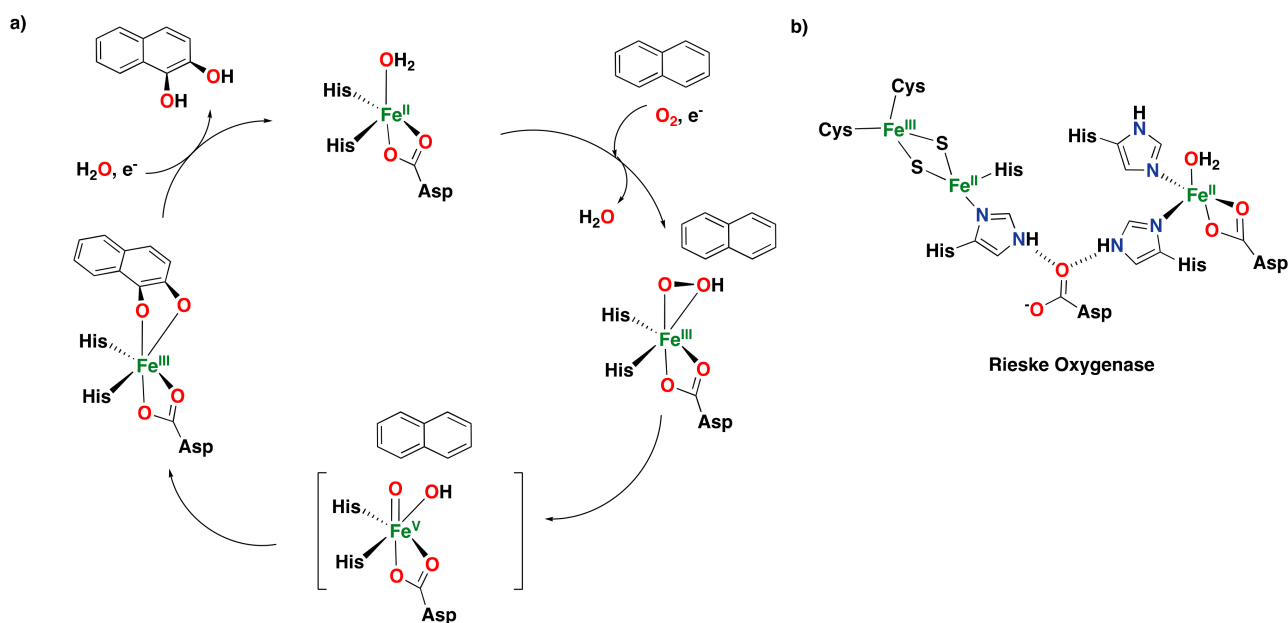
Figure 5. (**a**) Proposed catalytic cycle for the oxidation of naphthalene catalyzed by Rieske dioxygenases, involving the generation of an Fe(V)(O)(OH) species. (**b**) Active site of naphthalene 1,2-dioxygenase (NDO), showing the Rieske [2Fe:2S] cluster (reductase component) and the catalytic iron center (oxygenase component) [113].

One particular member of this family of enzymes is naphthalene-1,2-dioxygenase (NDO), which was crystallographically characterized in 1998 [111–113]. The proposed catalytic cycle for the *syn*-dihydroxylation of naphthalene consists of the reaction of dioxygen and an electron with the iron center to generate an Fe(III)-peroxo intermediate [79,112,116,117].

The cycle follows with the heterolytic cleavage of the O–O bond of the peroxo intermediate to generate what is proposed to be an Fe(V)(O)(OH) species, responsible for the oxidation of the substrate to form the syn-diol product (Figure 5a) [23,71,118,119]. Overall, the mechanism proposed for Rieske oxygenases resembles that of cytochrome P450 regarding the activation of dioxygen via a heterolytic O–O bond cleavage step. Moreover,

NDO can also perform the reaction in the presence of hydrogen peroxide via a "peroxide shunt" [120].

2.1.3. Bacterial Multicomponent Monooxygenases

Bacterial multicomponent monooxygenases (BMMs) are a family of non-heme iron enzymes that comprise a carboxylate-bridged diiron core in the active site [121–123]. Such enzymes catalyze the oxidation of various hydrocarbons, such as alkanes, alkenes, and aromatic compounds [124–127]. Within this family, we can distinguish several classes of multicomponent monooxygenases, such as soluble methane monooxygenases (sMMOs), toluene/*o*-xylene monooxygenases (ToMOs), and phenol hydroxylases (PHs) [128–130]. Among these, sMMO is the only enzyme that can catalyze the difficult conversion of methane to methanol, which is one of the most challenging reactions found in nature, 124 whereas ToMO performs the hydroxylation of aromatics and alkenes [126,131] and PH hydroxylates aromatic compounds (Figure 6 left) [130]. The hydroxylation of toluene by ToMO occurs through the generation of an epoxide and a subsequent NIH shift that forms *p*-cresol in 95% yield (*o*- and *m*-cresols are formed in ~4% yield) [106,121,132].
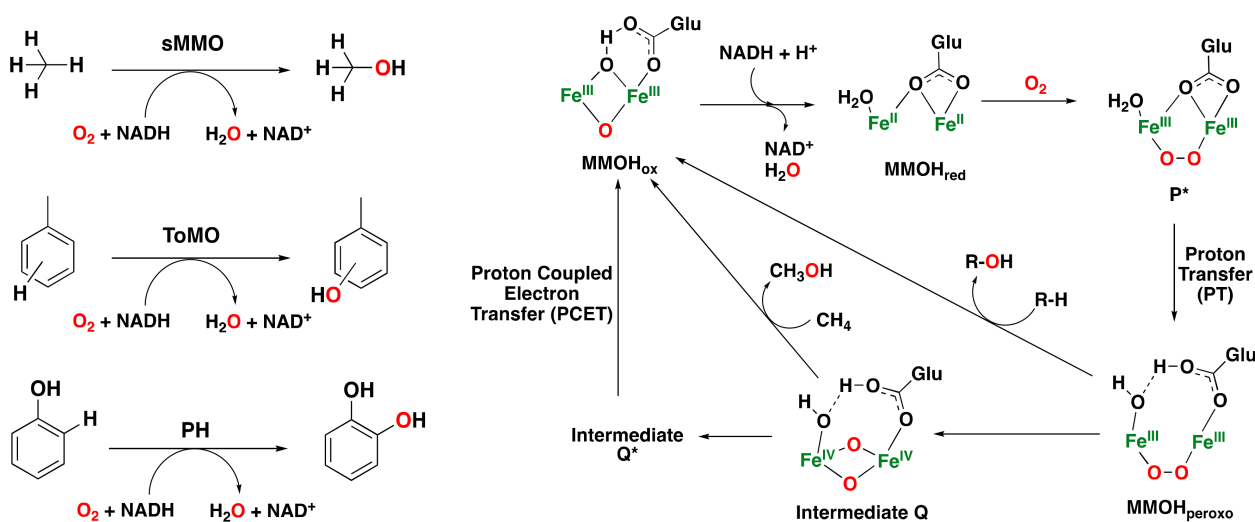

Figure 6. Left: Hydroxylation reactions catalyzed by some of the most representative bacterial multicomponent monooxygenases [14,121]. **Right**: catalytic mechanism of sMMO for dioxygen activation and substrate oxidation, involving the MMOHox, MMOHred, intermediate P*, MMOHperoxo, and intermediate Q species [14,121,133].

One of the most studied catalytic cycles is the one of sMMO for methane hydroxylation (Figure 6 right). In addition, sMMO is capable of oxidizing benzene to phenol [134]. Initially, the oxidized diiron(III) species (MMOH$_{ox}$) is activated by two-electron reduction to a diiron(II) species (MMOH$_{red}$). Then, the reaction with dioxygen forms the peroxo intermediate P* (via a superoxo species). Intermediate P* undergoes a proton transfer to form MMOH$_{peroxo}$, which can either decay to MMOH$_{ox}$ through the oxidation of electrophilic substrates or transform into diiron(IV) intermediate Q via homolytic cleavage of the O–O bond. The diiron(IV) intermediate Q can hydroxylate methane. In the absence of methane, intermediate Q decays to intermediate Q* and then to MMOH$_{ox}$ [14,121,124,133,135–138].

The mechanisms of ToMO and PH have also been investigated in detail, but they are less well understood compared to those of sMMO. Overall, these classes of bacterial multicomponent monooxygenases show a very similar diiron active site, which may imply a similar mechanism regarding the activation of dioxygen-generating peroxodiiron(III) and Q-type species [129,139]. Nevertheless, an unprecedented peroxodiiron(III) species has been elucidated for ToMO, and no evidence of Q-type intermediates is known yet, which suggests that the mechanism may differ from that described for sMMO. The general mechanism for dioxygen activation and substrate oxidation has been proposed to proceed

through an electrophilic attack by a peroxodiiron(III) intermediate on the arene to form an arene epoxide that ultimately leads to the aromatic oxidized product bound to the diiron(III) core (see Figure 7 for a representative scheme of phenol oxidation) [140].
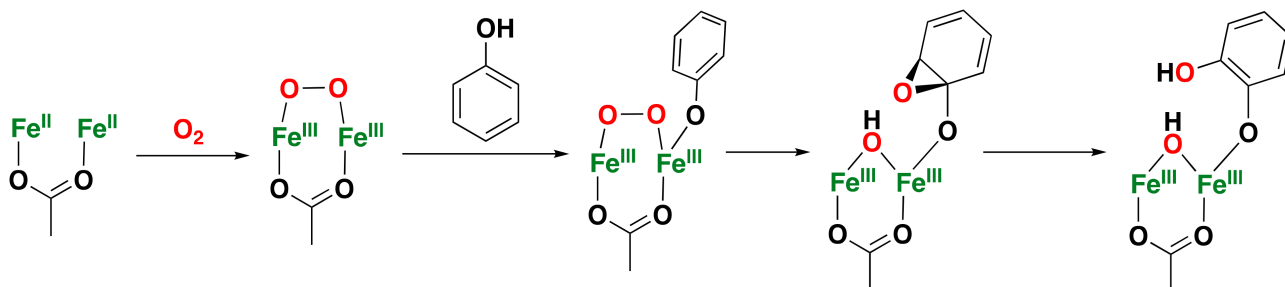
Figure 7. Schematic representation of the mechanism of PH for dioxygen activation and phenol hydroxylation. A similar mechanism is postulated for toluene hydroxylation; however, substrate orientation is controlled by residues of the active site rather than by coordination with the diiron core [140].

### 2.1.4. Pterin-Dependent Aromatic Amino Acid Hydroxylases

Aryl amino acid hydroxylases, also known as pterin-dependent oxygenases, are a class of enzymes that utilize tetrahydrobiopterin (BH_4) as a two-electron cofactor. Within this family, we can distinguish phenylalanine (PheOH), tyrosine (TyrOH), and tryptophan hydroxylases (TrpOH), which perform the hydroxylation of phenylalanine, tyrosine, and tryptophan, respectively (Figure 8) [23,34,141–145]. In addition, pterin-dependent hydroxylases can also perform epoxidations and benzylic hydroxylation reactions, in a similar way as the reactivity observed for cytochrome P450 enzymes [73,141].
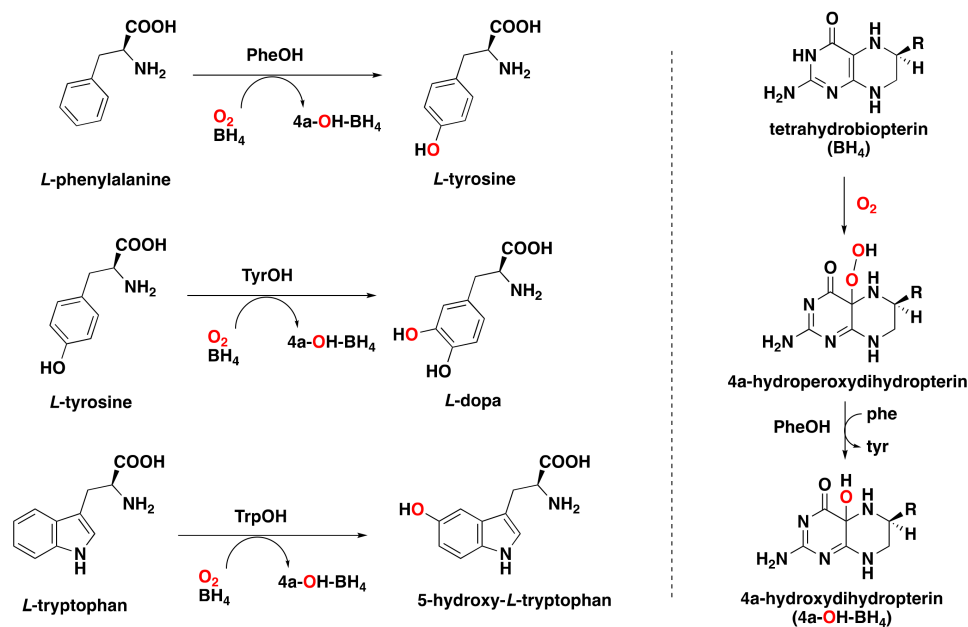
Figure 8. Left: arene hydroxylation reactions catalyzed by pterin-dependent amino acid hydroxylases. **Right**: reaction of the tetrahydropterin cofactor with dioxygen in the presence of aryl amino acid hydroxylases.

A general mechanism has been proposed regarding oxygen activation and substrate oxidation by these enzymes (Figure 9). Initially, tetrahydrobiopterin (BH_4) reacts with dioxygen to form a hydroperoxydihydropterin intermediate that reacts with the iron(II) center of the active site of the enzyme to generate an Fe(II)–O–O–pterin intermediate [34,141,143,146]. Alternatively, the direct reaction of dioxygen with the iron center to form an Fe(III)–

peroxo complex may take place, which then reacts with the tetrahydrobiopterin compound [144,147–149]. Subsequently, heterolytic cleavage of the O–O bond takes place to form a hydroxydihydropterin compound and an Fe(IV) oxo species responsible for the arene hydroxylation reaction. Several studies using labeled dioxygen have corroborated this last step because of the incorporation of labelled oxygen into both the amino acid and the hydroxydihydropterin product [150–152]. Once the hydroxylated amino acid is formed, the resting state of the enzyme is restored, and the oxidized tetrahydrobiopterin undergoes dehydration to generate a quinonoid dihydropterin. This latter compound is reduced by an external reductase to regenerate the tetrahydrobiopterin and start a new catalytic turnover [146]. Computational studies have also been performed to investigate the mechanism of pterin-dependent aromatic amino acid hydroxylases [153,154].
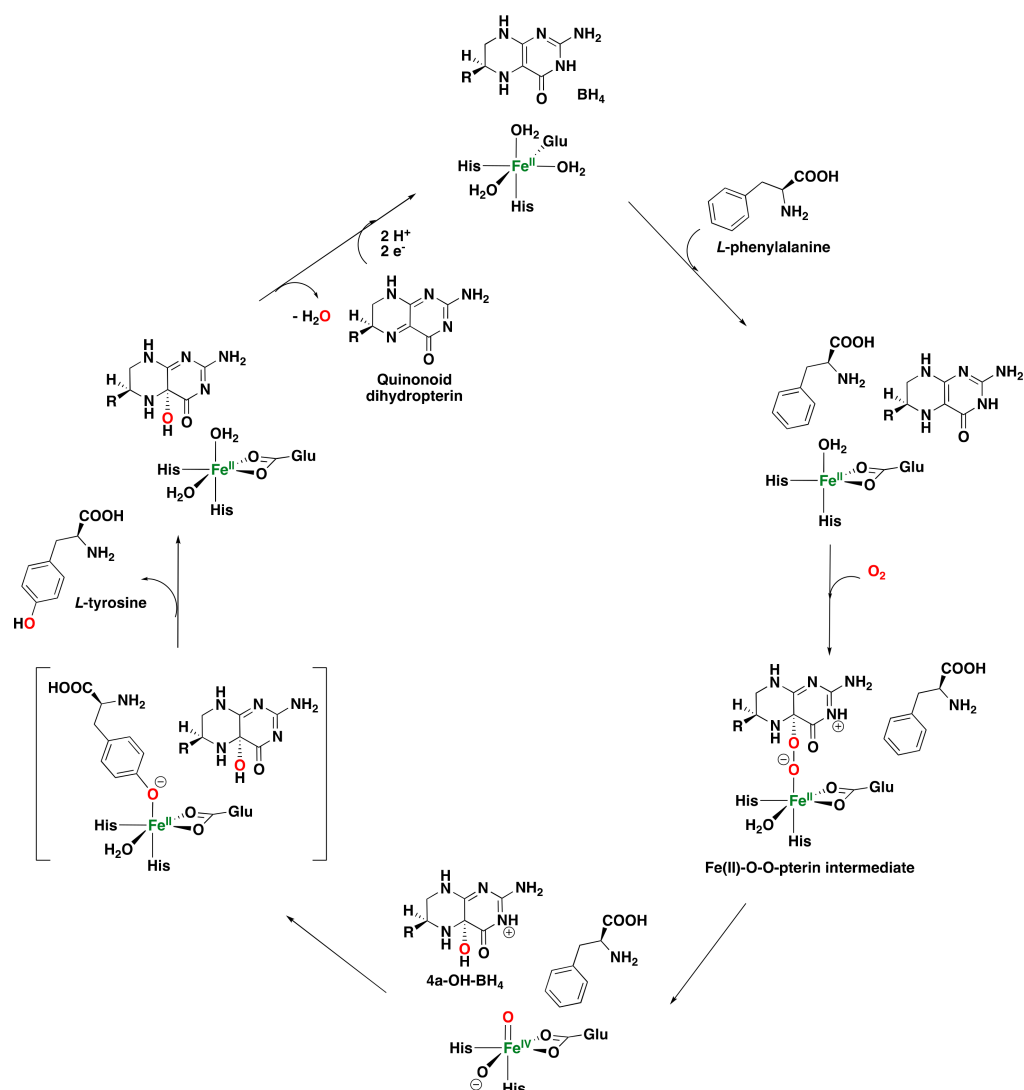
**Figure 9.** Proposed catalytic mechanism for phenylalanine hydroxylases (PheOH) [23,34].

2.2. Synthetic Iron Systems

Most of the synthetic iron complexes reported for aromatic oxidation are supported by polydentate N-based donor ligands and make use of the environmentally benign $2e^-$ oxidant H_2O_2. Overall, these systems have been extensively studied for the oxidation of inert $C(sp^3)$–H and C=C bonds, whereas aromatic oxidations using these complexes have mostly been studied in recent years. The mechanism of action of these bioinspired non-heme iron complexes has been extensively studied and is proposed to proceed through the involvement of highly stereoselective, high oxidation-state metal-based oxidants [26,155–160].

2.2.1. Iron-Based Systems and Oxidation Mechanism

The first example of a stereospecific hydrocarbon hydroxylation reaction catalyzed by a bioinspired non-heme iron complex was reported by Que and co-workers in 1997 using Fe(II) complex **8** supported by the tpa ligand (tpa = tris(2-pyridylmethyl)amine) with H_2O_2 as the oxidant [161]. The results shown in this study, based on the ratio of alcohol/ketone (A/K) products in the oxidation of cylcohexane (A/K > 5), retention of configuration in specific oxidation reactions (such as the oxidation of *cis*-1,2-dimethylcyclohexane), regioselectivity in the oxidation of tertiary C–H bonds over secondary C–H bonds (adamantane oxidation), and kinetic isotope effect (KIE) experiments, pointed towards a metal-based species as the active oxidant. Furthermore, the idea of a metal-based oxidant was also proposed in other studies using different aminopyridine ligands based on the tpa ligand scaffold [162].

Generally, this type of iron catalyst is supported by tetradentate aminopyridine ligands, with the ligands being either tripodal or linear. Different geometries around the metal center can be adopted in the case of linear tetradentate aminopyridine ligands, such as the bpmcn ligand (bpmcn = *N,N'*-dimethyl-*N,N'*-bis(2-picolyl)cyclohexane-*trans*-1,2-diamine). On the one hand, complexes with two *cis* positions open for coordination can form, whereas, on the other hand, the two open coordination sites can be *trans* to each other. For the *cis* topologies, two configurations are possible, namely *cis*-α and *cis*-β, and different reactivities have been found depending on the specific geometry that the complex may adopt (Figure 10) [72,158,161–167].
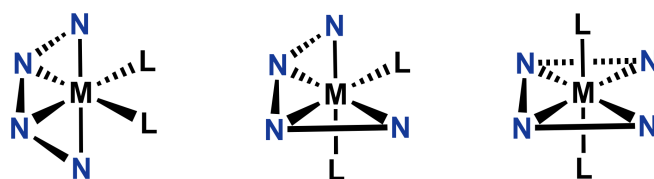

Figure 10. Different topologies for complexes with linear tetradentate aminopyridine ligands. L is an open coordination site.

A lot of debate has emerged regarding the mechanism of activation of H_2O_2 by non-heme iron complexes that can perform the hydroxylation reaction. Nevertheless, a general mechanistic pathway has been elucidated for iron complexes supported by strong-field tetradentate aminopyridine ligands with two *cis* open sites. This pathway proposes the generation of an Fe(V)(O)(OH) species generated via the O–O bond cleavage of an Fe(III)(OOH) intermediate with the help of a proton provided by a water molecule, reminiscent of the mechanism of Rieske dioxygenases (Figure 11) [26,157–159,168,169].

This pathway has been called the "water-assisted mechanism," and several studies on olefin epoxidation and *syn*-dihydroxylation reactions have pointed out the involvement of Fe(V)(O)(OH) species as the electrophilic oxidant responsible for the oxidation reactions by these kinds of complexes [170–172]. Indeed, several pieces of evidence that demonstrate the existence of these high-valent iron oxo-hydroxo species have been reported in recent years [173–176].

Another very important aspect of this chemistry was the introduction of carboxylic acid additives, which act as co-ligands binding to the metal center and modulating the reactivity of the complexes towards H_2O_2. For the first time in 2001, Jacobsen and co-workers introduced the use of acetic acid in combination with an iron complex supported by the bpmen ligand (bpmen = *N,N'*-dimethyl-*N,N'*-bis(2-picolyl)ethylenediamine) and H_2O_2, which enhanced the catalytic activity of the iron system in the epoxidation of olefins [177]. Later, White and co-workers demonstrated the same beneficial effect of carboxylic acids in aliphatic C–H bond oxidations [178]. This remarkable study showed for the first time that an iron complex supported by the robust bpbp ligand (bpbp = *N,N'*-bis(2-pyridylmethyl)-2,2'-bipyrrolidine) can perform C–H oxidations in synthetically useful yields. In addition, it can discriminate between different C–H bonds within a complex substrate molecule [179,180].

Various mechanistic studies have been carried out to elucidate the effect of the carboxylic acid in the activation of H_2O_2 and have led to a proposed mechanistic pathway now known as the "carboxylic acid assisted mechanism" (Figure 12) [26,59,72,157–159,168,169,181]. In this pathway, an Fe(V)(O)(OCOR) intermediate is postulated as the active species, which forms through the heterolytic cleavage of the O–O bond of an Fe(III)(OOH) intermediate with the help of the carboxylic acid instead of a water molecule. Overall, the use of carboxylic acid as an additive and co-ligand in aliphatic and aromatic oxidations, as well as epoxidation reactions, has been found to generate catalytic systems with higher activities in most cases.
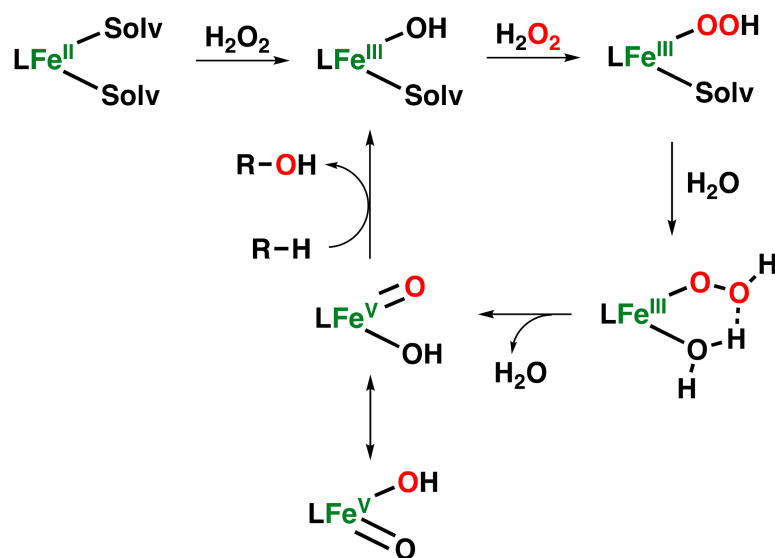
Figure 11. Water-assisted mechanism is proposed for the generation of an Fe(V)(O)(OH) species in hydroxylation reactions catalyzed by non-heme iron complexes supported by strong-field tetradentate aminopyridine ligands with two cis open sites.
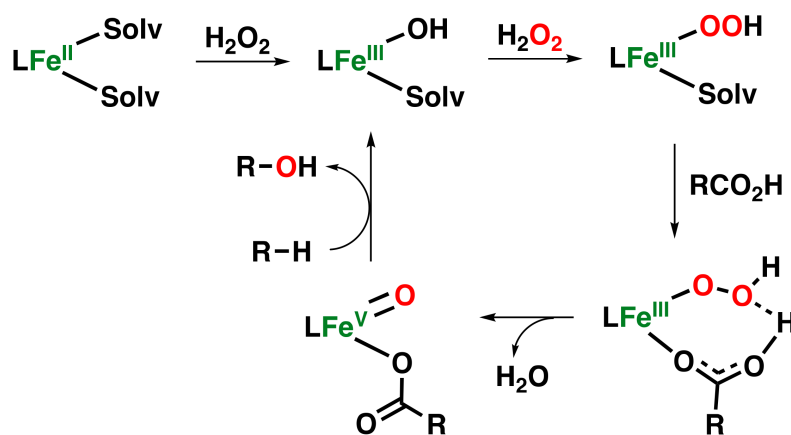
Figure 12. Carboxylic acid-assisted mechanism is proposed for the generation of an Fe(V)(O)(OCOR) species in the hydroxylation reaction catalyzed by non-heme iron complexes supported by strong-field tetradentate aminopyridine ligands with two cis open sites.

2.2.2. Iron-Catalyzed Arene Oxidation

As discussed previously, bioinspired non-heme iron complexes have been widely investigated in the field of aliphatic C(sp^3)–H oxidation and alkene epoxidation reactions, whereas catalytic arene oxidations with such complexes have remained challenging until recently [182]. Initial reports on aromatic oxidation reactions using iron are based on the incorporation of an aromatic ring into the ligand structure of the complex and therefore

represent examples of intramolecular arene hydroxylation reactions. Even though these examples do not represent catalytic systems, their study has allowed for further insight into the mechanism of these reactions. In 1993, Moro-oka and co-workers described the hydroxylation of a series of trispyrazolylborate-based ferric bis-phenoxo complexes (1, 2, and 3) to form catecholato complexes using mCPBA as the oxidant, resulting in a system that acts as a functional model for tyrosine hydroxylase [183]. The reaction of the Fe(III) complexes with 1 equiv. of mCPBA resulted in the formation of the corresponding catechol in quantitative yields, and a proposed reaction mechanism includes the formation of an acylperoxo intermediate (Figure 13a). However, attempts to detect the (acylperoxo)-phenoxo intermediate were unsuccessful. Later, Fontecave and co-workers reported on diiron complexes that act as models for methane monooxygenase, based on an ethylenediamine tetraacetic acid (EDTA) derived ligand bearing two electron-rich phenyl groups [184,185]. Complex 4 can react with aqueous H_2O_2, which leads to the ortho-hydroxylation of one of the phenyl groups of the ligand, generating a monomeric iron species (Figure 13b). This intramolecular reaction also proceeds in the presence of dioxygen and excess ascorbate as a reductant, while alkylhydroperoxides, sodium hypochlorite, and mCPBA do not oxidize the diiron complex. Similar iron complexes supported by the N,N'-bis(13yridine-2-ylmethyl)-N,N'-bis(3,4,5-trimethoxybenzyl)ethane-1,2-diamine ligand ([Fe(II)(L)X$_2$], 5 and 6) were reported to react with aqueous H_2O_2, leading to ortho-hydroxylation of one of the substituted phenyl moieties of the ligand as well (Figure 13c) [186]. However, for complex 6, in which the chloride ligands have been exchanged by acetonitrile solvent molecules, the organic ligand does not undergo aromatic hydroxylation, but instead N-dealkylation of the ligand was observed. In addition, this complex showed activity for epoxidation reactions and hydroxylation of alkanes [186]. For complex 5, it was proposed that the hydroxylation reaction proceeds through the reaction with H_2O_2 via an outer-sphere electron transfer to generate hydroxyl radicals that add to the aromatic ring of the ligand. In contrast, complex 6 is proposed to generate iron peroxo and oxo complexes because of the more labile sites of this complex, which allow for an inner-sphere reaction of H_2O_2 with the metal center [186].

In 1999, Que and co-workers reported on iron complex **7** based on a modified tpa ligand containing a pendant phenyl group, Fe(6-Ph-tpa)(NCCH$_3$)$_2$](ClO$_4$)$_2$ (6-Ph-tpa = bis(2-pyridylmethyl)-6-phenyl-2-pyridylmethylamine), that is capable of performing an intramolecular hydroxylation of the phenyl group of the ligand to form an Fe(III)-phenolate species (Figure 14a) [187]. The reaction of complex **7** with TBHP at low temperature afforded a transient blue species formulated as Fe(III)(OOtBu)(6-Ph-tpa) that decays over 4 h at −60 °C to give the final iron complex bearing the hydroxylated ligand.

Indirect evidence suggests the involvement of an Fe(IV) oxo species as the active oxidant in this reaction. Complex **7** also performs the *ortho*-hydroxylation of the ligand's phenyl ring efficiently and selectively by reaction with iodosobenzene [188]. The same reactivity with TBHP was also demonstrated for other iron complexes with modified versions of the 6-Ph-tpa ligand [189]. In 2005, it was shown that the parent iron complex **8** supported by the tpa ligand is capable of oxidizing ligated perbenzoic acids through the self-hydroxylation of the aromatic ring forming iron(III)-salicylate complexes (Figure 14b) [190].

Iron complex **9**, supported by the linear tetradentate bpmen ligand, was also found to perform the *ortho*- and *ipso*-hydroxylation of benzoic acids to afford salicylates and phenolates, respectively (Figure 14c) [191,192]. Later on, hydroxylation of externally added aromatic substrates without directing groups was found to be effective using iron complex **9** in combination with H_2O_2 as an oxidant, although strong coordination of the generated phenolates to the resulting iron(III) center prevented efficient catalysis, i.e., **9** performs up to 1.4 turn-overs (Figure 14d) [193].
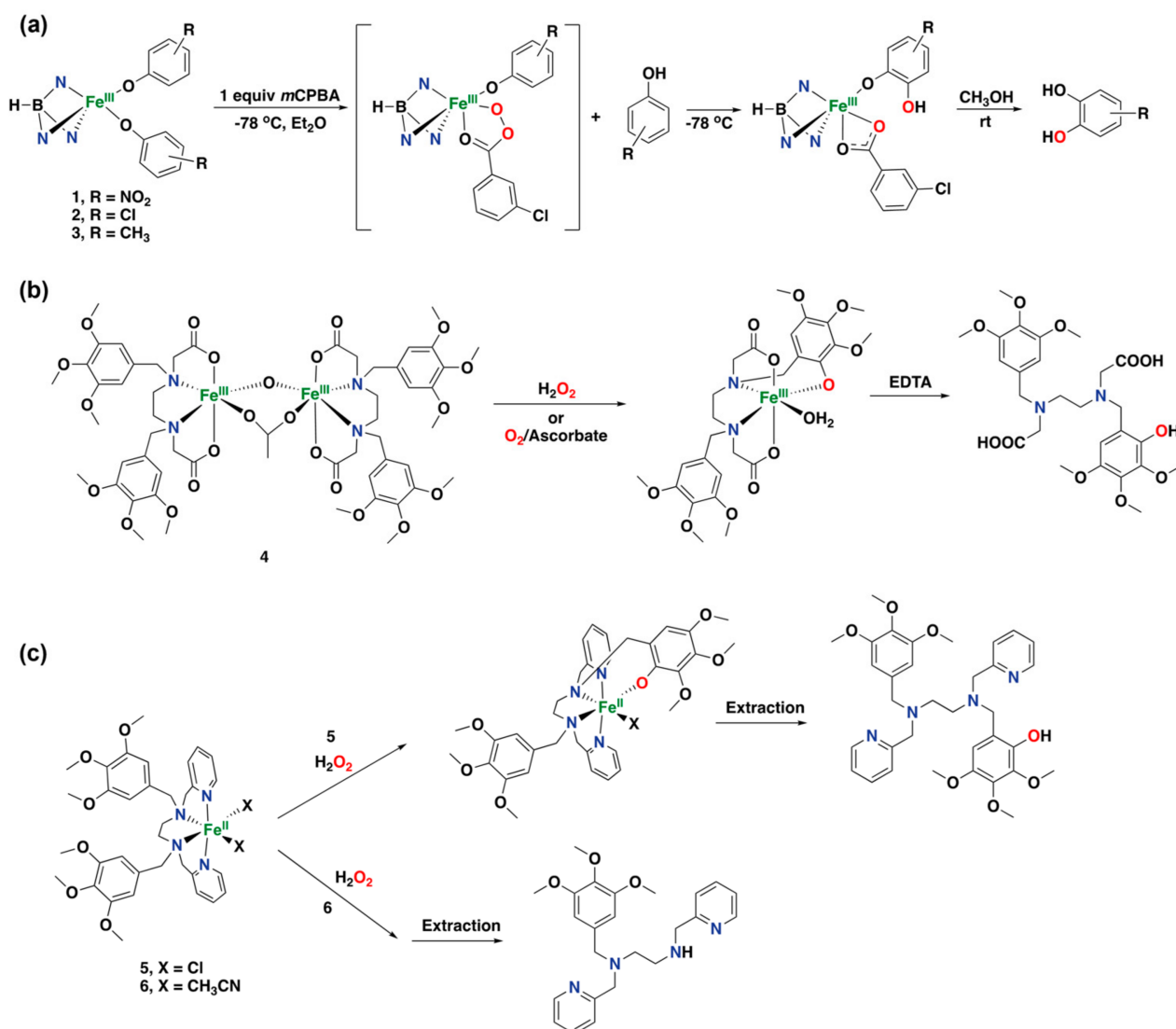
Figure 13. Early examples of iron complexes capable of intramolecular aromatic hydroxylation of the organic ligand. (**a**) Hydroxylation of trispyrazolylborate-based ferric bis-phenoxo complexes using mCPBA. (**b**) Intramolecular hydroxylation of a diiron complex to form a monomeric iron species. (**c**) Intramolecular hydroxylation of a series of iron complexes to yield the corresponding hydroxylated ligand.

A lot of effort has been devoted to the investigation of the active oxidant responsible for the arene hydroxylation reaction using these iron complexes. While for some an Fe(IV)-oxo species generated via the homolysis of the O–O bond has been postulated as the oxidant responsible for the oxidation reaction [187,189], an Fe(V)-oxo species has been proposed as an alternative active species in other cases [155,160,190,192–194].

Computational studies have also been performed to provide mechanistic insight into the *ortho*-hydroxylation of aromatic compounds by non-heme iron complexes. Particularly, DFT calculations have clearly shown that Fe(III)-hydroperoxo species are sluggish oxidants, whereas the heterolytic cleavage of the former species to generate a transient Fe(V)-oxo oxidant has been postulated as a plausible reaction mechanism for arene oxidations [195]. Moreover, some studies have demonstrated that Fe(IV)-oxo species are inactive in the hydroxylation of externally added aromatic substrates [193,196–198].
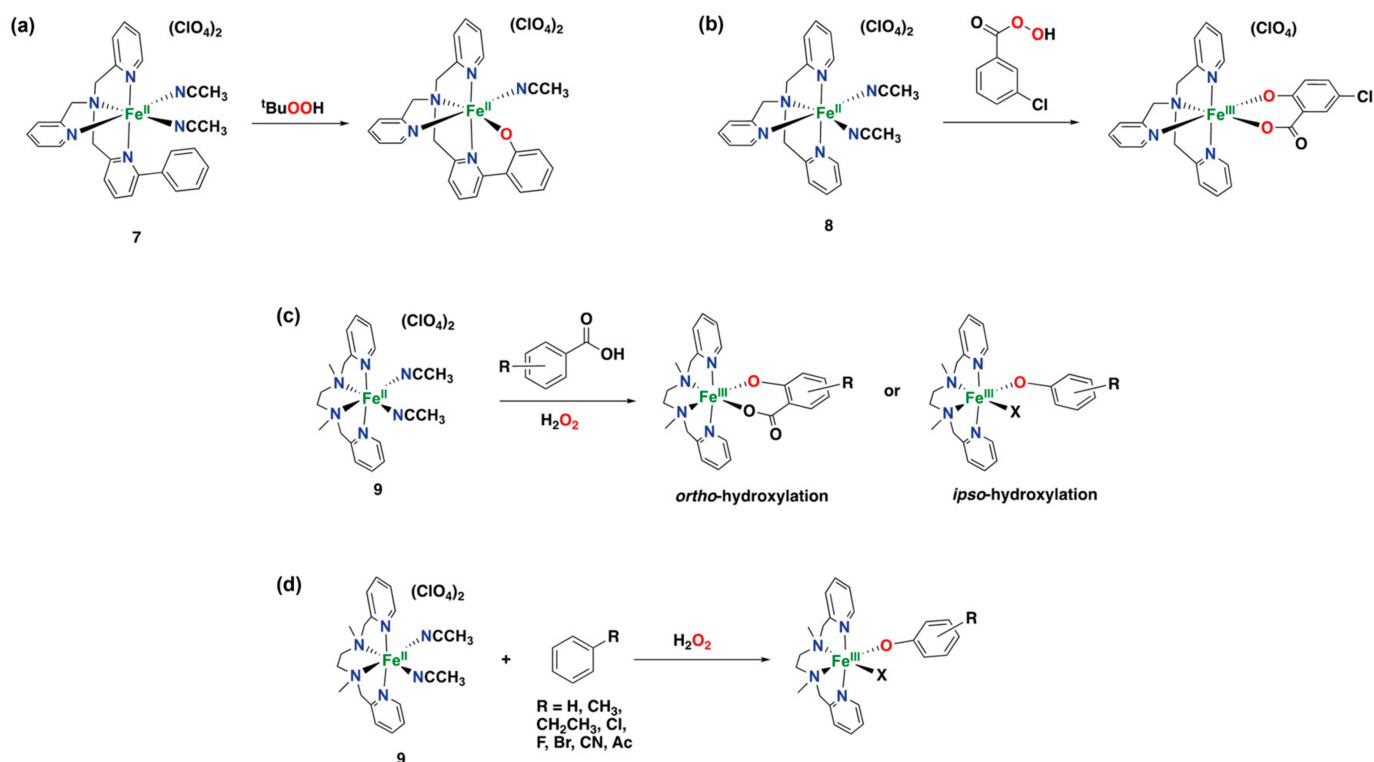
Figure 14. Iron(II) complexes are capable of performing arene hydroxylation reactions with different oxidants, generating phenolate or salicylate species. (**a**) Intramolecular hydroxylation of a monomeric iron complex supported by a modified tpa ligand. (**b**) Oxidation of perbenzoic acid with an iron-tpa complex complex. (**c**) Oxidation of benzoic acids with an iron-bpmen complex. (**d**) Oxidation of aromatic substrates without directing groups with an iron-bpmen complex.

Nam and co-workers provided further insight into the capabilities and reaction mechanisms of the oxidation of aromatic substrates by non-heme iron(IV)-oxo complexes [199]. In these studies, iron complexes containing Bn-tpen and N4Py ligands (Bn-tpen = *N*-benzyl-*N,N′,N′*-tris(2-pyridylmethyl)ethane-1,2-diamine and N4Py = *N,N*-bis(2-pyridylmethyl)-*N*-bis(2-pyridyl)methylamine) were considered. Experimental data, such as a large and negative Hammett *p*-value and an inverse C–H/C–D KIE effect, together with computational investigations indicated that arene hydroxylation by these iron(IV)-oxo complexes do not occur via a hydrogen atom abstraction but instead proceeds through an electrophilic aromatic substitution pathway. Oxidation of anthracene as the substrate produced anthraquinone as the product, which is generated via the reaction of two metal oxo complexes, as has been described previously for the generation of quinone compounds [15–17]. Worth mentioning is that these non-heme iron(IV)-oxo complexes do not perform the hydroxylation of benzene or naphthalene, which highlights the low reactivity of bioinspired iron(IV)-oxo species in arene hydroxylation reactions [199].

In 2002, Mansuy and co-workers described a non-heme iron complex supported by the TPAA ligand (TPAA = tris-[*N*-2-pyridylmethyl-2-aminoethyl]amine), which is effective in the hydroxylation of aromatic compounds using H_2O_2 as an oxidant, whereas this complex shows poor catalytic activity for olefin epoxidation and alkane hydroxylation (see Figure 15a for the structure of the TPAA ligand) [200]. Overall, this complex shows up to 10 turnovers for the oxidation of anisole (53% yield based on the oxidant) but shows poor activities for the oxidation of less electron-rich substrates, such as benzene or chlorobenzene. Non-heme iron complexes with tetradentate and pentadentate aminopyridine ligands, namely L_4^3, $L_5^{2'}$ and L_5^3 (Figure 15a), have shown comparable arene hydroxylation capabilities in combination with H_2O_2. In addition, for most of these iron complexes, it has been demonstrated that the addition of an appropriate reducing agent, such as hydroquinones,

thiophenol, or tetrahydropterins, dramatically enhances the yields of the hydroxylation aromatic products (up to 69% yield for anisole oxidation based on the oxidant catalyzed by an iron complex based on the L_5^2 ligand, i.e., TON = 13.8) [201].
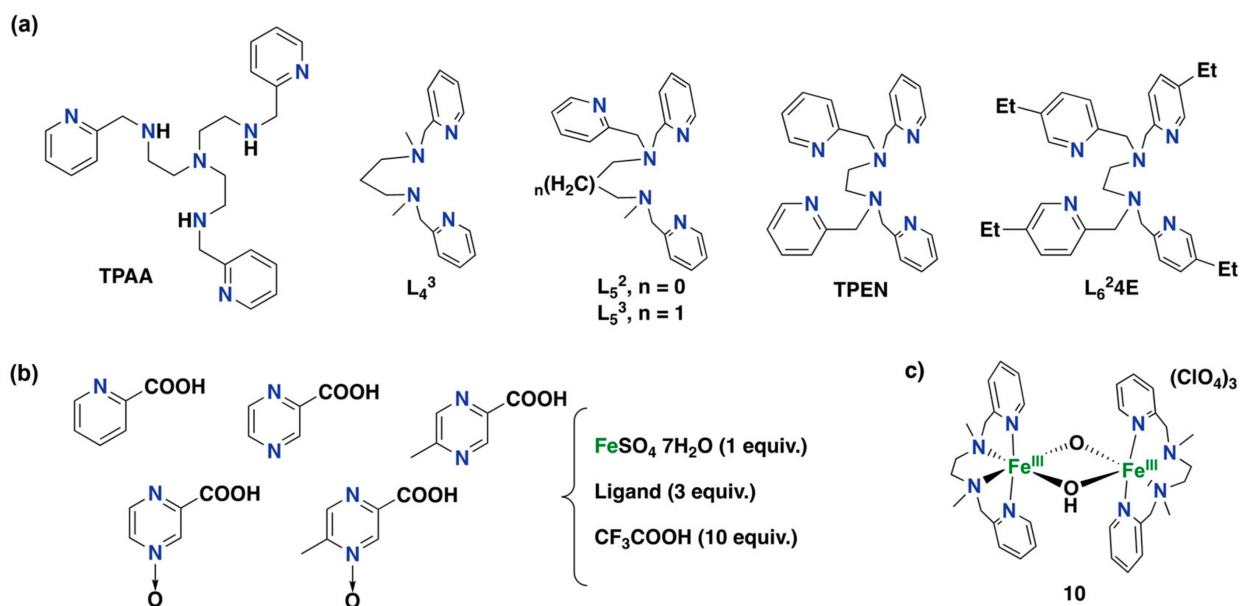
Figure 15. (**a**) Aminopyridine ligands were studied in iron-mediated arene hydroxylation reactions under substrate-excess conditions in the presence of a reductant [200–202]. (**b**) Three-component system for the hydroxylation of aromatics using a biphasic reaction medium under substrate-excess conditions [203–205]. (**c**) Example of a diiron complex that mimics the reactivity of toluene monooxygenases [206].

A more recent study on the non-heme iron complexes containing the TPEN (TPEN = *N, N,N′,N′*-tetrakis-(2-pyridylmethyl)ethane-1,2-diamine) and $L_6^2$4E ligands has shown activity for the hydroxylation of electron-rich anisole, as well as for benzene and chlorobenzene. In particular, the former complex performed best in the presence of 1-naphthol as a reducing agent, with a yield of up to 86% for anisole oxidation (TON = 17.2), whereas the latter complex performed best employing thiophenol as a reducing agent, with a yield up to 38% for anisole oxidation (TON = 7.6) [202]. Worth mentioning is that these systems make use of substrate-excess conditions, providing high product selectivities with low substrate conversions.

Bianchi and co-workers described a method for the selective hydroxylation of benzene to phenol catalyzed by an iron complex using H_2O_2 as a benign oxidant and trifluoroacetic acid as a co-catalyst in a biphasic system [203]. The study investigated a series of bidentate *N,N-*, *N,O-* and *O,O*-based ligands, finding that the most efficient catalyst system was obtained by using 5-carboxy-2-methylpyrazine-*N*-oxide as a ligand (see Figure 15b for ligand structures). The system was used under substrate-excess conditions, providing poor benzene conversions while H_2O_2 conversion was 94%. Selectivity for the phenol product was 85% based on benzene conversion. Remarkably, the use of a biphasic system (mixture of water, acetonitrile, and aromatic substrate) allowed easy recovery and recycling of the catalyst. Later, the same authors reported on the use of a similar system, using pyrazine-3-carboxylic acid *N*-oxide as the ligand (Figure 15b), for the direct hydroxylation of a series of aromatic substrates to the corresponding phenol products [204]. The authors highlight the low selectivity obtained for the oxidation of electron-rich arenes as well as possible competition for hydroxylation of the lateral alkyl chain in the case of alkylbenzenes. Finally, another study showed how small modifications in the structure of the ligand used in this biphasic system can produce significant differences in activities for the oxidation of

benzene and toluene. The system used pyrazine-3-carboxylic acid *N*-oxide as the ligand, which is the most efficient for the synthesis of phenols [205].

Biswas and co-workers have also described an iron system for the hydroxylation of aromatic C–H bonds under substrate-excess conditions [206]. This system consists of diiron(III) complex **10**, supported by the bpmen ligand (Figure 15c), which can carry out the hydroxylation of benzene and alkylbenzenes with high selectivities, albeit with very low turnover numbers. The addition of acetic acid was found to produce a small increase in phenol yields. For alkylbenzene oxidations, products derived from the hydroxylation of the lateral alkyl chain were also observed. Based on its dinuclear nature, this system mimics the activity of toluene monooxygenase and methane monooxygenase.

In 2014, Kühn and co-workers reported iron complex **11** capable of hydroxylating aromatic substrates to the corresponding phenol products under catalytic conditions with equimolar amounts of substrate/oxidant or excess of the oxidant [207]. This particular catalyst is based on a chelating di-pyridyl-di-NHC ligand (NHC = N-heterocyclic carbene; Figure 16). The difference between this complex and other complexes typically used in oxidation chemistry is that the iron center is coordinated in part by NHC-based carbon donors [208]. NHCs are considered good σ-donors and, therefore, the authors anticipated that the corresponding complex would exhibit high kinetic stability towards oxidation conditions [209,210]. Complex **11** can oxidize benzene to phenol using equimolar amounts of H_2O_2 and substrate, albeit with low conversion (7.4%) and phenol yield (6.9%, i.e., TON = 6.9) but high selectivity (94%). The major by-product of this reaction is *para*-benzoquinone. The involvement of hydroxyl radicals in this catalytic system was discarded since no formation of biphenyl was observed. Based on an experimental inverse C–H/C–D KIE of 0.9, the authors have postulated a mechanism that involves an sp^2-to-sp^3 hybridization change during the attack of a putative high-valent iron-oxo on the aromatic ring forming a σ-complex. Complex **11** is also capable of hydroxylating methyl substituted arene substrates, such as toluene, *p*-xylene, and pseudocumene (Figure 16). In some cases, mixtures of phenol products were observed together with some alkyl side chain oxidation products, overall showing a high selectivity for arene oxidation over benzylic oxidation reactions (up to 11.9% total yield for the aromatic oxidation of toluene and up to 12.6% total yield for *p*-xylene oxidation). A so-called NIH-shift for a methyl group was observed for the current system in the oxidation of *p*-xylene. This resembles the same process observed for arene oxidations catalyzed by cytochrome P450 or pterin-dependent aromatic amino acid hydroxylases. The system was also tested for the oxidation of pseudocumene, affording trimethylbenzoquinone (TMBQ) in a 7.5% yield (a valuable chemical for vitamin E synthesis) [207,211].

In 2016, Silva and co-workers reported on the reactivity of a series of iron complexes (**12**–**17**) based on acetylacetonate and Schiff base ligands in the direct hydroxylation of benzene to phenol with H_2O_2 (Figure 17a) [42]. Within this study, it was found that the complex based on a N_4-donor Schiff base ligand shows the highest activity and selectivity for the hydroxylation of benzene under substrate-limiting conditions, with 65% conversion and 98% phenol selectivity, generating *para*-benzoquinone as an overoxidized side-product [42]. This system has shown some of the highest conversions and phenol selectivities ever reported for arene hydroxylation using iron catalysts with H_2O_2 as an oxidant.

A later study by Antunes et al. describes the reactivity of a series of iron(III) complexes (**18**–**21**) based on the BMPA and similar ligands as catalysts for the hydroxylation of toluene with H_2O_2 as an oxidant (BMPA = bis-(2-pyridylmethyl)amine; Figure 17b) [212]. All complexes tested in this study showed reactivity for the oxidation of toluene, generating mixtures of phenol products (*ortho*-, *meta*- and *para*-isomers), as well as products derived from lateral alkyl chain oxidation (benzaldehyde and benzyl alcohol). Complex **18**, based on the BMPA ligand, showed the highest yields of all catalysts tested in this study, with a 30% total product yield for the oxidation of toluene at 50 °C after 24 h [212].
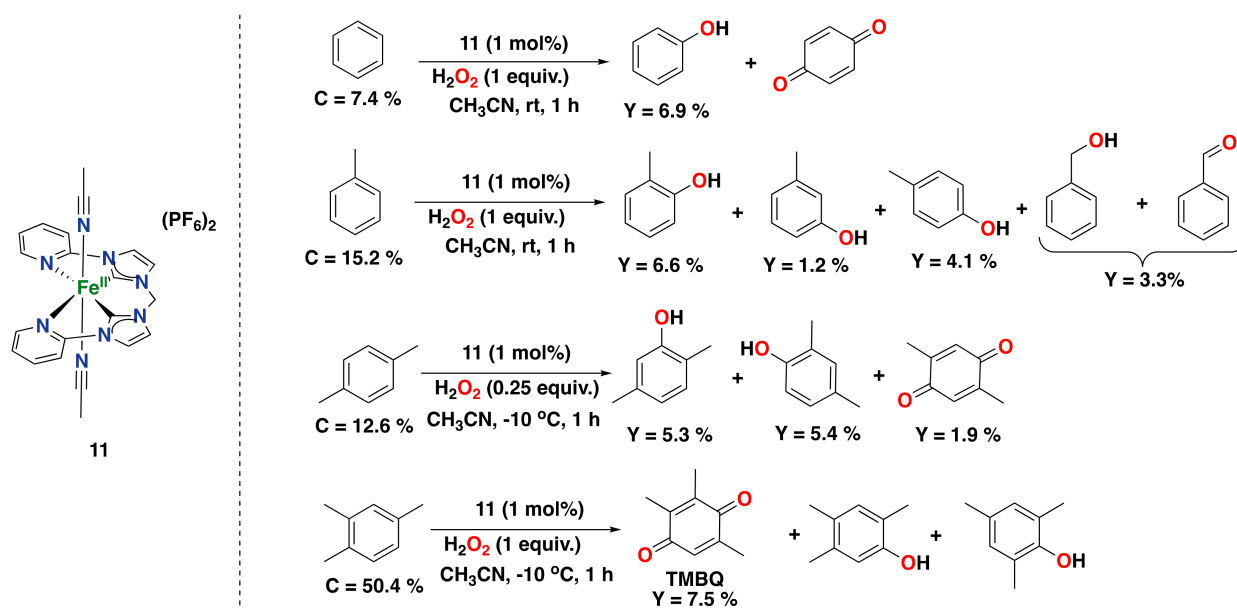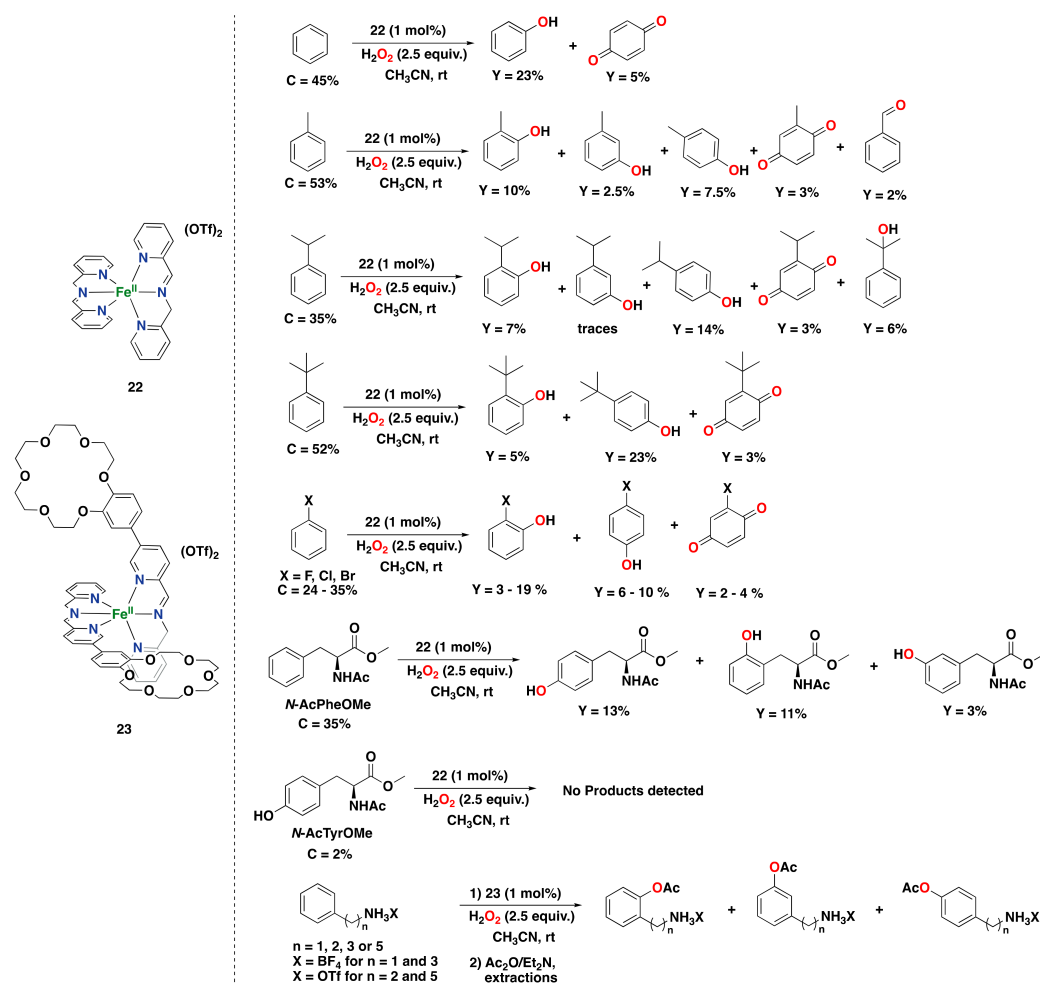
Figure 16. Reaction products of the catalytic oxidation of benzene and benzene derivatives catalyzed by NHC-based iron complex **11**, with H_2O_2 as the oxidant [207,211]. C: substrate conversion. Y: product yield.
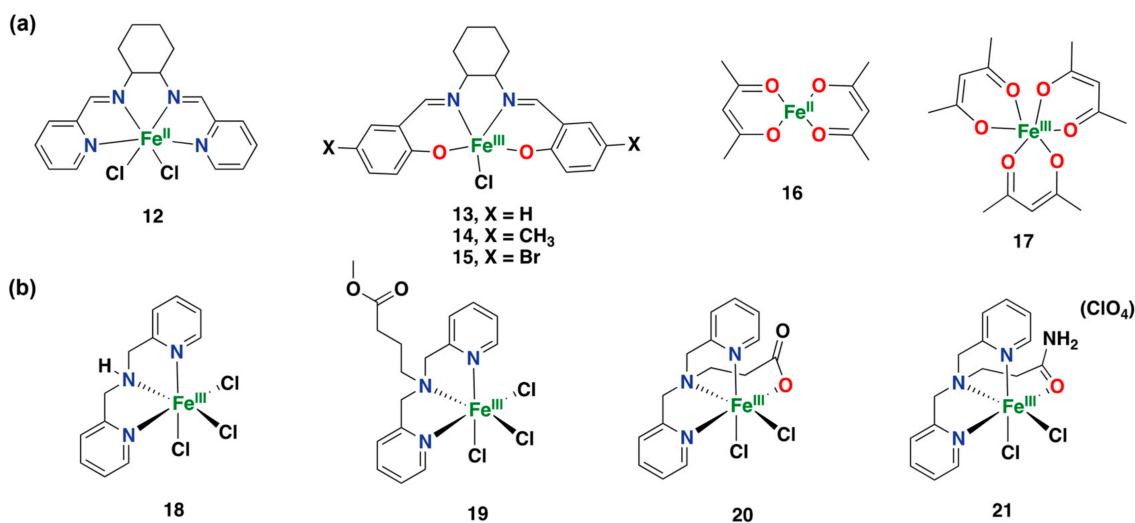
Figure 17. (**a**) Iron complexes supported by acetylacetonate and Schiff base ligands were tested for the direct aromatic hydroxylation of benzene to phenol with H_2O_2 [42]. (**b**) Iron(III) complexes were tested for the hydroxylation of toluene with H_2O_2 as an oxidant [212].

Despite the extensive investigation of non-heme iron complexes based on aminopyridine ligands, studies have also shown the effectiveness of imine-based non-heme iron complexes for different oxidative processes [213]. A remarkable example in the field of arene oxidations catalyzed by imine-based iron complexes was recently reported by Di Stefano and co-workers using iminopyridine iron(II) complex **22**, prepared in situ by self-assembly of commercial starting materials (iron(II) triflate, 2-picolylamine, and 2-picolylaldehyde), and H_2O_2 as an oxidant under mild reaction conditions (Figure 18) [214]. The authors found that complex **22** is capable of oxidizing benzene in a 23% phenol yield after 90 min of reaction time, generating benzoquinone as an overoxidized by-product in only a 5% yield. The oxidation of benzene was also effective on a 0.5 g scale, generating phenol with a 26% yield. A metal-based reaction was postulated as a plausible mechanism for this system since no biphenyl product was detected, suggesting that oxygen-centered radicals are likely

not involved. Additionally, the oxidation of benzene derivatives was also performed with this iminopyridine iron system. Oxidation of phenol afforded *para*-benzoquinone in a 13% yield exclusively. Oxidation of toluene afforded the corresponding cresol products (mixture of *ortho*-, *meta*- and *para*-isomers) a total yield of 20%, as well as overoxidized methyl-p-benzoquinone in a 3% yield, and the alkyl chain oxidation product benzaldehyde in a 2% yield. Oxidation of ethylbenzene provided products derived from hydroxylation at the aromatic ring as well as from alkyl side chain oxidation, albeit in smaller amounts. However, when cumene was considered, which bears a more encumbered isopropyl substituent with a weak tertiary benzylic C–H bond, the yield for the alkyl side chain oxidation alcohol product increased (6% yield). Hydroxylation of *tert*-butylbenzene was also proven to be effective, generating phenols with a total yield of 28% and a *tert*-butyl-p-benzoquinone by-product with only a 3% yield. For all the alkylbenzenes tested, mixtures of *ortho* and *para*-phenols were obtained, whereas *meta*-phenols formed in small amounts, suggesting that an electrophilic aromatic substitution-type mechanism is operative for this catalytic system. Oxidation of halobenzenes was also effective, exclusively generating *ortho*- and *para*-phenols, together with quinone by-products. The electron-rich substrate anisole was oxidized in 21% total yield, providing a mixture of *ortho*-phenol, *para*-phenol, and benzoquinone. This product profile agrees with the fact that electron-donating groups favor oxidation by electrophilic oxidants. On the contrary, electron-withdrawing substituents suppress the reactivity of the catalyst toward the aromatic ring.

Figure 18. Reaction products of the catalytic oxidation of benzene, benzene derivatives, and aromatic amino acids catalyzed by iminopyridine iron(II) complexes **22** and **23** with H_2O_2 as an oxidant [214–216]. C: substrate conversion. Y: product yield.

Iron complex **22** has also been found to be effective for the oxidation of several aliphatic C–H bonds [217], as well as alcohol oxidation to ketones [218]. Noteworthy is that benzylic alcohols are oxidized in low yields due to competitive arene hydroxylation, showing that the **22**/H_2O_2 catalytic system has a preference for oxidizing aromatic over aliphatic sites. Moreover, the oxidation of monocyclic and polycyclic aromatic systems showed clear chemoselectivity for aromatic over aliphatic side chain oxidation. However, for more activated polycyclic substrates with lower BDEs of the benzylic C–H bond, the chemoselectivity decreased [219].

A mechanism for H_2O_2 activation and substrate oxidation by complex **22** has been proposed to include the decoordination of one of the pyridine donor arms [214,220]. Initially, the starting Fe(II) complex is oxidized to an Fe(III) intermediate, after which detachment of one of the pyridine arms of the ligand allows the complex to react with H_2O_2 to generate an Fe(III) hydroperoxo species (Figure 19). Further generation of the active species is still a matter of debate, but the generation of a high-valent Fe(V) oxo species is proposed to be unlikely since imine-based ligands usually favor low oxidation states of the metal center [220].
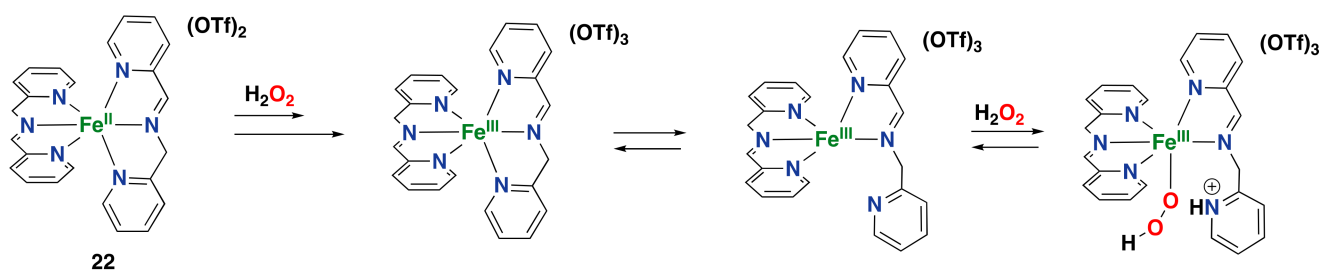

Figure 19. Proposed mechanism for H_2O_2 activation with iminopyridine iron(II) complex **22** [220].

Complex **22** was also shown to be capable of oxidizing an aromatic amino acid derivative with H_2O_2. Particularly, the oxidation of protected phenylalanine (*N*-AcPheOMe) yields the corresponding tyrosine (*N*-AcTyrOMe) as the main product (13% yield), together with the two isomeric phenolic derivatives in 14% total yield (Figure 18) [215]. Interestingly, no products deriving from benzylic hydroxylation were observed. An important point to highlight is that **22** does not seem to suffer from irreversible phenolate binding to the iron center, which generally avoids catalytic turnover by catalyst inhibition, as found in several examples presented in this review.

More recently, Di Stefano and co-workers designed a modified version of iminopyridine iron(II) complex **22** by decorating the ligand with crown-ether moieties. Complex **23** catalyzes the oxidation of aromatic compounds endowed with an alkylammonium anchoring group with H_2O_2 with moderate activity (up to 31% total yield) and selectivity for hydroxylation of the *meta* over the *ortho* site (up to 1.5 for *meta*/*ortho* ratio; Figure 18) [216]. The selectivity observed was proposed to be guided by the steric bulk provided by the crown-ether moieties of the ligand, with a minor contribution from substrate recognition.

In 2018, Talsi and co-workers described iron complex **24** based on a bpbp type ligand as a catalyst for the hydroxylation of aromatics with H_2O_2 or peracetic acid as oxidants and carboxylic acid as a co-ligand (Figure 20) [221]. Particularly, iron complex **24** is based on a diferric core, which was previously found to be effective in other oxidative processes, such as alkane hydroxylations and alkene epoxidation reactions [222–224].
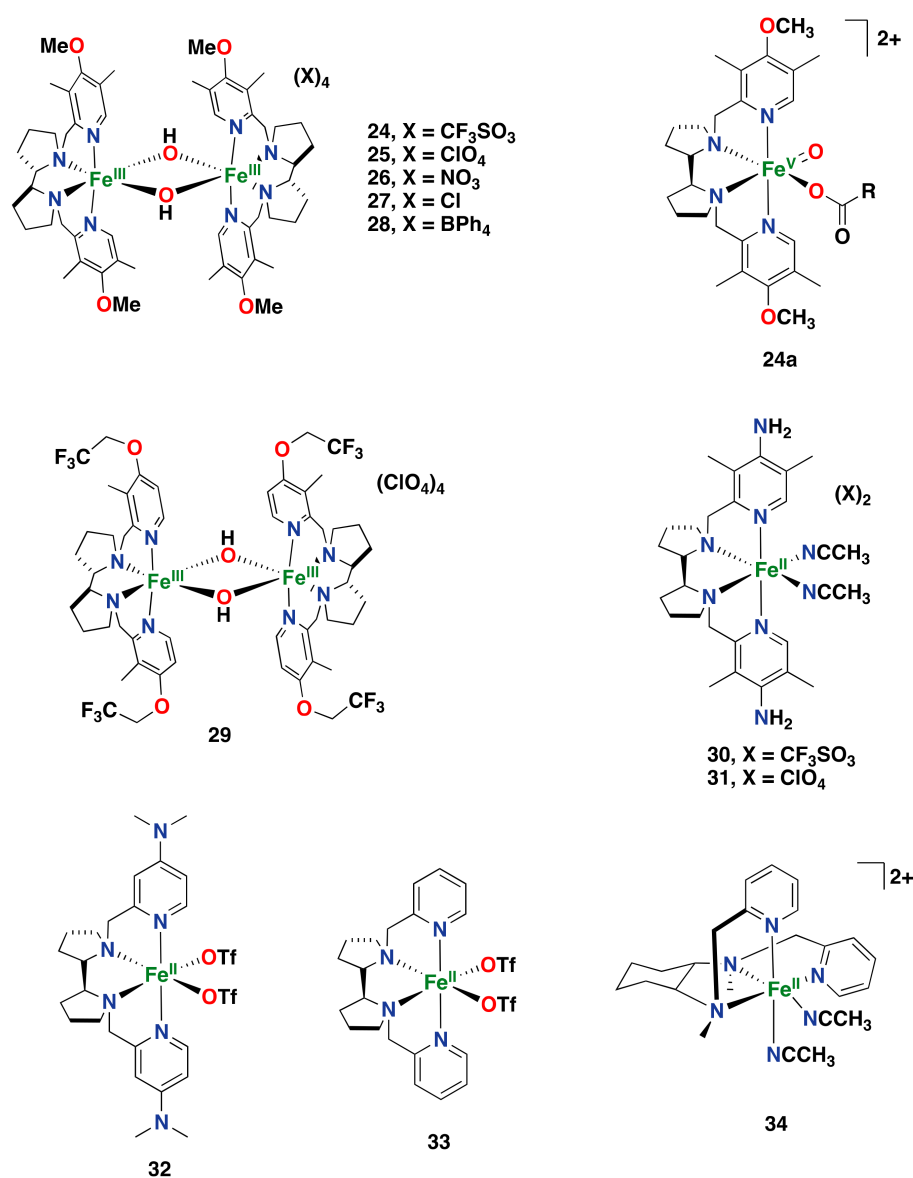
Figure 20. Structures of iron complexes supported by tetradentate aminopyridine ligands that catalyze aromatic oxidation using H_2O_2.

Complex **24** was also found to be effective in the oxidation of different aromatic substrates, such as benzene and mono- and dialkylbenzenes (Figure 21). With 0.62 mol% of catalyst loading, 4 equiv. aqueous H_2O_2, and 10 equiv. acetic acid, a total TON of 12.6 in benzene oxidation was achieved, forming hydroquinone (TON = 11.4) as the major, overoxidized product, next to phenol as a minor product (TON = 1.2). For the oxidation of toluene, cresols were obtained in only 1.9 turnovers as a mixture of *ortho*- and *para*-phenols, whereas the major products were the corresponding methylhydroquinone (TON = 8.2) and 4-(hydroxymethyl)phenol (TON = 4.9). Products derived exclusively from the oxidation of the alkyl side chain were also obtained. Oxidation of other alkylbenzene derivatives provided similar results, with the corresponding hydroquinones as the major product (Figure 21). Overall, overoxidized products and poor selectivities for the oxidation of the aromatic ring were obtained, resulting in mixtures of products in which oxidation has taken place on aromatic as well as aliphatic positions [221]. Regarding the active oxidant responsible for the arene hydroxylation reaction, the mechanism was proposed to proceed through the Fe(V)-oxo species **24a**, which is formed as a monomeric species upon the reaction of differic complex **24** with H_2O_2 and the carboxylic acid additive at low

temperatures [222,223,225]. This assignment was based on characteristic EPR parameters that were similar to those for previously reported non-heme Fe(V)-oxo species [226,227].
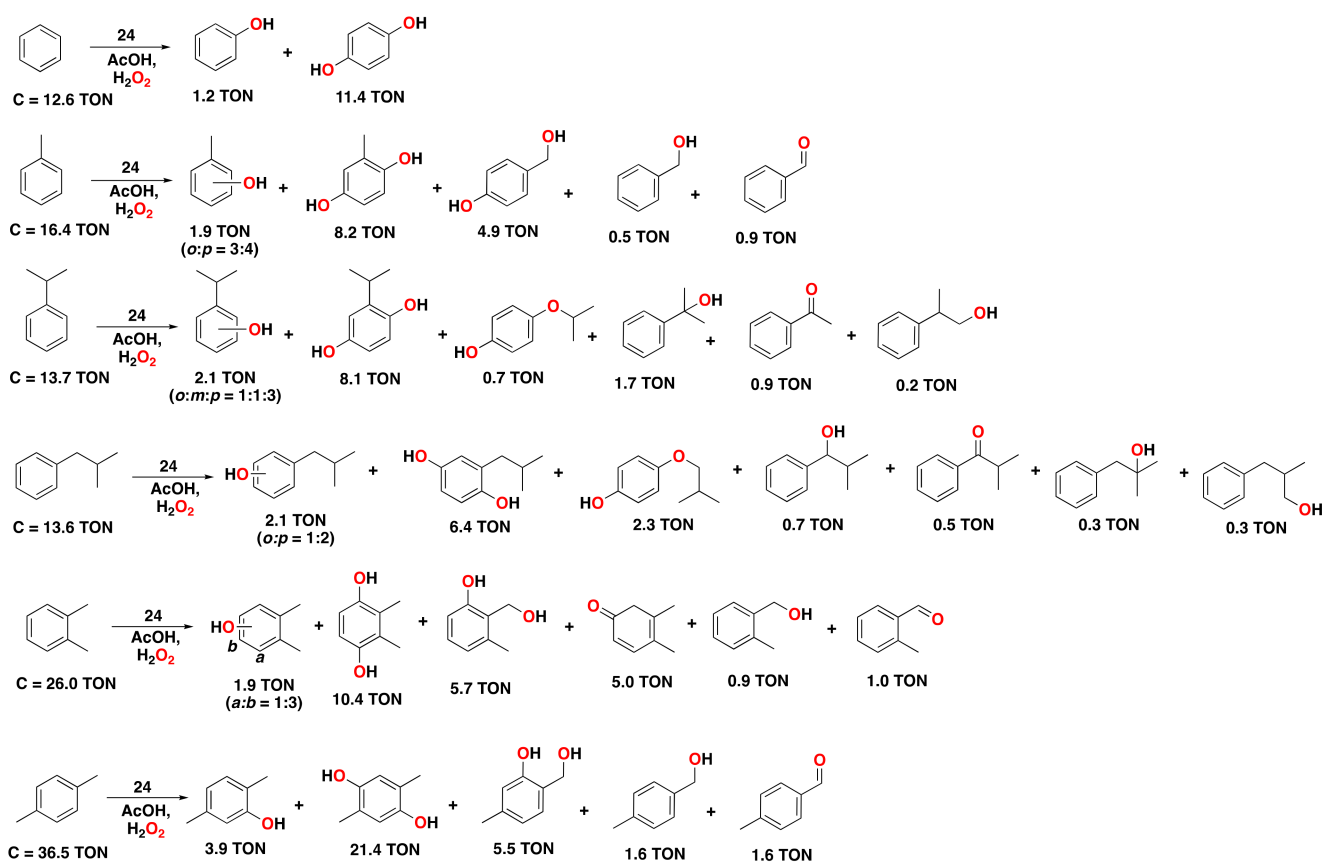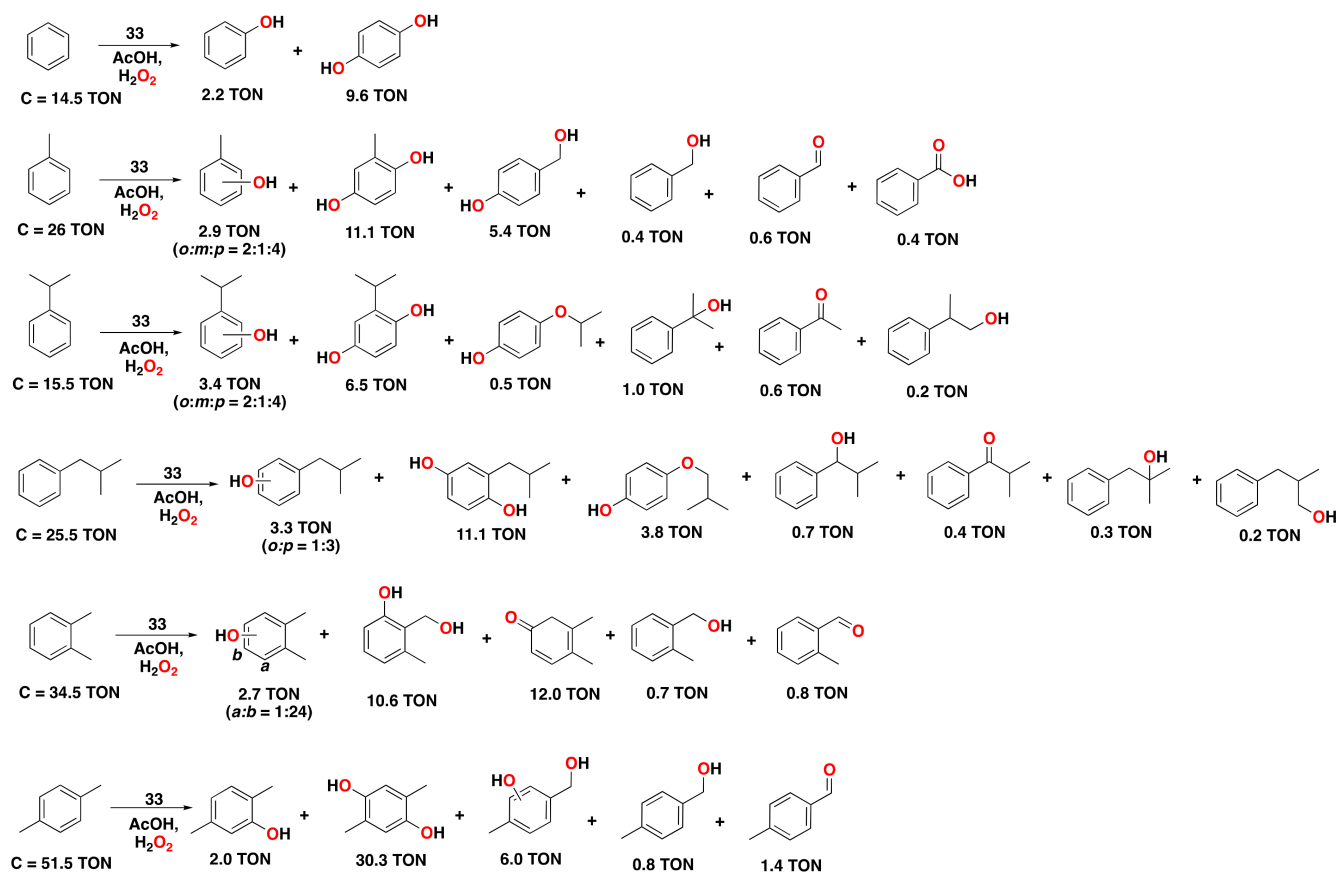

Figure 21. Reaction products of the catalytic oxidation of benzene and benzene derivatives catalyzed by diferric complex **24** as catalyst with H_2O_2 as an oxidant and AcOH as a carboxylic acid additive. Reaction conditions: complex **24** (0.62 mol% cat./1.24 μmol Fe), substrate (100 μmol), H_2O_2 (400 μmol), and AcOH (1000 μmol) in CH_3CN at 0 °C for 1.5 h. See the corresponding reference for further details on the oxidation of other alkylbenzene substrates [221].

Subsequently, Bryliakov and co-workers explored a series of related iron complexes **24–33** based on (substituted) bpbp ligands and containing different counter anions for the oxidation of alkylbenzenes [228]. Among the different counter anions tested, it was found that complex **24**, containing triflate ions, performed the best, with the highest efficiency and selectivity for the oxidation of *o*-xylene. Complex **25**, with perchlorate counter anions, showed a slightly lower catalytic activity, whereas complexes **26–28**, with other counter anions, performed less efficiently for arene oxidation. Importantly, all these iron complexes are active in aromatic oxidation but show low selectivities, as shown by the formation of considerable amounts of mixed aromatic/aliphatic double oxygenation products.

Among the series of iron complexes tested in this study, it was found that the mononuclear, non-substituted bpbp complex **33** (1.24 mol%) performed best for the oxidation of several aromatic substrates with H_2O_2 (4 equiv.), employing acetic acid (10 equiv.) as an additive (Figure 22) [228]. Complex **33** is capable of oxidizing benzene, providing hydroquinone as the major product (TON = 9.6), together with small amounts of phenol (TON = 2.2). For toluene oxidation, hydroquinone was again generated as the main product (TON = 11.1), together with small amounts of cresol products (TON = 2.9). Products in which oxidation has taken place at the benzylic position were also observed in considerable amounts. Oxidation of other alkylbenzene substrates, including mono and dialkylbenzenes, was also performed. Of interest is the oxidation of *p*-xylene, in which a high conversion (TON = 51.5) and yield for the hydroquinone product (TON = 30.3) were observed. Overall,

hydroquinone products were obtained as the main product, with small amounts of phenol products and benzylic oxidation products, in a similar way as observed for complex **24** (compare Figures 21 and 22).
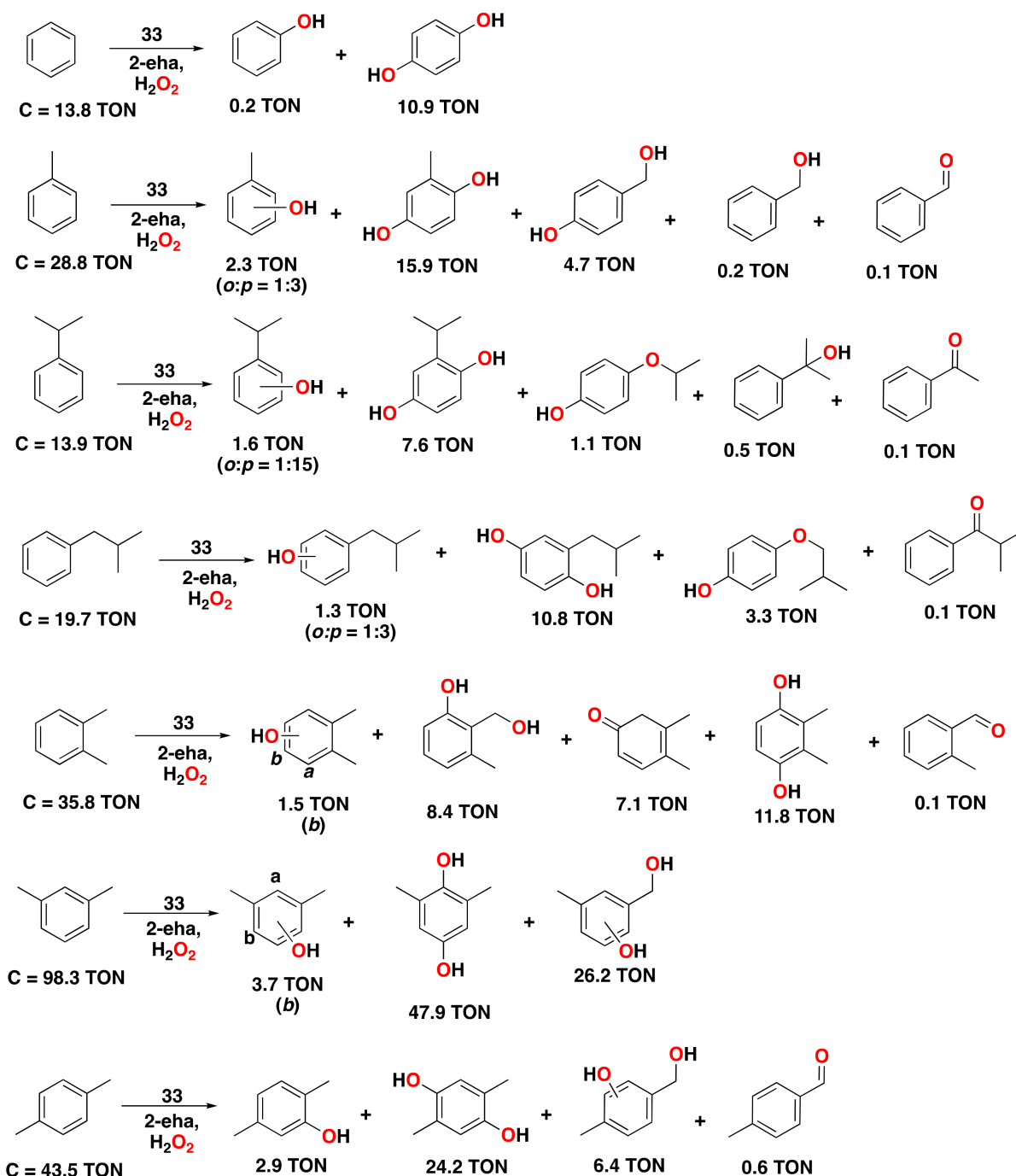

Figure 22. Reaction products of the catalytic oxidation of benzene and benzene derivatives catalyzed by complex **33** as catalyst with H_2O_2 as an oxidant and AcOH as a carboxylic acid additive. Reaction conditions: complex **33** (1.24 μmol Fe), substrate (100 μmol), H_2O_2 (400 μmol), and AcOH (1000 μmol) in CH_3CN at 0 °C for 1.5 h. See the corresponding reference for further details on the oxidation of other alkylbenzene substrates [228].

The authors also tested other mononuclear iron complexes based on the parent bpbp ligand and comprising differently substituted pyridine rings, but these were found to perform less efficiently compared to parent complex **33**. For instance, the use of mononuclear complexes **30** and **31**, containing an amino group at the pyridine ring instead of a methoxy group, did not improve the reactivity in the oxidation of *o*-xylene with respect to that of complexes **24** or **33**. A similar reactivity was also found when the diferric trifluoroethoxy iron complex **29** was employed, whereas complex **32**, bearing dimethylamino substituents, was less efficient. Finally, complex **8**, which contains the parent tripodal tpa ligand, was also tested in this same study, also showing poor catalytic activity.

An exploration of different carboxylic acid additives in the aromatic oxidation of *m*-xylene catalyzed by complex **33** revealed that 2-ethylhexanoic acid provided the best results among a series of different linear and branched carboxylic acids tested [229]. Using optimized conditions, i.e., complex **33** (1.24 mol%), with 2-ethylhexanoic acid additive (10 equiv.) and H_2O_2 (4 equiv.), the oxidation of a series of aromatic substrates was performed (Figure 23). Benzene was oxidized to hydroquinone (TON = 10.9), with small amounts of phenol product being formed (TON = 0.2). For the oxidation of toluene, the corresponding hydroquinone was formed in 15.9 turnovers, with small amounts of phenol products and products derived from oxidation at the aliphatic side chain. Catalytic

oxidation of a series of mono and dialkylbenzene substrates gave similar results to those obtained when acetic acid was employed. However, yields for the oxidized products were slightly higher when 2-ethylhexanoic acid was used (compare Figures 22 and 23). Interestingly, *m*-xylene was oxidized with a conversion of 98.3 turnovers under these conditions, providing the corresponding hydroquinone in up to 47.9 turnovers.

Figure 23. Reaction products of the catalytic oxidation of benzene and benzene derivatives catalyzed by complex **33** with H_2O_2 as an oxidant and 2-eha as a carboxylic acid additive. Reaction conditions: complex **33** (1.24 µmol Fe), substrate (100 µmol), H_2O_2 (400 µmol), and 2-eha (1000 µmol) in CH_3CN at 0 °C for 1.5 h. See the corresponding reference for further details on the oxidation of other alkylbenzene substrates [229]. 2-eha = 2-ethylhexanoic acid.

In an independent study, Que and co-workers tested the reactivity of iron complex **34** ([Fe(β-bpmcn)(CH$_3$CN)$_2$]$^{2+}$) in the oxidation of benzene (Figure 20), which was found to perform several catalytic turnovers to generate phenol in the presence of Sc(OTf)$_3$ or HClO$_4$ additives [230]. Generally, it has been established that iron complex **34** is a sluggish oxidation catalyst with H$_2$O$_2$ as the oxidant [166]. Nevertheless, it was found that by adding a strong Lewis acid such as Sc(OTf)$_3$ or a Brønsted acid such as HClO$_4$, a highly electrophilic oxidant is formed that is able to carry out four catalytic turnovers in the hydroxylation of benzene to phenol at -40 °C. The authors have proposed that an interaction between Sc^{3+} and the iron-oxo oxidant or its iron-hydroperoxo precursor occurs, in a similar way as has been proposed in other studies for related iron complexes [231–235]. In another study, Que and co-workers showed that activation of the non-heme iron-hydroperoxo species generated with the **34**/H$_2$O$_2$ system can also be accomplished using Fe^{III}(OTf)$_3$ as a Lewis acid, leading to the formation of the iron(V)-oxo oxidant [236]. This system was found to be slightly more active in the hydroxylation of benzene to phenol, affording up to 5.4 turnovers. This finding is of interest since it provided insight into the role of a second iron center, which can be related to the activity of diiron active sites found in metalloenzymes, such as in sMMOs.

Finally, in 2021, Han and co-workers reported on an iron complex supported by the *L*-cystine-derived BCPOM ligand and its activity in the arene hydroxylation reaction with H$_2$O$_2$ as an oxidant (Figure 24) [237]. The selectivity of this system is excellent, with good yields and compatibility with a broad range of substrates. For instance, for the oxidation of protected anilines, oxidation takes place at the *para*-position with respect to the amide substituent, with up to 68% isolated product yield. Oxidation of arenes containing methyl, dimethyl, or isopropyl substituents was also tested and afforded the phenol products in up to 70% isolated yield. The BCPOM-based system is also active in the oxidation of strongly electron-deficient arene substrates, including aryl ketones and aldehydes. Of note, the system makes use of 10 mol% of FeCl$_2$ as the metal salt precursor and 20 mol% of ligand.
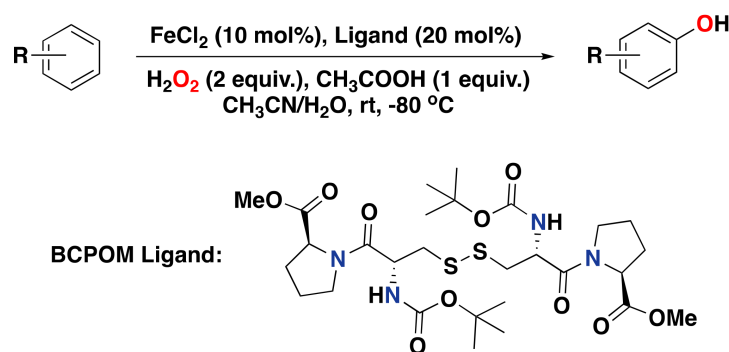
Figure 24. Arene oxidation reaction catalyzed by FeCl$_2$, the L-cystine-derived BCPOM ligand, and H$_2$O$_2$ as an oxidant.

3. Copper in Biological and Synthetic Systems

3.1. Copper-Containing Metalloenzymes

Copper-containing enzymes also play an important role in biological oxidation chemistry and, accordingly, are a big source of inspiration in the area of homogeneous oxidation catalysis [22,25,27]. Copper enzymes can be classified by the number of copper centers in their active site: either one copper center (mononuclear) [238] or two or more copper centers (di- or polynuclear) [27,239]. Examples that stand out among this class of copper-containing metalloenzymes are galactose oxidase (i.e., radical copper oxidases that use copper(II)-tyrosyl radical intermediates), amine oxidase, dopamine β-monooxygenase and peptidylglycine α-hydroxylating monooxygenase (i.e., enzymes that involve monocopper-oxygen species as intermediates during catalysis), and tyrosinase and catechol oxidases (i.e., enzymes that contain dicopper(I) active sites).

Tyrosinase and Catechol Oxidases

In this section, we briefly discuss copper-containing metalloenzymes capable of performing the oxidation of aromatic substrates. Tyrosinase and catechol oxidases are well-known copper-containing metalloenzymes that catalyze the two-electron oxidation of catechols to *o*-quinones [240]. The difference is that tyrosinase oxidases can also perform the *o*-hydroxylation of phenols to catechols, along with the further oxidation to *o*-quinones [241,242]. This reactivity is important in melanin biosynthesis.

The active site of tyrosinase comprises a dinuclear copper(I) center in which each metal center is coordinated to three histidine residues (catechol oxidases and haemocyanin share a similar active site) [243]. Reaction with O_2 forms a (peroxo)dicopper(II) species in which oxygen is bound in a side-on bridging (μ-η^2:η^2) binding mode [244]. The overall catalytic cycle for phenol oxidation by tyrosinase (phenolase cycle) to generate a quinone product is depicted in Figure 25 [14,106,239,241,242]. The *deoxy* species can bind O_2 to form the *oxy* intermediate, as stated above. Then, the phenol substrate (in its phenolate form) coordinates to the *oxy* intermediate at only one of the copper centers and *ortho*-hydroxylation occurs to generate an *o*-catecholate dianion that binds in single-bridging mode to both copper centers and in a bidentate fashion to only one of the copper centers. Subsequently, two-electron oxidation yields the final *o*-quinone, thereby restoring the *deoxy* species. An additional catalytic cycle involves the oxidation of external catechol substrates to form *o*-quinones (diphenolase activity; not shown).
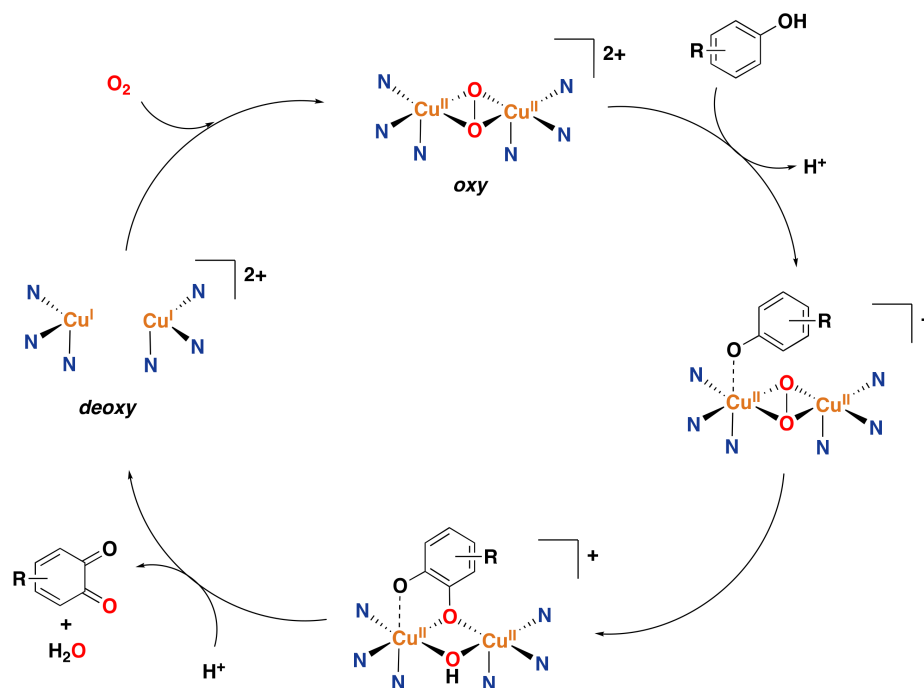
Figure 25. Oxidation of monophenols to o-quinones catalyzed by tyrosinase oxidase [14,106,241,242,245].

3.2. Synthetic Copper Systems

Inspired by copper-containing metalloenzymes, chemists have tried to copy their interesting activity and selectivity by mimicking their active sites. Accordingly, various studies have reported on the synthesis of bioinspired model complexes for these copper-containing metalloenzymes. In general, the ligands used in these models contain nitrogen atom donors to reproduce the histidine environment around the catalytic active site of the metalloenzyme. Within this context, these studies have mainly employed pyridines, secondary and tertiary amines, and benzimidazole donor groups.

Within this field, Karlin and co-workers have published numerous examples of copper complexes capable of performing oxidation processes related to the reactions catalyzed by tyrosinase oxidase [246–254]. Generally, the ligands used in their studies contain

a *meta*-xylyl linker, which allows for the proper orientation of the two copper centers to react with external reagents cooperatively. Earlier examples are based on dinuclear copper(I) complexes of the general structure presented in Figure 26 for complex **35**, bearing two aminopyridine moieties bridged by a *m*-xylyl linker, which react with O_2 to form an intermediate species **36** that contains a side-on (μ-η^2:η^2) coordinated peroxo ligand. Intermediate **36** is responsible for the intramolecular hydroxylation of the aromatic ring in the *m*-xylyl linker of the ligand to afford compound **37** [246–248,252].
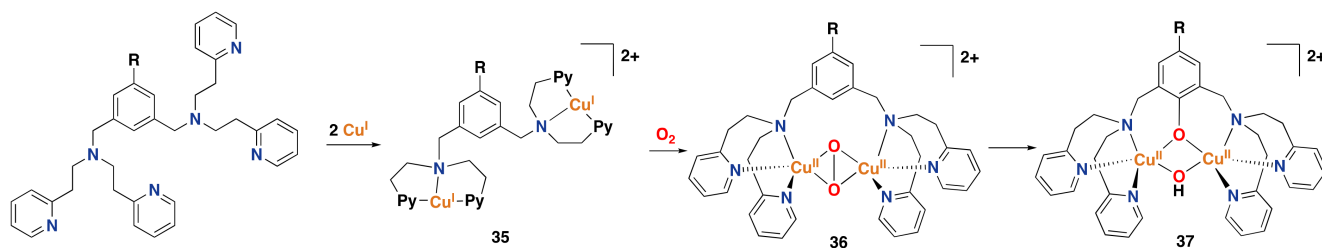
Figure 26. Representative synthetic copper complex **35** inspired by tyrosinase oxidase, reported by Karlin et al. [246–248]. Upon complexation of copper with the dinucleating aminopyridine ligand, reaction with dioxygen leads to a side-on (μ-η^2 : η^2) peroxo copper intermediate that can perform an intramolecular aromatic hydroxylation. Py = pyridine; R = H, MeO, tBu, F, CN, NO_2.

Other dicopper model complexes have also been found to react with dioxygen, to subsequently display arene hydroxylation reactivity (Figure 27). For instance, a dicopper complex supported by triazacyclononan-based ligands bridged by *m*-xylyl groups reacts with dioxygen at -80 °C to form species **38** with a (μ-η^2:η^2) peroxo moiety that could be spectroscopically traced using UV–Vis and resonance Raman. Such species are subsequently able to hydroxylate the bridging arene group of the ligand [255]. A dicopper complex supported by the 1,3-bis{[3-(*N*,*N*-dimethyl)propyl]iminomethyl}benzene ligand also reacts with dioxygen to afford a Cu_2O_2 species that performs arene hydroxylation of the ligand to afford compound **39**, which was isolated and characterized by X-ray crystallography [256]. Similarly, a dicopper complex ligated to a dinucleating hexaaza macrocycle is capable of performing intramolecular arene hydroxylation of the ligand to yield compound **40** [257]. Casella and co-workers reported a synthetic dicopper complex derived from the ligand L-66 (L-66 = α,α'-bis{bis[2-(1'-methyl-2'-benzimidazolyl)ethyl]amino}-*m*-xylene), which for the first time performed the intermolecular hydroxylation of phenols, therefore displaying similar reactivity as found for tyrosinase oxidase [258]. The reaction of the dicopper(I) complex with dioxygen was shown by low-temperature UV–Vis and resonance Raman to generate intermediate **41** with a highly reminiscent structure to that of prototypical intermediate **36**. Species **41** can hydroxylate external phenol substrates, such as the *o*-hydroxylation of 4-carbomethoxyphenolate to the catecholate product (about 40% yield concerning intermediate **41**) and the oxidation of 3,5-di-*tert*-butyl-catechol to the corresponding quinone (the formation of the product was demonstrated by low temperature UV–Vis) [258]. Later, related benzimidazole-based copper-oxygen intermediates, such as **42**, were also found to react with external phenols to form quinones at different temperatures [259].
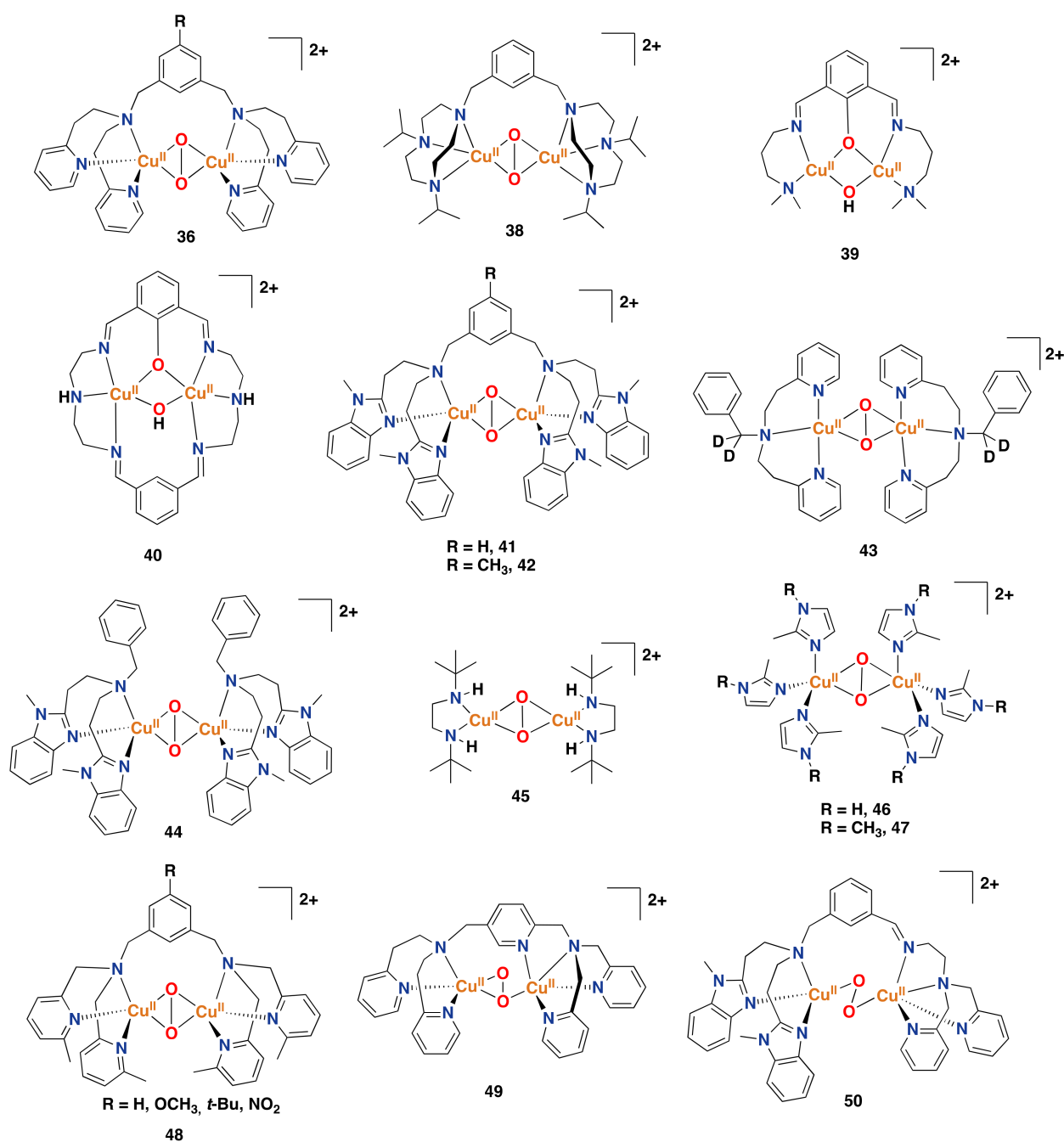
Figure 27. Selected examples of dicopper(II) dioxygen complexes (supported by mono- and dinucleating ligands as well as non-symmetrical dinucleating ligands) that mimic the activity of tyrosinase [255–266].

Mononuclear copper complexes have also been used to generate Cu_2O_2 intermediates that can mimic the activity of tyrosinase [260,261]. For instance, Itoh and co-workers reported the synthesis of a side-on (μ-η^2:η^2) peroxo complex **43**, supported by the *N,N*-bis[2-(2-pyridyl)-ethyl]-α,α-dideuteriobenzylamine ligand. This complex can perform the intermolecular hydroxylation of lithium salts of phenols (*p*-X-C_6H_4-OLi; X = Cl, Me and CO_2Me) to generate the corresponding catechols with up to 90% isolated yield in a stoichiometric reaction [260]. Another mononuclear copper complex supported by *N,N*-bis(2-(*N*-methylbenzimidazol-2-yl)ethyl)benzylamine has also been found to react with dioxygen to generate a binuclear (μ-η^2:η^2) peroxo complex **44** that can perform the *o*-hydroxylation of externally added phenols [261]. Next, (μ-η^2:η^2) peroxo dicopper complexes supported by bidentate ligands have also been reported. For instance, complex **45** (supported by a

bidentate secondary diamine ligand) was synthesized from the reaction of its corresponding mononuclear copper(I) complex with dioxygen, and its reactivity with phenolates to yield catechols and quinone products was described [267,268]. The mechanism through which complex **45** reacts with phenolate substrates in the presence of dioxygen has been shown to involve the formation of a bis(μ-oxo)dicopper(III) intermediate before the aromatic hydroxylation step (see Figure 28b) [269]. (μ-η^2:η^2) Peroxo dicopper(II) complexes **46** and **47** supported by monodentate imidazole ligands have also been reported, and their reactivity has been explored towards the hydroxylation of exogenous phenolic substrates to afford catechols in good stoichiometric yields at −125 °C, representing more recent examples of bioinspired copper complexes based on the active site of the tyrosinase enzyme [262]. Along the same line, mononuclear copper complexes supported by imine-based ligands containing pyrazole groups have been reported, and their reaction with dioxygen has been proposed to generate a side-on (μ-η^2:η^2) bound dicopper species that can react with 2,4-di-*tert*-butyl-phenolate (DTBP-H) to generate 3,5-di-*tert*-butyl-*o*-quinone (DTBQ) [270]. Suzuki and co-workers have reported on the side-on (μ-η^2:η^2)-peroxo dicopper(II) complex **48** supported by H-L-H-type ligands (H-L-H = 1,3-bis-[bis(6-methyl-2-pyridylmethyl)aminomethyl]benzene). This species is very similar to species **36** previously reported by Karlin and co-workers and not only performs the aromatic ligand hydroxylation of the *m*-xylyl linker but also the intermolecular epoxidation of styrene and the hydroxylation of THF [266].

Unsymmetrical dinucleating ligands have also been employed in the field of synthetic copper-oxygen chemistry. For instance, Itoh and co-workers reported on a dicopper complex supported by an asymmetric pentapyridine dinucleating ligand [264]. Upon reaction with dioxygen, they postulated that dicopper(II) species **49** with an unprecedented (μ-η^1:η^2) binding mode is formed by comparison of its UV–Vis spectra and resonance Raman features with those of well-characterized (μ-η^1:η^1)-peroxo dicopper(II) and (μ-η^2:η^2)-peroxo dicopper(II) complexes. Later, Costas and co-workers reported on a non-symmetrical dicopper(I) complex supported by a non-symmetric dinucleating ligand, which upon reaction with dioxygen generates (μ-η^1:η^1) peroxo dicopper(II) complex **50** [265]. The reactivity of this species was studied using experimental and computational methods, and it was found to perform the *ortho* hydroxylation of externally added sodium *p*-chlorophenolate to form *p*-chlorocatechol in 39% yield with respect to **50**.

Generally, a side-on (μ-η^2:η^2) coordination mode of the O$_2$-ligand in these kinds of Cu:O$_2$ complexes has been proposed to be responsible for the hydroxylation reaction. However, an equilibrium has been demonstrated to exist between the side-on (μ-η^2:η^2) peroxo dicopper species and a bis(*μ*-oxo)dicopper(III) species, in which the latter can be formed upon cleavage of the O–O bond [271–274]. Accordingly, the capability of bis(*μ*-oxo)dicopper(III) species to perform aromatic hydroxylation reactions was scrutinized, and indeed, in some cases, this reactivity has been demonstrated [242,257,263,269,271,272,275,276]. For example, Tolman and co-workers made use of a mononuclear copper(I) complex containing a bidentate pyridine/amine ligand with a pendant phenyl group, which, upon reaction with dioxygen, formed bis(*μ*-oxo) dicopper(III) species **51** that can perform the intramolecular aromatic hydroxylation of a phenyl group (Figure 28a) [276]. Stack and co-workers have studied the reactivity of (μ-η^2:η^2)-peroxo dicopper(II) complex **45** towards phenols, and they could demonstrate that upon addition of the substrate at −120 °C a bis(*μ*-oxo)dicopper(III)-phenolate complex **52** formed prior to the hydroxylation step (Figure 28b) [269]. This intermediate was characterized by UV–Vis, resonance Raman, and Cu K-edge X-ray absorption spectroscopy. Later, Costas and co-workers reported a dicopper(I) complex containing a tertiary N-methylated hexaaza ligand with a bridging *m*-xylyl linker, which generates the bis(*μ*-oxo)dicopper(III) species **53** upon reaction with dioxygen at −90 °C (Figure 28c). Intermediate **53** can bind and hydroxylate phenolates, and indeed, the authors were able to trap and spectroscopically characterize the species that results from the reaction of sodium *p*-chlorophenolate with species **53** and that precedes phenolate hydroxylation. The 4-chlorocatechol product was formed in a 67% yield with respect to the initial dicopper(I)

complex [263]. Stack and co-workers reported another bis(μ-oxo)dicopper(III) species (**54**) supported by a permethylated-amine-guanidine ligand based on the 1,3-propanediamine backbone that can perform the *ortho*-hydroxylation of phenolates to afford catechol products (Figure 28d) [277].
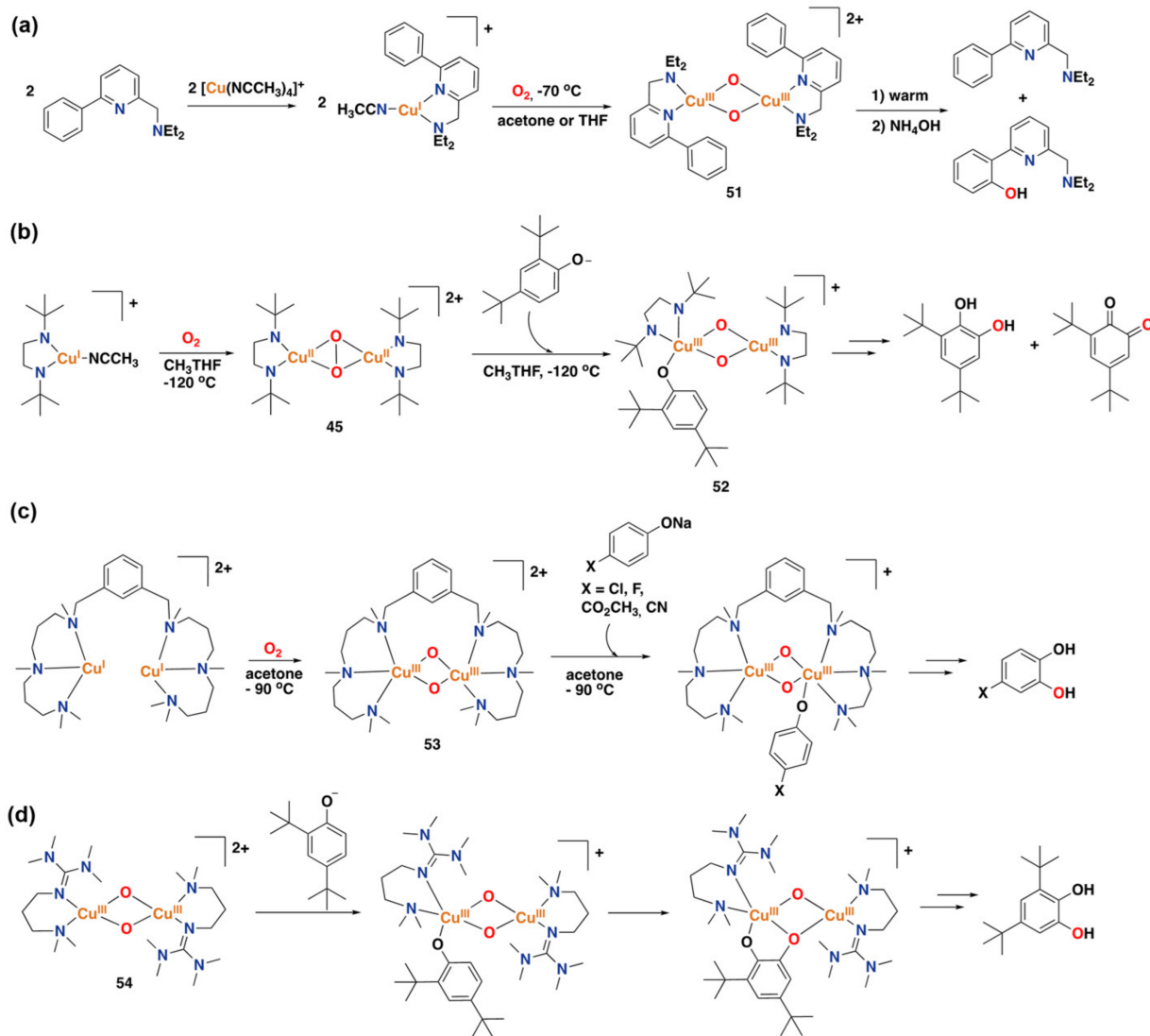
Figure 28. (**a**) Synthesis of a copper(I) complex that performs the hydroxylation of an arene of the ligand upon reaction with dioxygen through the bis(μ-oxo)dicopper(III) intermediate **51** [276]. (**b**) Mechanism of phenolate oxidation by a mononuclear copper(I) complex, involving the formation of intermediates **45** and **52** [269]. (**c**) Mechanism of phenolate oxidation by a dinuclear copper(I) complex, involving a bis(μ-oxo)dicopper(III) intermediate **53** [263]. (**d**) The reaction of bis(μ-oxo)dicopper(III) complex **54** with phenolates to afford catechol products [277].

Mononuclear oxygenated copper complexes, such as end-on bound superoxo copper(II) species or copper(II)-alkylperoxide complexes, have also been shown to perform aromatic oxidation reactivity (Figure 29a,b) [278]. For instance, copper(II) complexes **55** supported by tridentate bis[(pyridin-2-yl)methyl]benzylamine ligands containing *m*-substituted phenyl substituents at the 6th position of each pyridine group were reported to react with H_2O_2 in acetone to form 2-hydroxy-2-hydroperoxypropane species **56**. The latter intermediate undergoes an aromatic ligand hydroxylation reaction to afford copper(II)-phenolate complex **57** (Figure 29a) [279]. This reaction pathway has been studied using spectroscopic and kinetic analysis, and an electrophilic aromatic substitution mechanism

has been proposed [280]. A carbonyl copper complex, supported by an electron-rich tripodal tetradentate aminopyridine ligand based on the tpa scaffold, was reported to react with dioxygen to generate end-on bound superoxo copper(II) compound **58**. The reactivity of the latter complex was tested for the oxidation of phenol substrates, leading to the decomposition of complex **58** to generate a phenoxyl radical in 40% yield, together with the generation of 1,4-benzoquinone (24% yield) and arylhydroperoxide (Figure 29c) [250]. Thus, the reactivity of complex **58** was not exclusively toward aromatic oxidation. Another study reported on the reactivity of a similar end-on superoxo copper(II) complex (**59**), supported by the TMG$_3$tren ligand (TMG$_3$tren = tris(2-(N-tetramethylguanidyl)ethyl)amine), towards external phenol substrates (Figure 29d) [251]. Complex **59** could be characterized using X-ray crystallography, providing structural evidence for the existence of an end-on superoxo copper(II) species [281]. Reaction with phenol substrates showed products in which aromatic oxidation had occurred, in a similar way as the reactivity previously found for complex **58**. Upon reaction of complex **59** with 4-MeO-2,6-tBu$_2$-phenol, 1,4-benzoquinone was formed in a 22% yield, together with the stabilized phenoxyl radical (37% yield) and the arylhydroperoxide product. Interestingly, for the generation of the 1,4-benzoquinone product, the displacement of a methoxy group has taken place. Reaction with 2,6-tBu$_2$-phenol and 2,4,6-tBu$_3$-phenol leads to the formation of the benzoquinone product in 33% and 35% yield, respectively. Finally, reaction with 3,5-tBu$_2$-catechol leads to the corresponding benzoquinone product in a 20% yield (Figure 29d). From all reactions of complex **59** with phenols, a hydroxylated copper(II) alkoxide complex in which a methyl group on the ligand has been hydroxylated was detected [251]. Later on, a new end-on bound superoxo copper(II) complex (**60**) supported by another electron-rich aminopyridine ligand containing dimethylmethoxy substituents on each pyridine ring was reported, and its reactivity towards *para*-substituted 2,6-di-*tert*-butyl-phenols was shown to afford 2,6-di-*tert*-butyl-1,4-benxoquinone in up to 50% yield [253]. Much more recently, copper(II)-superoxo species **61**, in which the metal center is coordinated to two pyridyl groups, one tertiary amine, and one thioether donor, was also described to perform the oxidation of 2,6-di-*tert*-butyl-4-methoxyphenol to 2,6-di-*tert*-butyl-1,4-benzoquinone [254].

All the examples reported until that point were based on stoichiometric reactions. However, in recent years, examples of catalytic copper systems have been developed, and their catalytic activity has been demonstrated toward the oxidation of aromatic substrates [282–286]. Generally, chemists have tried to develop systems that generate metal-based oxidants to perform aromatic hydroxylation reactions, whereas systems that generate hydroxyl radicals through Fenton-type processes were aimed to be avoided because of their non-selective oxidation chemistry (see above). However, some examples have shown that hydroperoxyl radicals generated through Fenton-type processes can perform the aromatic oxidation of benzene to phenol with high activities and selectivities. For instance, Karlin, Fukuzumi, and co-workers reported on a system based on a mononuclear copper complex supported by the tpa ligand, which reacts with H$_2$O$_2$ to generate hydroperoxyl radicals and performs the oxidation of benzene to phenol [287]. Particularly, they demonstrated that by incorporating the copper complex into mesoporous silica-alumina (Al-MCM-41), they could enhance the activity of the system, reaching up to 4320 turnovers for phenol formation [288].

A study reported by Pérez and co-workers showed that catalytic amounts of copper complexes supported by trispyrazolylborate type ligands can perform the direct oxidation of aromatic C–H bonds with H$_2$O$_2$ under acid-free conditions (Figure 30, complex **62** for general structure) [282]. Particularly, they tested the system for the oxidation of benzene to phenol (and 1,4-benzoquinone as an overoxidized product), showing conversions within the range of 14–30% and selectivities towards phenol of 67–85%. In addition, the oxidation of anthracene to 9,10-anthraquinone (98% isolated yield) and 2-ethylanthracene to 2-ethyl-9,10-anthraquinone (98% isolated yield) occurred successfully. In a follow-up study, the same authors reported on a mechanistic investigation, combining experimental and DFT studies, in which they demonstrated that these copper systems perform aromatic hydroxylation

through a copper-oxyl species [283]. Moreover, they proposed that hydroxylation occurs through two competing pathways either via an electrophilic aromatic substitution pathway in which the copper-oxyl species acts as the electrophile, or via a rebound mechanism in which the hydrogen on the substrate is abstracted by the copper-oxyl species before C–O bond formation [283].
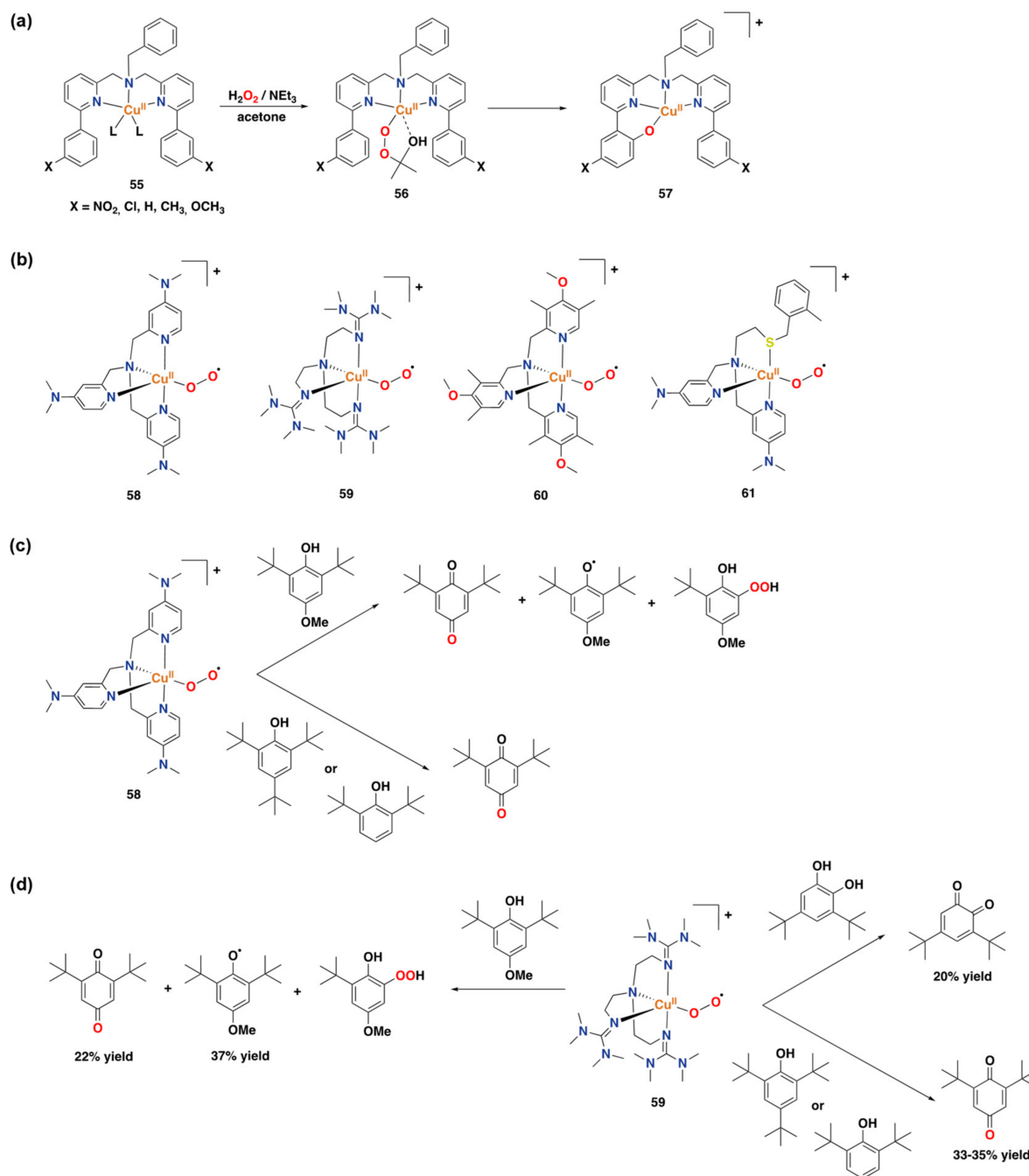

Figure 29. (**a**) Aromatic hydroxylation reactivity of a mononuclear copper(II)-alkylperoxo complex [279,280]. (**b**) Selected end-on bound superoxo copper(II) complexes [250,251,253,254]. (**c**) Reactivity of complex **58** towards phenol substrates [250]. (**d**) Reactivity of complex **59** towards phenol substrates [251].
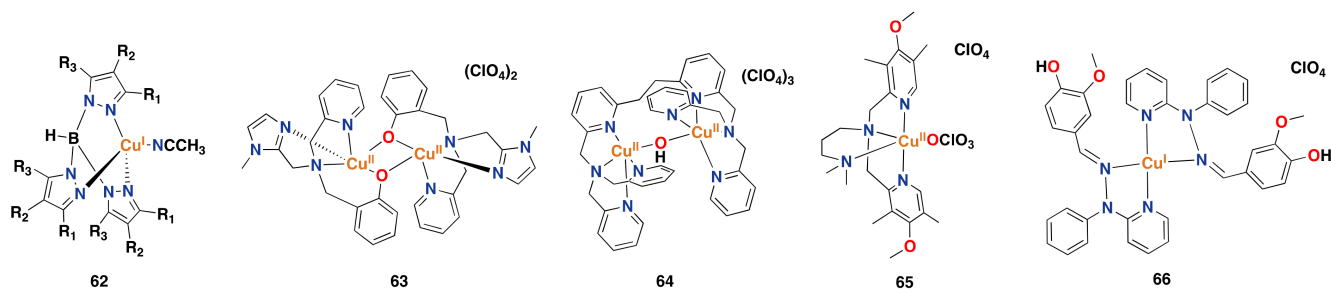
Figure 30. Synthetic copper complexes display catalytic activity for the hydroxylation of aromatic substrates through a metal-based mechanism [282,284–286,288].

Liu and co-workers reported a catalyst based on dicopper(II) complex **63**, supported by two 2-(((((1-methyl-1H-imidazol-2-yl)methyl)(pyridin-2-ylmethyl)amino)methyl)phenol ligands (Figure 30), that can perform the direct hydroxylation of benzene to phenol using H_2O_2 as an oxidant, with up to 11.9% phenol yield and 79.3 turnovers [284]. Later on, Kodera and co-workers developed the dicopper(II) complex **64** based on the bis(tpa) ligand (6-hpa). This complex was reported to catalyze the selective hydroxylation of benzene to phenol using H_2O_2, reaching a turnover number higher than 12,000 after 40 h for phenol formation in CH_3CN at 50 °C and with a turnover frequency [mol phenol·(mol catalyst)$^{-1}$·h^{-1}] of 1010 [285]. Noteworthy, these are the highest values reported until now for benzene hydroxylation with H_2O_2 catalyzed by a homogeneous catalyst.

Concerning the mechanism for H_2O_2 activation and benzene hydroxylation, the authors proposed that upon the addition of 1 equiv. of H_2O_2 in the presence of Et_3N at −40 °C, an end-on *trans*-peroxodicopper(II) (Cu_2O_2) complex is formed (Figure 31). Then, in the presence of excess amounts of H_2O_2, Cu_2O_2 decomposes to form the hydroperoxocopper(II) complex ($CuO_2H)_2$. This latter complex is proposed to release H_2O reversibly with the assistance of H_2O to give a copper-bound oxyl and peroxyl radical, which is stabilized by hydrogen-bonding interactions with H_2O. Then, the copper-oxyl radical is proposed to react with benzene in the rate-limiting step through an electrophilic aromatic oxidation mechanism to form phenol [285].
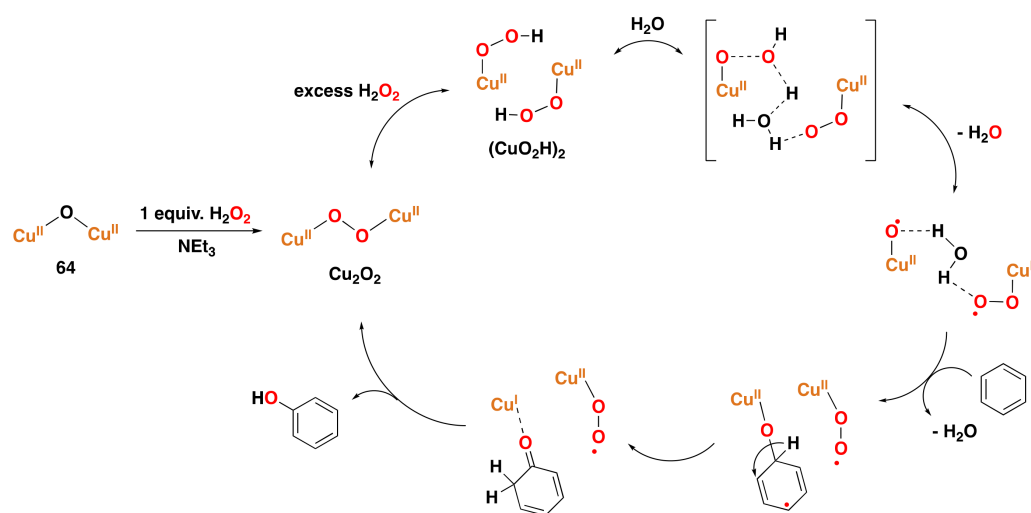
Figure 31. Proposed mechanism for the activation of H_2O_2 and hydroxylation of benzene to phenol catalyzed by complex **64** supported by the 6-hpa ligand [285].

Recently, Mayilmurugan and co-workers have described a set of copper(II) complexes based on tripodal tetradentate aminopyridine ligands and have reported that complex **65**, containing an electron-rich pyridine, is the best for the aromatic hydroxylation of benzene with H_2O_2, affording phenol in 37% yield and with 98% selectivity [286]. The

authors proposed that oxidation of benzene occurs, most likely, through the generation of a copper(II) hydroperoxo intermediate (Figure 32), and evidence for such species has been obtained using vibrational and electronic spectra, as well as ESI mass spectrometry.
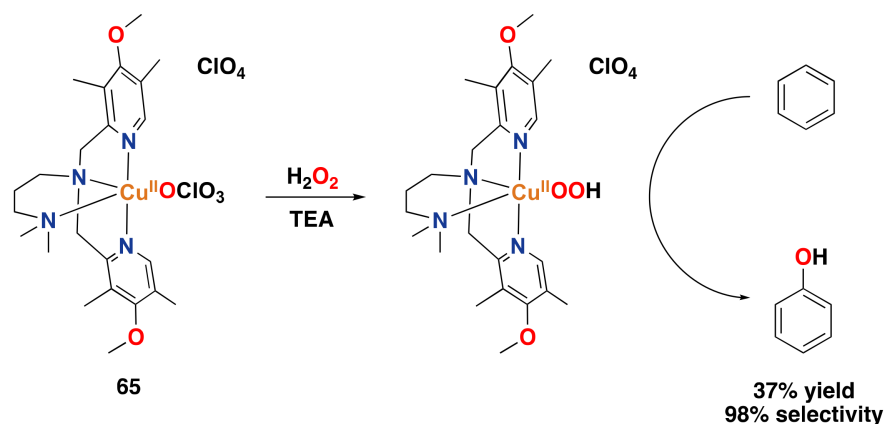
Figure 32. Proposed mechanism for benzene hydroxylation catalyzed by complex **61** through a copper(II) hydroperoxo species [286]. TEA = triethylamine.

Mayilmurugan, Ghosh, and co-workers also reported on catalyst **66**, in which copper(I) is supported by bidentate nitrogen ligands (Figure 30), which can perform the direct hydroxylation of benzene to phenol in 29% yield with the benzoquinone by-product being generated in <1% yield [288]. The authors also reported on the effectiveness of using this catalyst for the oxidation of toluene, which afforded *p*-cresol and *o*-cresol in 37% yield and benzaldehyde in 21% yield, showing 42% selectivity for aromatic oxidation.

4. Nickel in Biological and Synthetic Systems

4.1. Nickel-Containing Metalloenzymes

Despite being less studied in the literature compared to iron and copper-containing metalloenzymes, several nickel enzymes are known to be involved in several different oxidation processes. Examples include glyoxalase I, quercetin 2,4-dioxygenase, acireductone dioxygenase, urease, superoxide dismutase, [NiFe]-hydrogenase, carbon monoxide dehydrogenase, acetyl-coenzyme A synthase/decarbonylase, methyl-coenzyme M reductase, and lactate racemase [289]. Among these nickel-based metalloenzymes, none of them is capable of performing arene hydroxylation, in contrast to what is known for iron- or copper-based Rieske oxygenases, pterin-dependent oxygenases, tyrosinase oxidases, and others. Despite this fact, several synthetic nickel-oxygen species have been identified and reported to be capable of performing aromatic and alkane oxidation as well as epoxidation reactions [290]. Because of that, chemists have also studied biological oxidation reactions proceeding in nickel-containing metalloenzymes, with a special interest in the (putative) reactive nickel–superoxo, nickel–peroxo, and nickel–oxo intermediates involved in these enzymatic oxidations. As an example, we briefly discuss nickel superoxide dismutases in this section in terms of their catalytic active site, their mechanism of action, and the nickel-oxygen intermediates involved.

Nickel Superoxide Dismutase

Superoxide dismutases (SOD) are a class of metalloenzymes that protect cells from the toxic products of aerobic metabolism. These nickel-containing metalloenzymes regulate the formation of superoxide by converting it into hydrogen peroxide and molecular oxygen (Figure 33) [31]. It was in 1996 that this class of NiSOD was found in Streptomyces and cyanobacteria [30].
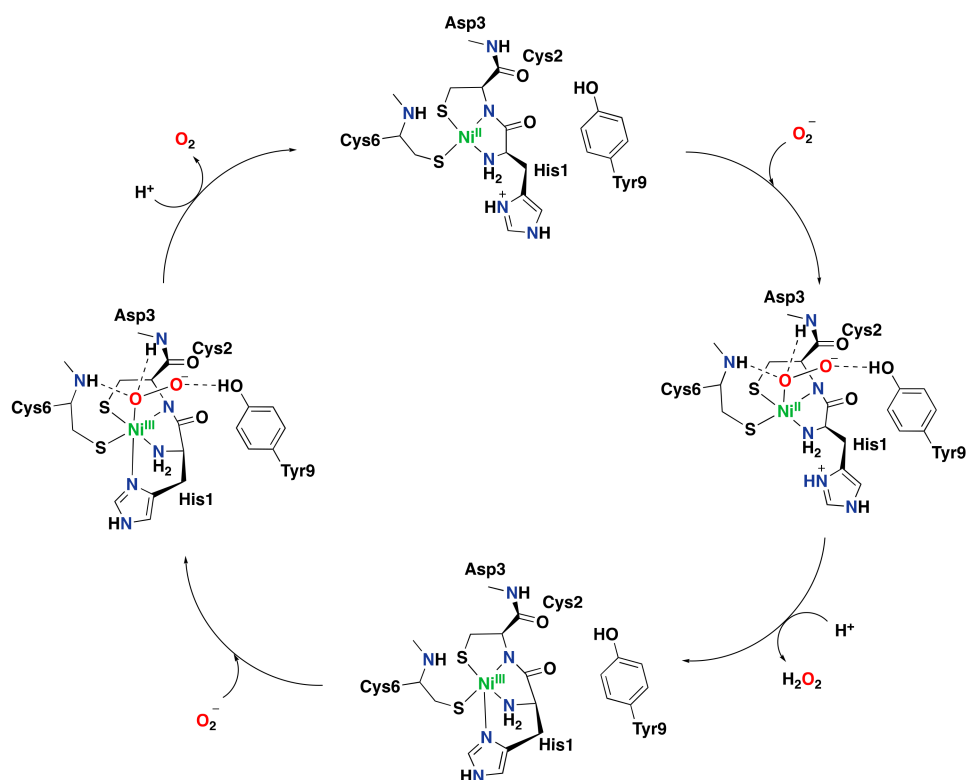
**Figure 33.** Catalytic cycle of nickel superoxide dismutase (NiSOD) [31].

4.2. Synthetic Aromatic Oxidation Systems Based on Nickel

An early study reported by Kimura and co-workers in 1984 described a nickel(II) compound supported by a macrocyclic polyamine that can activate dioxygen and oxidize aromatic substrates to generate hydroxylated products [291]. This study represents an early example of nickel-based systems that model biological monooxygenases in the selective hydroxylation of aromatic substrates.

More recently, Suzuki and co-workers reported on the development of bis(µ-oxo) dinickel(III) complexes supported by H-L-H-type ligands (H-L-H = 1,3-bis-[bis(6-methyl-2-pyridylmethyl)aminomethyl]benzene), in which different substituents were introduced onto the xylyl linker of the ligand [292]. This study was a follow-up on the exploration of copper complexes based on the same type of ligands performed by the same authors (Figure 27, complex **48** for general structure) [266]. Whereas the nickel complexes reacted with H_2O_2 to generate a bis(µ-oxo)dinickel(III) species, the copper counterparts reacted with dioxygen to form a (µ-η^2:η^2)-peroxo dicopper(II) complex. Both species have been demonstrated to undergo arene hydroxylation of the xylyl linker [266,292].

As a follow-up to the study on copper(II) complexes containing tridentate bis[(pyridin-2-yl)methyl]benzylamine ligands carrying *m*-substituted 6-phenyl rings on each pyridine group, in which intramolecular aromatic ligand hydroxylation occurred (see Figure 29a), Itoh and co-workers extended their investigation to the corresponding nickel complexes [293]. In this particular study, the authors synthesized and characterized a series of nickel(II) complexes supported by tridentate ligands that contain different substituents at the *meta* position of the phenyl substituents (OCH_3, CH_3, H, Cl, NO_2) (Figure 34, complex **63** for general structure). These complexes were found to react with H_2O_2 in acetone give the bis(µ-oxo)dinickel(III) intermediate **64**. This species decomposes to form the (µ-phenoxo)(µ-hydroxo)dinickel(II) species **65**, in which one of the phenyl groups on the ligand has been hydroxylated. This aromatic hydroxylation reaction was proposed to proceed through an electrophilic aromatic substitution mechanism. Finally, mononuclear nickel(II) complex **66** is formed, containing the hydroxylated ligand together with a (µ-hydroxo)dinickel(II) species. Complex **66** was characterized by ESI-MS and X-ray crystallographic analysis

(see Figure 34) [293]. Worthy of note is that the mechanism of action proposed for these nickel(II) complexes differs from the one proposed for the analogs copper(II) complexes. For the former complexes, a bis(μ-oxo)dinickel(III) species seems to be involved, whereas for the latter complexes, a 2-hydroxy-2-hydroperoxypropane adduct is generated (see Figures 29a and 34 for comparison) [279,280,293].
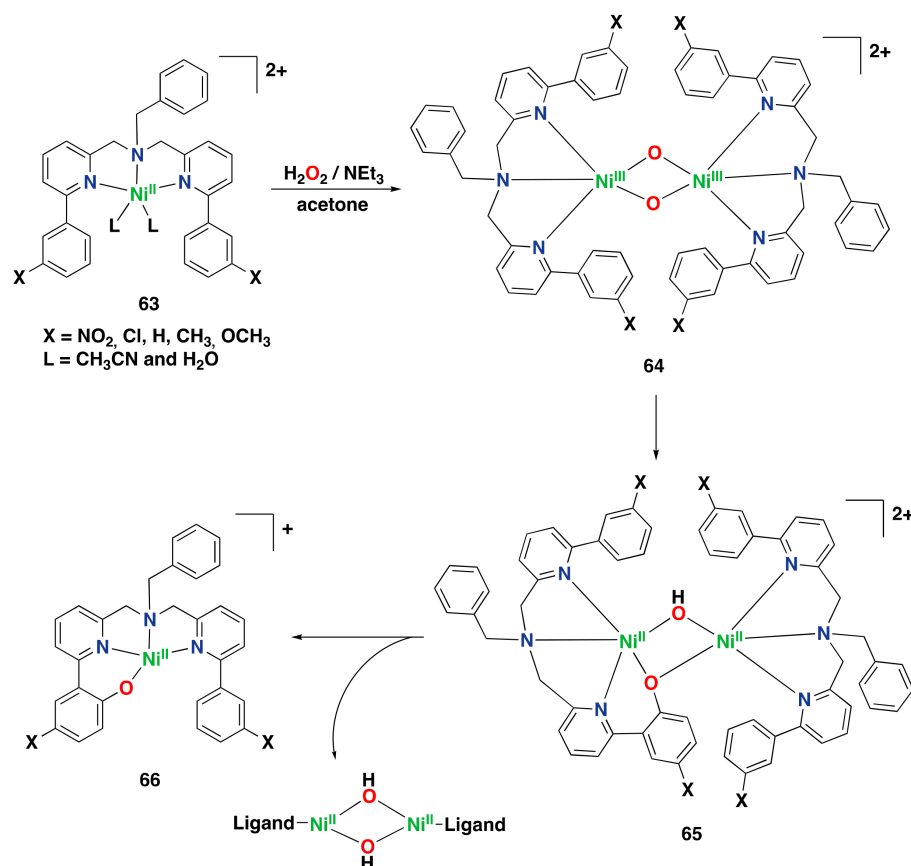
Figure 34. Reaction of nickel(II) complex **63** with H$_2$O$_2$ and triethylamine at low temperature to yield bis(μ-oxo)dinickel(III) intermediate **64** that can hydroxylate a phenyl ring of one of the ligands through the formation of intermediate **65** [292].

Itoh and co-workers have also investigated nickel complexes derived from tpa ligands bearing one, two, or three aryl substituents [294]. Particularly, they found that nickel complexes with two (**67**) or three aryl substituents react with H$_2$O$_2$ to afford bis(μ-oxo)dinickel(III) species (such as complex **68**) at low temperatures (Figure 35). This contradicted what was observed for the nickel complexes derived from tpa ligands bearing fewer aryl rings, which hardly react with the oxidant. Bis(μ-oxo)dinickel(III) species (such as complex **68**) were detected using UV–Vis and resonance Raman, and their features were compared with other known bis(μ-oxo)dinickel(III) intermediates [295–300]. Interestingly, it was reported that the former complexes can undergo intramolecular aromatic hydroxylation of the aminopyridine ligand to afford mononuclear nickel species **69**, in which one aryl ring on the ligand has been hydroxylated and binds to the metal center [294]. Remarkably, complex **67** was found to be capable of hydroxylating externally added benzene substrates at 60 °C, although phenol was only obtained in a 3% yield. The authors described that the extremely low yield can be attributed to the competition between intermolecular and intramolecular reactions.
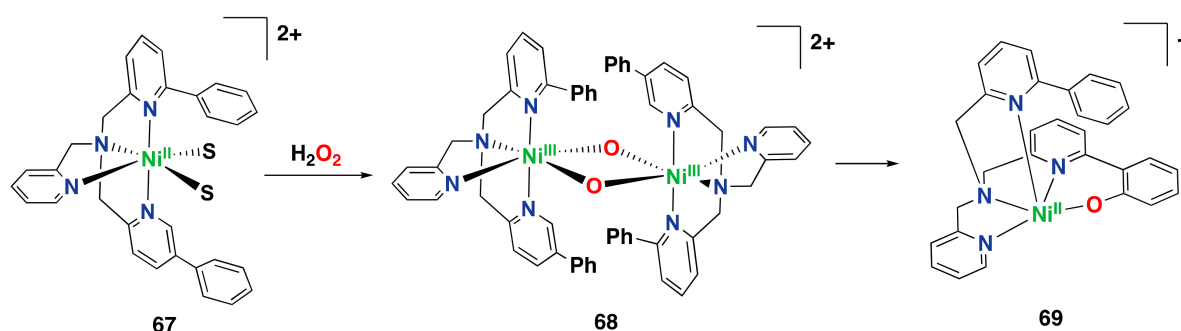
**Figure 35.** Formation of a bis(μ-oxo)dinickel(III) intermediate, and intramolecular arene hydroxylation of the ligand [293,300].

In 2015, the same group reported an interesting study in which they described the catalytic ability of nickel(II) complexes as homogeneous catalysts for the direct hydroxylation of benzene to phenol employing H_2O_2 as an oxidant [301]. In these catalytic reactions, the substrate is mixed with H_2O_2 in the presence of a catalytic amount of the nickel complex (10 mol% catalyst loading) and triethylamine. The best catalyst in this study proved to be nickel complex **70**, supported by the tepa ligand (tepa = tris[2-(pyridine-2-yl)ethyl]amine), which provided 21% phenol yield based on the amount of substrate and small amounts of overoxidized products. The same complex was also used for the oxidation of the alkylbenzene substrates toluene, ethylbenzene, and cumene. Interestingly, the selectivity for aromatic oxidation was up to 90% for these substrates. Nevertheless, reactions do not exceed two turnovers per nickel. In an independent experiment, the authors reported high turnover numbers using extremely low concentrations of the nickel complex and very long reaction times (TON = 749 after 216 h). Based on an experimental kinetic isotope effect, the authors excluded the involvement of hydroxyl radicals in these reactions and postulated a metal-based mechanism. In addition, it was proposed that the aromatic hydroxylation occurs via an electrophilic aromatic substitution mechanism and through the formation of a bis(μ-oxo)dinickel(III) intermediate (Figure 36) [301]. However, no experimental evidence was provided for the involvement of such an active oxidant. Recently, Itoh and co-workers reported on the synthesis and characterization of a bis(μ-oxo)dinickel(III) complex bearing a similar ligand that exhibited hydrogen abstraction and oxygenation reactivity towards external substrates but no aromatic oxidation reactivity [302]. In a study on a series of complexes related to complex **70**, including complex **70** itself, Klein Gebbink and co-workers cast doubt on the molecular nature of the active catalyst [303].
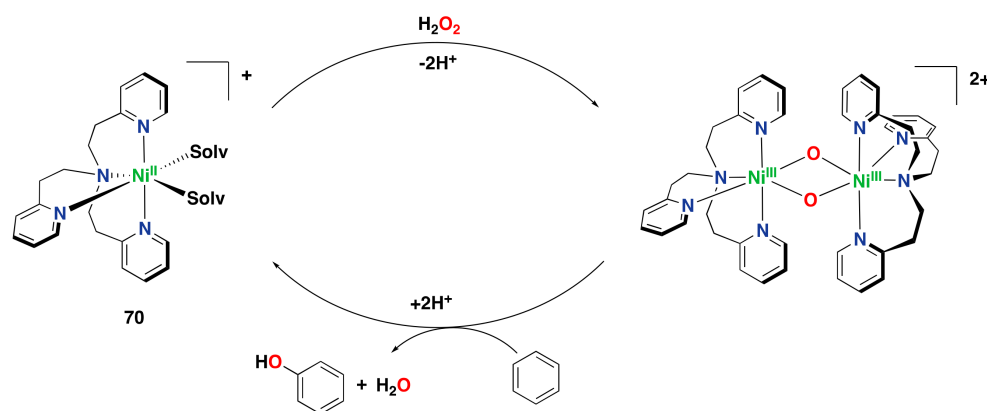
Figure 36. Proposed catalytic mechanism for the direct hydroxylation of benzene to phenol catalyzed by nickel(II) complex **70** supported by a tripodal tetradentate aminopyridine ligand and involving a bis(μ-oxo)dinickel(III) intermediate [301].

Recently, Mayilmurugan and co-workers reported on related nickel(II) complexes supported by tetradentate aminopyridine ligands for the direct hydroxylation of benzene and toluene to the corresponding phenol products with H_2O_2 as an oxidant (Figure 37) [304]. Interestingly, oxidation did not occur when phenol was used as a substrate, thus preventing overoxidation to hydroquinone or benzoquinone products. By employing nickel(II), complex **71** bearing an electron-rich ligand (0.05 mol% catalyst loading), the authors reported up to 41% phenol yield and 820 turnovers. Aromatic hydroxylation was proposed to occur through the formation of a bis(μ-oxo)dinickel(III) intermediate, in a similar way as in the mechanism proposed by Itoh and co-workers (Figure 36) [304].
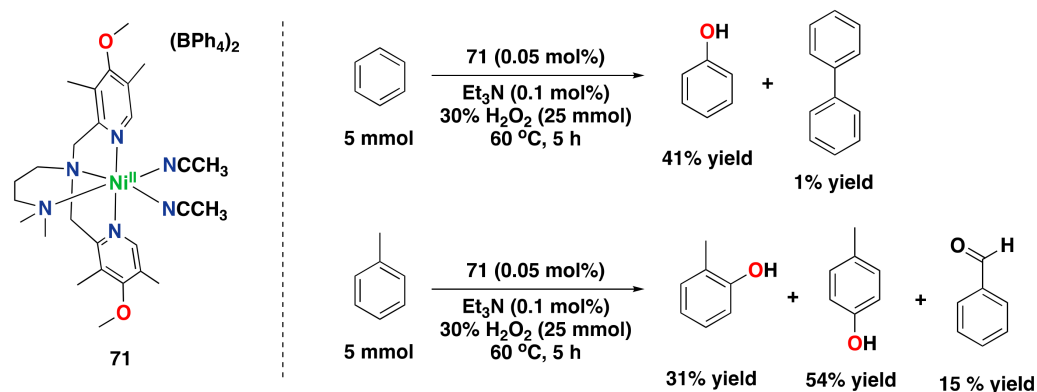
Figure 37. Reaction products of the catalytic oxidation of benzene and toluene catalyzed by nickel(II) complex **71** with H_2O_2 as an oxidant and triethylamine as an additive.

5. Manganese in Biological and Synthetic Systems

5.1. Manganese-Containing Metalloenzymes

Manganese, in a similar way to iron, is a non-toxic, inexpensive, and earth-abundant first-row transition metal. So far, no manganese-containing enzymes are known to perform aromatic oxidation in nature. Nevertheless, manganese plays an important role in the oxygen-evolving complex (OEC) in photosystem II (PS II). PS II is an enzyme present in the thylakoid membranes of oxygenic photosynthetic organisms. Particularly, it is in the oxygen-evolving complex (OEC) where the oxidation of water to dioxygen occurs [305,306]. Several X-ray crystal structure determinations have been successfully achieved for PS II, thus allowing for a better understanding of the structure geometry and components involved in the oxidation reaction [307]. The OEC consists of an oxo-bridged structure containing four Mn atoms and one Ca atom, linked via three di-μ-oxo and one mono-μ-oxo-bridged Mn–Mn interactions, and the Ca cofactor is linked by single-O bridging to two Mn centers [308].

5.2. Synthetic Manganese Systems

Due to the advantages of manganese (i.e., earth-abundant, non-toxic, and cheap), in the last few years, researchers have focused on the exploration of the reactivity of synthetic manganese-based complexes. This element has several available oxidation states (−3 to +7), consequently resulting in a great variety of reactivities for manganese-containing coordination complexes [309,310]. For instance, complexes in which the manganese center has a low oxidation state can perform chemistry similar to that of main-group elements, whereas high-oxidation manganese complexes can perform oxidation chemistry. Along this vein, manganese complexes have been widely studied in various catalytic oxidation reactions, such as asymmetric epoxidation reactions [311] and enantioselective aliphatic C–H oxidation [312,313], whereas only a few examples are known for aromatic oxidation reactions.

Nam and co-workers reported on manganese(II) complex **72** (Figure 38) bearing the Bn-TPEN ligand (Bn-TPEN = *N*-benzyl-*N*,*N'N'*-tris(2-pyridylmethyl)-1,2-diaminoethane), which upon reaction with iodosylbenzene forms a manganese(IV)-oxo complex that is

active in the oxidation of naphthalene, among other types of oxidation reactions [314]. Nevertheless, no efficient catalytic turnover numbers were achieved.
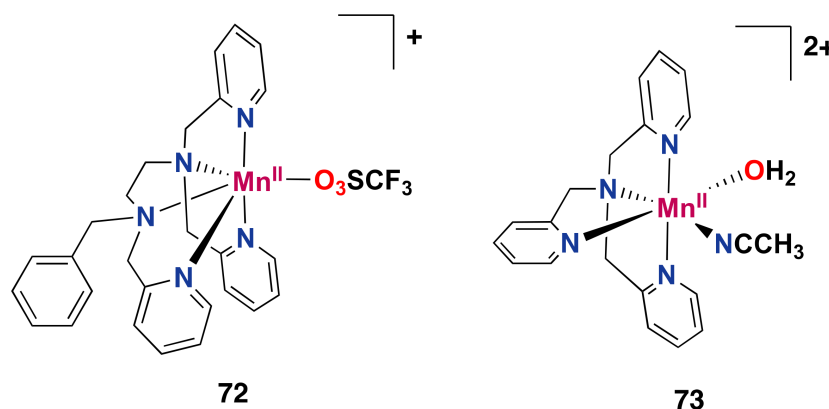
Figure 38. Synthetic manganese complexes that display aromatic oxidation reactivity. Complex **73** is incorporated into a mesoporous silica-alumina (Al-MCM-41) [312,313].

In 2015, Fukuzumi and co-workers described the remarkably selective hydroxylation of benzene derivatives to phenols with H_2O_2 employing manganese-tpa complex **73** incorporated into mesoporous silica-alumina (Al-MCM-41) [315]. The selectivity obtained for phenol formation was excellent, and the authors showed the importance of the incorporation of the complex into the solid support, which prevents the formation of bis(μ-oxo)dimanganese(III,IV) species that are catalytically much less active.

More recently, Klein Gebbink et al. have reported on the oxidation of aromatic substrates to phenols using H_2O_2 as a benign oxidant in fluorinated alcohol solvents in combination with Mn-complexes derived from bpmcn-type aminopyridine ligands [316]. An initial screening of bpmcn-type ligands in the oxidation of propylbenzene showed a critical dependence of the product selectivity on the nature of the bpmcn ligand, i.e., the use of the electron-rich ^{dMM}bpmcn ligand in complex **75** resulted in preferential oxidation at the benzylic position, whereas the bulky ^{tips}bpmcn ligand resulted in preferential aromatic oxidation (Figure 39). The likely role of the bulky silyl groups in the ^{tips}bpmcn ligand in complex **76** was attributed to the prevention of binding of phenol products to the manganese center (product inhibition), resulting in higher catalytic turn-over numbers.

	74	**75**	**76**
Arom./Aliph.	2.1/1	1/13.5	7.3/1
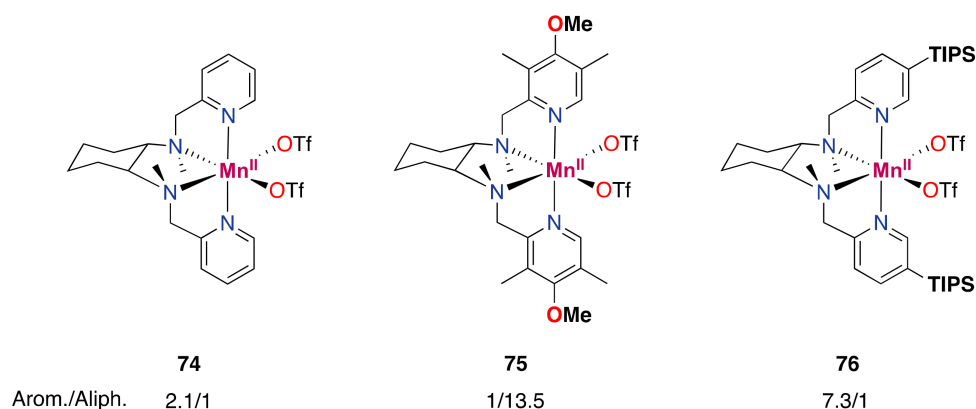
Figure 39. Bpmcn-based Mn-complexes studied in the oxidation of propylbenzene [314]. Ratio Arom./Aliph. represents the ratio between aromatic and aliphatic oxidation products.

The catalytic reaction conditions for complex **76** were further optimized using the oxidation of *tert*-butylbenzene. The highest yield of 29% 4-*tert*-butylphenol at 65% substrate conversion was obtained using 1 mol% of complex **76**, 1 equiv. oxidant (H_2O_2; slow addition), 0.5 equiv. dichloroacetic acid (DCA), and either hexafluoro-isopropanol (HFIP)

or trifluoroethanol (TFE) as the solvent. Using these optimized conditions, a series of different (substituted) benzene substrates can be converted to the corresponding *para*-phenols with reasonable yields (Figure 40). Side products typically include the corresponding ortho-phenol and quinone, as well as traces of benzyl alcohol. The mass balance of these reactions ranges from 66–94%, which was attributed to the formation of overoxidized products that did not show up in the GC analysis. Mechanistic investigations pointed out that **76** operates via an electrophilic, metal-based oxidant with no significant involvement of hydroxyl radicals and that phenol formation proceeds via an arene oxide intermediate. Overall, complex **76** is among the most competent molecular catalysts for aromatic oxidation reactions, showing some of the highest product yields reported to date.
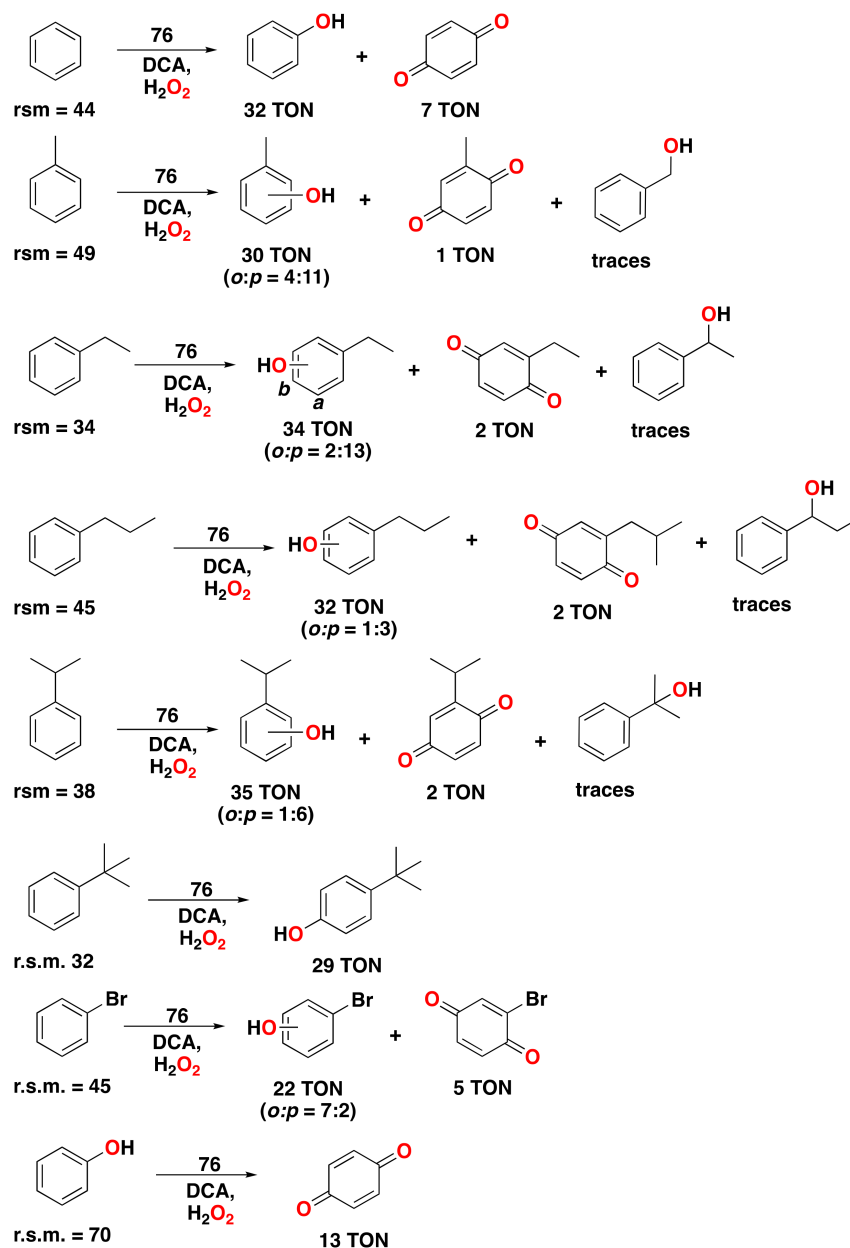
Figure 40. Reaction products of the catalytic oxidation of benzene and benzene derivatives catalyzed by complex **76** with H_2O_2 as an oxidant and DCA as a carboxylic acid additive. Reaction conditions: complex **76** (1 mol%), substrate, H_2O_2 (1.0 equiv., slow addition in 30 min), and DCA (0.5 equiv.) in HFIP at 0 °C for 0.5 h. See the corresponding reference for further details on the oxidation of other alkylbenzene substrates [316]. rsm = remaining starting material (%).

6. Concluding Remarks

This review has highlighted the inspiration that is drawn from the active site design of metallo-enzymes capable of catalyzing aromatic oxidation reactions to develop molecular catalysts that can form phenol products from benzene substrates. This field has undergone significant development over the past years. The initial endeavors resulted in synthetic metal complexes, such as those based on copper, which were capable of forming phenols in a (sub)stoichiometric fashion. However, more recent studies have led to the development of complexes based on, e.g., iron and manganese that can catalyze aromatic oxidation reactions with significant catalytic turnover numbers. To showcase the progress in the field, Figure 41 highlights the most proficient catalysts in terms of turnover numbers in the oxidation of benzene reported to date for each of the metals included in this review. Based on this development, it is to be expected that further activities in the field will yield molecular catalysts based on first-row transition metal ions that can catalyze aromatic oxidation reactions with high turn-over numbers and high selectivity for the phenol products, such that these may be part of the synthetic chemist's toolbox.
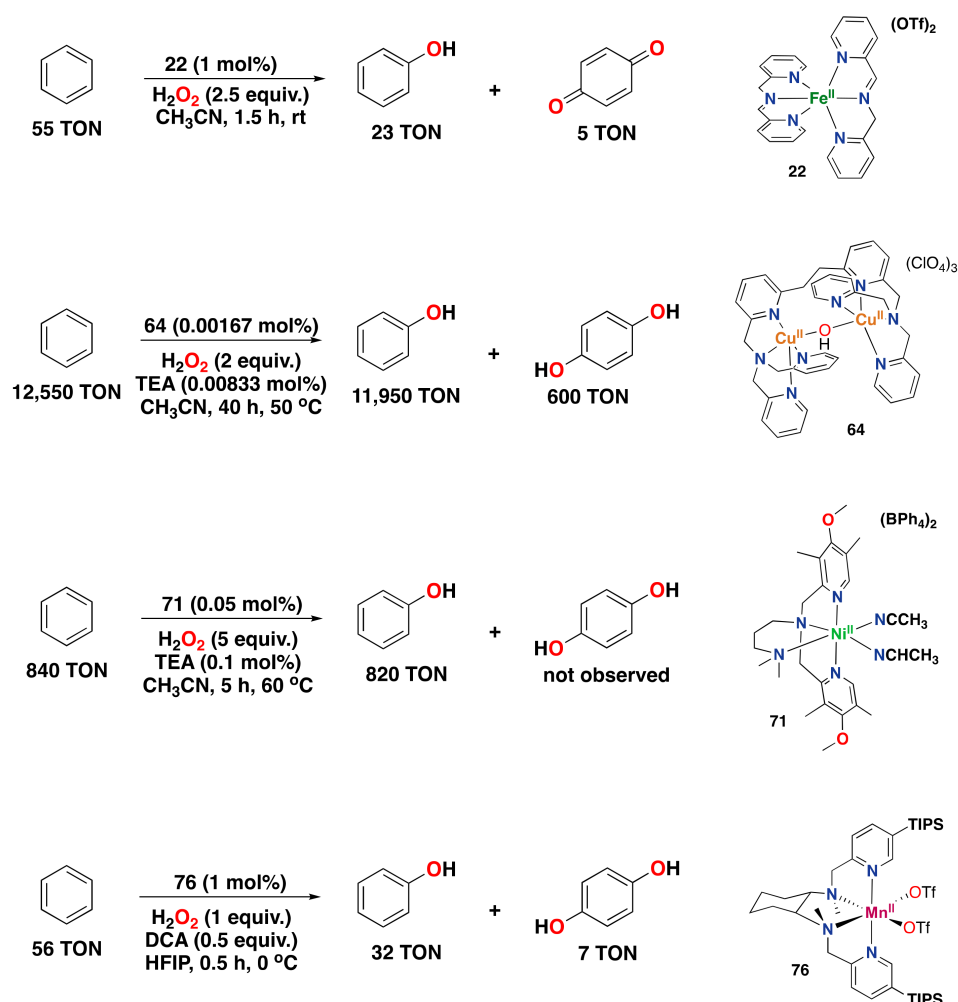
Figure 41. The best-performing catalysts per metal covered in this review are for the oxidation of benzene to phenol. Catalyst performance is expressed in terms of turnover numbers.

These research endeavors face several challenges. One of the challenges is the overmass balance of the reactions. In many cases, poor mass balances are encountered, i.e., significant substrate conversion may be achieved, yet the total amount of (identified) products is significantly less. These low mass balances may be the result of several site reactions occurring during catalysis. In particular, the occurrence of secondary, tertiary, or further oxidation reactions will result in the formation of more polar, over-oxidized

products that may be harder to trace, characterize, and quantify. Yet, an in-depth analysis of all oxidation products formed in aromatic oxidation reactions will provide a detailed "map" of the chemical landscape that is built up during the reactions. This analysis will not only significantly improve our understanding of these reactions but will also aid in the development of more selective and efficient catalysts. A second challenge is also related to product selectivity and relates to substrates on which different sites for oxidation are present on the same aromatic target structure. As shown by many examples in this review, singly substituted benzene substrates most often yield a mixture of differently substituted phenol products (ortho, meta, and para). The formation of such products may be inherent to the chemical reaction being carried out, as in electrophilic aromatic substitution reaction, and might therefore be difficult to tackle. On the other hand, recent advances in such as site-selective aromatic C–H activation reactions have shown that inherent selectivity patterns may be overcome by intricate catalyst design. The design of such catalysts for the aromatic oxidation reactions described in this review has yet to be accomplished. A final challenge in the field is the productive conversion of complex substrates beyond a single turnover. Most of the examples described in this review deal with reactions on relatively simple aromatic substrates comprised of a single aromatic core with one or two substituents and no further functional groups, ring structures, chirality, etc. A true challenge in the field is to design first-row transition metal catalysts capable of dealing with complex substrates while converting them with decent turnover numbers. This is particularly important in order to produce real synthetic and catalytic tools. Overall, these challenges sketch out an interesting and motivating scenario for the further development of the types of catalysts described in this review and may also ask for more "disruptive" approaches to come to the next generation of catalysts that can tackle these challenges.

References

1. Arakawa, H.; Aresta, M.; Armor, J.N.; Barteau, M.A.; Beckman, E.J.; Bell, A.T.; Bercaw, J.E.; Creutz, C.; Dinjus, E.; Dixon, D.A.; et al. Catalysis Research of Relevance to Carbon Management: Progress, Challenges, and Opportunities. *Chem. Rev.* **2001**, *101*, 953–996. [CrossRef] [PubMed]
2. Punniyamurthy, T.; Velusamy, S.; Iqbal, J. Recent Advances in Transition Metal Catalyzed Oxidation of Organic Substrates with Molecular Oxygen. *Chem. Rev.* **2005**, *105*, 2329–2363. [CrossRef] [PubMed]
3. White, M.C.; Zhao, J. Aliphatic C–H Oxidations for Late-Stage Functionalization. *J. Am. Chem. Soc.* **2018**, *140*, 13988–14009. [CrossRef] [PubMed]
4. Hong, B.; Luo, T.; Lei, X. Late-Stage Diversification of Natural Products. *ACS Cent. Sci.* **2020**, *6*, 622–635. [CrossRef] [PubMed]
5. Feng, K.; Quevedo, R.E.; Kohrt, J.T.; Oderinde, M.S.; Reilly, U.; White, M.C. Late-stage oxidative $C(sp^3)$–H methylation. *Nature* **2020**, *580*, 621–627. [CrossRef] [PubMed]
6. Genovino, J.; Sames, D.; Hamann, L.G.; Touré, B.B. Accessing Drug Metabolites via Transition-Metal Catalyzed C–H Oxidation: The Liver as Synthetic Inspiration. *Angew. Chem. Int. Ed.* **2016**, *55*, 14218–14238. [CrossRef]
7. Börgel, J.; Tanwar, L.; Berger, F.; Ritter, T. Late-stage aromatic C–H oxygenation. *J. Am. Chem. Soc.* **2018**, *140*, 16026–16031. [CrossRef]
8. Haggin, J. Chemists seek greater recognition for catalysis. *Chem. Eng. News* **1993**, *71*, 22. [CrossRef]
9. Cornils, B.; Herrmann, W.A. Concepts in homogeneous catalysis: The industrial view. *J. Catal.* **2003**, *216*, 23–31. [CrossRef]
10. Weber, M.; Weber, M.; Kleine-Boymann, M. *Ullmann's Encyclopedia of Industrial Chemistry*; Wiley-VCH: Weinheim, Germany, 2004; pp. 503–519.
11. Fukuzumi, S.; Ohkubo, K. One-Step Selective Hydroxylation of Benzene to Phenol. *Asian J. Org. Chem.* **2015**, *4*, 836–845. [CrossRef]
12. Sheldon, R.A.; Kochi, J.K. *Metal-Catalyzed Oxidations of Organic Compounds*; Academic Press: New York, NY, USA, 1981; pp. 315–339.
13. Luo, Y.-R. *Comprehensive Handbook of Chemical Bond Energies*; CRC Press: Boca Raton, FL, USA, 2007.

14. Lewis, J.C.; Coelho, P.S.; Arnold, F.H. Enzymatic functionalization of carbon–hydrogen bonds. *Chem. Soc. Rev.* **2011**, *40*, 2003–2021. [CrossRef] [PubMed]

15. Song, R.; Sorokin, A.; Bernadou, J.; Meunier, B. Metalloporphyrin-catalyzed oxidation of 2-methylnaphthalene to vitamin K3 and 6-methyl-1,4-naphthoquinone by potassium monopersulfate in aqueous solution. *J. Org. Chem.* **1997**, *62*, 673–678. [CrossRef] [PubMed]

16. Sorokin, A.; Meunier, B. Oxidation of polycyclic aromatic hydrocarbons catalyzed by iron tetrasulfophthalocyanine FePcS: Inverse isotope effects and oxygen labeling studies. *Eur. J. Inorg. Chem.* **1998**, *1998*, 1269–1281. [CrossRef]

17. Higuchi, T.; Satake, C.; Hirobe, M. Selective quinone formation by oxidation of aromatics with heteroaromatic N-oxides catalyzed by ruthenium porphyrins. *J. Am. Chem. Soc.* **1995**, *117*, 8879–8880. [CrossRef]

18. Khavasi, H.R.; Davarani, S.S.H.; Safari, N. Remarkable solvent effect on the yield and specificity of oxidation of naphthalene catalyzed by iron(III) porphyrins. *J. Mol. Catal. A Chem.* **2002**, *188*, 115–122. [CrossRef]

19. Klein Gebbink, R.J.M.; Moret, M.-E. *Non-Noble Metal Catalysis: Molecular Approaches and Reactions*; John Wiley & Sons: Weinmar, Germany, 2019.

20. Wallar, B.J.; Lipscomb, J.D. Dioxygen activation by enzymes containing binuclear non-heme iron clusters. *Chem. Rev.* **1996**, *96*, 2625–2658. [CrossRef]

21. Que, L., Jr.; Ho, R.Y. Dioxygen activation by enzymes with mononuclear non-heme iron active sites. *Chem. Rev.* **1996**, *96*, 2607–2624. [CrossRef]

22. Holm, R.H.; Kennepohl, P.; Solomon, E.I. Structural and functional aspects of metal sites in biology. *Chem. Rev.* **1996**, *96*, 2239–2314. [CrossRef]

23. Costas, M.; Mehn, M.P.; Jensen, M.P.; Que, L. Dioxygen activation at mononuclear nonheme iron active sites: Enzymes, models, and intermediates. *Chem. Rev.* **2004**, *104*, 939–986. [CrossRef]

24. Bruijnincx, P.C.; van Koten, G.; Klein Gebbink, R.J.M. Mononuclear non-heme iron enzymes with the 2-His-1-carboxylate facial triad: Recent developments in enzymology and modeling studies. *Chem. Soc. Rev.* **2008**, *37*, 2716–2744. [CrossRef]

25. Que, L.; Tolman, W.B. Biologically inspired oxidation catalysis. *Nature* **2008**, *455*, 333–340. [CrossRef] [PubMed]

26. Guo, M.; Corona, T.; Ray, K.; Nam, W. Heme and nonheme high-valent iron and manganese oxo cores in biological and abiological oxidation reactions. *ACS Cent. Sci.* **2019**, *5*, 13–28. [CrossRef] [PubMed]

27. Solomon, E.I.; Chen, P.; Metz, M.; Lee, S.K.; Palmer, A.E. Oxygen binding, activation, and reduction to water by copper proteins. *Angew. Chem. Int. Ed.* **2001**, *40*, 4570–4590. [CrossRef]

28. Pecoraro, V.L.; Baldwin, M.J.; Gelasco, A. Interaction of manganese with dioxygen and its reduced derivatives. *Chem. Rev.* **1994**, *94*, 807–826. [CrossRef]

29. Law, N.A.; Caudle, M.T.; Pecoraro, V.L. Manganese redox enzymes and model systems: Properties, structures, and reactivity. *Adv. Inorg. Chem.* **1998**, *46*, 305–440.

30. Youn, H.-D.; Kim, E.-J.; Roe, J.-H.; Hah, Y.C.; Kang, S.-O. A novel nickel-containing superoxide dismutase from *Streptomyces* spp. *Biochem. J.* **1996**, *318*, 889–896. [CrossRef]

31. Barondeau, D.P.; Kassmann, C.J.; Bruns, C.K.; Tainer, J.A.; Getzoff, E.D. Nickel superoxide dismutase structure and mechanism. *Biochemistry* **2004**, *43*, 8038–8047. [CrossRef]

32. Ragsdale, S.W. Nickel-based enzyme systems. *J. Biol. Chem.* **2009**, *284*, 18571–18575. [CrossRef]

33. Kirby, A.J.; Hollfelder, F. *From Enzyme Models to Model Enzymes*; Royal Society of Chemistry: Cambridge, UK, 2009.

34. Solomon, E.I.; Brunold, T.C.; Davis, M.I.; Kemsley, J.N.; Lee, S.-K.; Lehnert, N.; Neese, F.; Skulan, A.J.; Yang, Y.-S.; Zhou, J. Geometric and electronic structure/function correlations in non-heme iron enzymes. *Chem. Rev.* **2000**, *100*, 235–350. [CrossRef]

35. Neidig, M.L.; Solomon, E.I. Structure–function correlations in oxygen activating non-heme iron enzymes. *Chem. Commun.* **2005**, *21*, 5843–5863. [CrossRef]

36. Matsumoto, K.; Tachikawa, S.; Hashimoto, N.; Nakano, R.; Yoshida, M.; Shindo, M. Aerobic C–H Oxidation of Arenes Using a Recyclable, Heterogeneous Rhodium Catalyst. *J. Org. Chem.* **2017**, *82*, 4305–4316. [CrossRef] [PubMed]

37. Santoro, S.; Kozhushkov, S.I.; Ackermann, L.; Vaccaro, L. Heterogeneous catalytic approaches in C–H activation reactions. *Green Chem.* **2016**, *18*, 3471–3493. [CrossRef]

38. Reay, A.J.; Fairlamb, I.J. Catalytic C–H bond functionalisation chemistry: The case for quasi-heterogeneous catalysis. *Chem. Commun.* **2015**, *51*, 16289–16307. [CrossRef] [PubMed]

39. Rahmani, N.; Amiri, A.; Ziarani, G.M.; Badiei, A. Review of some transition metal-based mesoporous catalysts for the direct hydroxylation of benzene to phenol (DHBP). *Mol. Catal.* **2021**, *515*, 111873. [CrossRef]

40. Vicens, L.; Olivo, G.; Costas, M. Rational Design of Bioinspired Catalysts for Selective Oxidations. *ACS Catal.* **2020**, *10*, 8611–8631. [CrossRef]

41. Bailey, C.L.; Drago, R.S. Utilization of O_2 for the specific oxidation of organic substrates with cobalt(II) catalysts. *Coord. Chem. Rev.* **1987**, *79*, 321–332. [CrossRef]

42. Carneiro, L.; Silva, A.R. Selective direct hydroxylation of benzene to phenol with hydrogen peroxide by iron and vanadyl based homogeneous and heterogeneous catalysts. *Catal. Sci. Technol.* **2016**, *6*, 8166–8176. [CrossRef]

43. Han, J.W.; Jung, J.; Lee, Y.-M.; Nam, W.; Fukuzumi, S. Photocatalytic oxidation of benzene to phenol using dioxygen as an oxygen source and water as an electron source in the presence of a cobalt catalyst. *Chem. Sci.* **2017**, *8*, 7119–7125. [CrossRef]

44. Anandababu, K.; Muthuramalingam, S.; Velusamy, M.; Mayilmurugan, R. Single-step benzene hydroxylation by cobalt(II) catalysts via a cobalt(III)-hydroperoxo intermediate. *Catal. Sci. Technol.* **2020**, *10*, 2540–2548. [CrossRef]

45. Lemke, K.; Ehrich, H.; Lohse, U.; Berndt, H.; Jähnisch, K. Selective hydroxylation of benzene to phenol over supported vanadium oxide catalysts. *Appl. Catal. A Gen.* **2003**, *243*, 41–51. [CrossRef]

46. Zhang, J.; Tang, Y.; Li, G.; Hu, C. Room temperature direct oxidation of benzene to phenol using hydrogen peroxide in the presence of vanadium-substituted heteropolymolybdates. *Appl. Catal. A Gen.* **2005**, *278*, 251–261. [CrossRef]

47. Masferrer-Rius, E. Manganese and Nickel Complexes as Catalysts for Aromatic Oxidation: Novel Methodologies for Non-Noble Metal Catalysis. Ph.D. Thesis, Utrecht University, Utrecht, The Netherlands, 2022.

48. Rajeev, A.; Balamurugan, M.; Sankaralingam, M. Rational Design of First-Row Transition Metal Complexes as the Catalysts for Oxidation of Arenes: A Homogeneous Approach. *ACS Catal.* **2022**, *12*, 9953–9982. [CrossRef]

49. Fenton, H. LXXIII.—Oxidation of tartaric acid in presence of iron. *J. Chem. Soc. Trans.* **1894**, *65*, 899–910. [CrossRef]

50. Haber, F.; Weiss, J. Üeber die Katalyse des Hydroperoxydes. *Naturwissenschaften* **1932**, *20*, 948–950. [CrossRef]

51. Haber, F.; Weiss, J. The catalytic decomposition of hydrogen peroxide by iron salts. *Proc. R. Soc. Lond. A Math. Phys. Sci.* **1934**, *147*, 332–351.

52. Walling, C. Intermediates in the reactions of Fenton type reagents. *Acc. Chem. Res.* **1998**, *31*, 155–157. [CrossRef]

53. MacFaul, P.A.; Wayner, D.; Ingold, K. A radical account of "Oxygenated Fenton chemistry". *Acc. Chem. Res.* **1998**, *31*, 159–162. [CrossRef]

54. Goldstein, S.; Meyerstein, D. Comments on the mechanism of the "Fenton-like" reaction. *Acc. Chem. Res.* **1999**, *32*, 547–550. [CrossRef]

55. Merz, J.; Waters, W. 511. The oxidation of aromatic compounds by means of the free hydroxyl radical. *J. Chem. Soc.* **1949**, 2427–2433. [CrossRef]

56. Smith, J.L.; Norman, R. 539. Hydroxylation. Part I. The oxidation of benzene and toluene by Fenton's reagent. *J. Chem. Soc.* **1963**, 2897–2905. [CrossRef]

57. Walling, C.; Johnson, R.A. Fenton's reagent. V. Hydroxylation and side-chain cleavage of aromatics. *J. Am. Chem. Soc.* **1975**, *97*, 363–367. [CrossRef]

58. Kurata, T.; Watanabe, Y.; Katoh, M.; Sawaki, Y. Mechanism of aromatic hydroxylation in the Fenton and related reactions. One-electron oxidation and the NIH shift. *J. Am. Chem. Soc.* **1988**, *110*, 7472–7478. [CrossRef]

59. Cussó, O.; Garcia-Bosch, I.; Ribas, X.; Lloret-Fillol, J.; Costas, M. Asymmetric epoxidation with H_2O_2 by manipulating the electronic properties of non-heme iron catalysts. *J. Am. Chem. Soc.* **2013**, *135*, 14871–14878. [CrossRef] [PubMed]

60. MacFaul, P.A.; Ingold, K.; Wayner, D.; Que, L. A Putative Monooxygenase Mimic Which Functions via Well-Disguised Free Radical Chemistry1. *J. Am. Chem. Soc.* **1997**, *119*, 10594–10598. [CrossRef]

61. Ingold, K.U.; MacFaul, P.A. *Biomimetic Oxidations Catalyzed by Transition Metal Complexes*; Meunier, B., Ed.; Imperial College Press: London, UK, 2000; p. 45.

62. Hiatt, R.; Clipsham, J.; Visser, T. The induced decomposition of tert-butyl hydroperoxide. *Can. J. Chem.* **1964**, *42*, 2754–2757. [CrossRef]

63. Udenfriend, S.; Clark, C.T.; Axelrod, J.; Brodie, B.B. Ascorbic acid in aromatic hydroxylation. I. A model system for aromatic hydroxylation. *J. Biol. Chem.* **1954**, *208*, 731–738. [CrossRef]

64. Brodie, B.B.; Axelrod, J.; Shore, P.A.; Udenfriend, S. Ascorbic acid in aromatic hydroxylation II. Products formed by reaction of substrates with ascorbic acid, ferrous ion, and oxygen. *J. Biol. Chem.* **1954**, *208*, 741–750. [CrossRef]

65. Slavik, R.; Peters, J.-U.; Giger, R.; Bürkler, M.; Bald, E. Synthesis of potential drug metabolites by a modified Udenfried reaction. *Tetrahedron Lett.* **2011**, *52*, 749–752. [CrossRef]

66. Mathieu, D.; Bartoli, J.F.; Battioni, P.; Mansuy, D. Monooxygenation of aromatic compounds by dioxygen with bioinspired systems using non-heme iron catalysts and tetrahydropterins: Comparison with other reducing agents and interesting regioselectivity favouring meta-hydroxylation. *Tetrahedron* **2004**, *60*, 3855–3862. [CrossRef]

67. Metelitsa, D.I. Mechanisms of the hydroxylation of aromatic compounds. *Russ. Chem. Rev.* **1971**, *40*, 563. [CrossRef]

68. Kunai, A.; Hata, S.; Ito, S.; Sasaki, K. The role of oxygen in the hydroxylation reaction of benzene with Fenton's reagent. Oxygen 18 tracer study. *J. Am. Chem. Soc.* **1986**, *108*, 6012–6016. [CrossRef] [PubMed]

69. Meunier, B.; De Visser, S.P.; Shaik, S. Mechanism of oxidation reactions catalyzed by cytochrome P450 enzymes. *Chem. Rev.* **2004**, *104*, 3947–3980. [CrossRef] [PubMed]

70. Poulos, T.L. Heme enzyme structure and function. *Chem. Rev.* **2014**, *114*, 3919–3962. [CrossRef] [PubMed]

71. Abu-Omar, M.M.; Loaiza, A.; Hontzeas, N. Reaction mechanisms of mononuclear non-heme iron oxygenases. *Chem. Rev.* **2005**, *105*, 2227–2252. [CrossRef] [PubMed]

72. Cussó, O.; Ribas, X.; Costas, M. Biologically inspired non-heme iron-catalysts for asymmetric epoxidation; design principles and perspectives. *Chem. Commun.* **2015**, *51*, 14285–14298. [CrossRef] [PubMed]

73. Sono, M.; Roach, M.P.; Coulter, E.D.; Dawson, J.H. Heme-containing oxygenases. *Chem. Rev.* **1996**, *96*, 2841–2888. [CrossRef] [PubMed]

74. De Montellano, P.R.O. *Cytochrome P450: Structure, Mechanism, and Biochemistry*, 3rd ed.; Kluwer Academic; Plenum Publishers: New York, NY, USA, 2005.

75. De Montellano, P.R.O.; Kunze, K.L.; Beilan, H.S. Chiral orientation of prosthetic heme in the cytochrome P-450 active site. *J. Biol. Chem.* **1983**, *258*, 45–47. [CrossRef]

76. Tshuva, E.Y.; Lippard, S.J. Synthetic models for non-heme carboxylate-bridged diiron metalloproteins: Strategies and tactics. *Chem. Rev.* **2004**, *104*, 987–1012. [CrossRef]

77. Hegg, E.L.; Que, L., Jr. The 2-His-1-carboxylate facial triad—An emerging structural motif in mononuclear non-heme iron(II) enzymes. *Eur. J. Biochem.* **1997**, *250*, 625–629. [CrossRef]

78. Que, L. One motif—Many different reactions. *Nat. Struct. Biol.* **2000**, *7*, 182–184. [CrossRef]

79. Koehntop, K.D.; Emerson, J.P.; Que, L. The 2-His-1-carboxylate facial triad: A versatile platform for dioxygen activation by mononuclear non-heme iron(II) enzymes. *J. Biol. Inorg. Chem.* **2005**, *10*, 87–93. [CrossRef] [PubMed]

80. Kryatov, S.V.; Rybak-Akimova, E.V.; Schindler, S. Kinetics and mechanisms of formation and reactivity of non-heme iron oxygen intermediates. *Chem. Rev.* **2005**, *105*, 2175–2226. [CrossRef] [PubMed]

81. Kovaleva, E.G.; Lipscomb, J.D. Versatility of biological non-heme Fe(II) centers in oxygen activation reactions. *Nat. Chem. Biol.* **2008**, *4*, 186–193. [CrossRef]

82. Gibson, D.; Resnick, S.; Lee, K.; Brand, J.; Torok, D.; Wackett, L.; Schocken, M.; Haigler, B. Desaturation, dioxygenation, and monooxygenation reactions catalyzed by naphthalene dioxygenase from *Pseudomonas* sp. strain 9816-4. *J. Bacteriol.* **1995**, *177*, 2615–2621. [CrossRef] [PubMed]

83. Wolfe, M.D.; Parales, J.V.; Gibson, D.T.; Lipscomb, J.D. Single Turnover Chemistry and Regulation of O_2 Activation by the Oxygenase Component of Naphthalene 1,2-Dioxygenase. *J. Biol. Chem.* **2001**, *276*, 1945–1953. [CrossRef]

84. Denisov, I.G.; Makris, T.M.; Sligar, S.G.; Schlichting, I. Structure and chemistry of cytochrome P450. *Chem. Rev.* **2005**, *105*, 2253–2278. [CrossRef]

85. Ortiz de Montellano, P.R. Hydrocarbon hydroxylation by cytochrome P450 enzymes. *Chem. Rev.* **2010**, *110*, 932–948. [CrossRef]

86. Meunier, B.; Bernadou, J. Active iron-oxo and iron-peroxo species in cytochromes P450 and peroxidases; oxo-hydroxo tautomerism with water-soluble metalloporphyrins. In *Metal-Oxo and Metal-Peroxo Species in Catalytic Oxidations*; Springer: New York, NY, USA, 2000; pp. 1–35.

87. Cooper, H.L.R.; Groves, J.T. Molecular probes of the mechanism of cytochrome P450. Oxygen traps a substrate radical intermediate. *Arch. Biochem. Biophys.* **2011**, *507*, 111–118. [CrossRef]

88. Kille, S.; Zilly, F.E.; Acevedo, J.P.; Reetz, M.T. Regio-and stereoselectivity of P450-catalysed hydroxylation of steroids controlled by laboratory evolution. *Nat. Chem.* **2011**, *3*, 738–743. [CrossRef]

89. Narayan, A.R.; Jiménez-Osés, G.; Liu, P.; Negretti, S.; Zhao, W.; Gilbert, M.M.; Ramabhadran, R.O.; Yang, Y.-F.; Furan, L.R.; Li, Z.; et al. Enzymatic hydroxylation of an unactivated methylene C–H bond guided by molecular dynamics simulations. *Nat. Chem.* **2015**, *7*, 653–660. [CrossRef]

90. Roiban, G.D.; Agudo, R.; Reetz, M.T. Cytochrome P450 Catalyzed Oxidative Hydroxylation of Achiral Organic Compounds with Simultaneous Creation of Two Chirality Centers in a Single C-H Activation Step. *Angew. Chem. Int. Ed.* **2014**, *53*, 8659–8663. [CrossRef] [PubMed]

91. Zhang, K.; Shafer, B.M.; Demars, M.D.; Stern, H.A.; Fasan, R. Controlled oxidation of remote sp^3 C–H bonds in artemisinin via P450 catalysts with fine-tuned regio-and stereoselectivity. *J. Am. Chem. Soc.* **2012**, *134*, 18695–18704. [CrossRef] [PubMed]

92. Poulos, T.L.; Finzel, B.; Gunsalus, I.; Wagner, G.C.; Kraut, J. The 2.6-Å crystal structure of Pseudomonas putida cytochrome P-450. *J. Biol. Chem.* **1985**, *260*, 16122–16130. [CrossRef] [PubMed]

93. Li, H.; Narasimhulu, S.; Havran, L.M.; Winkler, J.D.; Poulos, T.L. Crystal structure of cytochrome P450cam complexed with its catalytic product, 5-exo-hydroxycamphor. *J. Am. Chem. Soc.* **1995**, *117*, 6297–6299. [CrossRef]

94. Schlichting, I.; Berendzen, J.; Chu, K.; Stock, A.M.; Maves, S.A.; Benson, D.E.; Sweet, R.M.; Ringe, D.; Petsko, G.A.; Sligar, S.G. The catalytic pathway of cytochrome P450cam at atomic resolution. *Science* **2000**, *287*, 1615–1622. [CrossRef] [PubMed]

95. Yano, J.K.; Wester, M.R.; Schoch, G.A.; Griffin, K.J.; Stout, C.D.; Johnson, E.F. The structure of human microsomal cytochrome P450 3A4 determined by X-ray crystallography to 2.05-Å resolution. *J. Biol. Chem.* **2004**, *279*, 38091–38094. [CrossRef]

96. Kells, P.M.; Ouellet, H.; Santos-Aberturas, J.; Aparicio, J.F.; Podust, L.M. Structure of cytochrome P450 PimD suggests epoxidation of the polyene macrolide pimaricin occurs via a hydroperoxoferric intermediate. *Chem. Biol.* **2010**, *17*, 841–851. [CrossRef]

97. Shah, M.B.; Jang, H.-H.; Zhang, Q.; Stout, C.D.; Halpert, J.R. X-ray crystal structure of the cytochrome P450 2B4 active site mutant F297A in complex with clopidogrel: Insights into compensatory rearrangements of the binding pocket. *Arch. Biochem. Biophys.* **2013**, *530*, 64–72. [CrossRef]

98. Dawson, J.H.; Sono, M. Cytochrome P-450 and chloroperoxidase: Thiolate-ligated heme enzymes. Spectroscopic determination of their active-site structures and mechanistic implications of thiolate ligation. *Chem. Rev.* **1987**, *87*, 1255–1276. [CrossRef]

99. Mueller, E.J.; Loida, P.J.; Sligar, S.G. Twenty-five Years of P450 cam Research. In *Cytochrome P450*; Springer: New York, NY, USA, 1995; pp. 83–124.

100. King, N.K.; Winfield, M. Oxygen uptake and evolution by iron porphyrin enzymes. *Aust. J. Chem.* **1959**, *12*, 47–64.

101. Dunford, H.; Stillman, J. Structure and functional properties of peroxidases and catalases. *Coord. Chem. Rev.* **1976**, *19*, 187–251. [CrossRef]

102. Meunier, B.; Bernadou, J. Metal-oxo species in P450 enzymes and biomimetic models. Oxo-hydroxo tautomerism with water-soluble metalloporphyrins. *Top. Catal.* **2002**, *21*, 47–54. [CrossRef]

103. Rittle, J.; Green, M.T. Cytochrome P450 compound I: Capture, characterization, and C–H bond activation kinetics. *Science* **2010**, *330*, 933–937. [CrossRef] [PubMed]

104. Groves, J.T.; McClusky, G.A. Aliphatic hydroxylation via oxygen rebound. Oxygen transfer catalyzed by iron. *J. Am. Chem. Soc.* **1976**, *98*, 859–861. [CrossRef]

105. Groves, J.T.; McClusky, G.A.; White, R.E.; Coon, M.J. Aliphatic hydroxylation by highly purified liver microsomal cytochrome P-450. Evidence for a carbon radical intermediate. *Biochem. Biophys. Res. Commun.* **1978**, *81*, 154–160. [CrossRef]

106. Ullrich, R.; Hofrichter, M. Enzymatic hydroxylation of aromatic compounds. *Cell. Mol. Life Sci.* **2007**, *64*, 271–293. [CrossRef]

107. de Montellano, P.R.O.; de Voss, J.J. Substrate oxidation by cytochrome P450 enzymes. In *Cytochrome P450—Structure, Mechanism and Biochemistry*, 3rd ed.; Kluwer Academic; Plenum Publishers: New York, NY, USA, 2005; pp. 183–245.

108. Groves, J.T. High-valent iron in chemical and biological oxidations. *J. Inorg. Biochem.* **2006**, *100*, 434–447. [CrossRef]

109. Guroff, G.; Daly, J.W.; Jerina, D.M.; Renson, J.; Witkop, B.; Udenfriend, S. Hydroxylation-induced migration: The NIH shift. *Science* **1967**, *157*, 1524–1530. [CrossRef]

110. Daly, J.; Jerina, D.; Witkop, B. Arene oxides and the NIH shift: The metabolism, toxicity and carcinogenicity of aromatic compounds. *Experientia* **1972**, *28*, 1129–1149. [CrossRef]

111. Barry, S.M.; Challis, G.L. Mechanism and catalytic diversity of Rieske non-heme iron-dependent oxygenases. *ACS Catal.* **2013**, *3*, 2362–2370. [CrossRef]

112. Karlsson, A.; Parales, J.V.; Parales, R.E.; Gibson, D.T.; Eklund, H.; Ramaswamy, S. Crystal structure of naphthalene dioxygenase: Side-on binding of dioxygen to iron. *Science* **2003**, *299*, 1039–1042. [CrossRef] [PubMed]

113. Kauppi, B.; Lee, K.; Carredano, E.; Parales, R.E.; Gibson, D.T.; Eklund, H.; Ramaswamy, S. Structure of an aromatic-ring-hydroxylating dioxygenase–naphthalene 1,2-dioxygenase. *Structure* **1998**, *6*, 571–586. [CrossRef] [PubMed]

114. Parales, R.E.; Parales, J.V.; Gibson, D.T. Aspartate 205 in the catalytic domain of naphthalene dioxygenase is essential for activity. *J. Bacteriol.* **1999**, *181*, 1831–1837. [CrossRef] [PubMed]

115. Perry, C.; De Los Santos, E.L.; Alkhalaf, L.M.; Challis, G.L. Rieske non-heme iron-dependent oxygenases catalyse diverse reactions in natural product biosynthesis. *Nat. Prod. Rep.* **2018**, *35*, 622–632. [CrossRef]

116. Martins, B.M.; Svetlitchnaia, T.; Dobbek, H. 2-Oxoquinoline 8-monooxygenase oxygenase component: Active site modulation by Rieske-[2Fe-2S] center oxidation/reduction. *Structure* **2005**, *13*, 817–824. [CrossRef]

117. Hsueh, K.-L.; Westler, W.M.; Markley, J.L. NMR investigations of the Rieske protein from Thermus thermophilus support a coupled proton and electron transfer mechanism. *J. Am. Chem. Soc.* **2010**, *132*, 7908–7918. [CrossRef]

118. Wolfe, M.D.; Altier, D.J.; Stubna, A.; Popescu, C.V.; Münck, E.; Lipscomb, J.D. Benzoate 1,2-dioxygenase from Pseudomonas putida: Single turnover kinetics and regulation of a two-component Rieske dioxygenase. *Biochemistry* **2002**, *41*, 9611–9626. [CrossRef]

119. Bugg, T.D.; Ramaswamy, S. Non-heme iron-dependent dioxygenases: Unravelling catalytic mechanisms for complex enzymatic oxidations. *Curr. Op. Chem. Biol.* **2008**, *12*, 134–140. [CrossRef]

120. Wolfe, M.D.; Lipscomb, J.D. Hydrogen peroxide-coupled *cis*-diol formation catalyzed by naphthalene 1,2-dioxygenase. *J. Biol. Chem.* **2003**, *278*, 829–835. [CrossRef]

121. Lippard, S.J. Hydroxylation of C–H bonds at carboxylate-bridged diiron centres. *Philos. Trans. R. Soc. Lond. Ser. A* **2005**, *363*, 861–877. [CrossRef]

122. Rosenzweig, A.C.; Frederick, C.A.; Lippard, S.J. Crystal structure of a bacterial non-haem iron hydroxylase that catalyses the biological oxidation of methane. *Nature* **1993**, *366*, 537–543. [CrossRef] [PubMed]

123. Que, L., Jr.; True, A.E. Dinuclear iron-and manganese-oxo sites in biology. *Prog. Inorg. Chem.* **1990**, *38*, 97–200.

124. Merkx, M.; Kopp, D.A.; Sazinsky, M.H.; Blazyk, J.L.; Müller, J.; Lippard, S.J. Dioxygen activation and methane hydroxylation by soluble methane monooxygenase: A tale of two irons and three proteins. *Angew. Chem. Int. Ed.* **2001**, *40*, 2782–2807. [CrossRef]

125. Notomista, E.; Lahm, A.; Di Donato, A.; Tramontano, A. Evolution of bacterial and archaeal multicomponent monooxygenases. *J. Mol. Evol.* **2003**, *56*, 435–445. [CrossRef] [PubMed]

126. Leahy, J.G.; Batchelor, P.J.; Morcomb, S.M. Evolution of the soluble diiron monooxygenases. *FEMS Microbiol. Rev.* **2003**, *27*, 449–479. [CrossRef]

127. Green, J.; Dalton, H. Substrate specificity of soluble methane monooxygenase. Mechanistic implications. *J. Biol. Chem.* **1989**, *264*, 17698–17703. [CrossRef]

128. Siewert, I.; Limberg, C. Low-Molecular-Weight Analogues of the Soluble Methane Monooxygenase (sMMO): From the Structural Mimicking of Resting States and Intermediates to Functional Models. *Chem. Eur. J.* **2009**, *15*, 10316–10328. [CrossRef]

129. Sazinsky, M.H.; Bard, J.; Di Donato, A.; Lippard, S.J. Crystal Structure of the Toluene/o-Xylene Monooxygenase Hydroxylase from *Pseudomonas stutzeri* OX1. *J. Biol. Chem.* **2004**, *279*, 30600–30610. [CrossRef]

130. Sazinsky, M.H.; Dunten, P.W.; McCormick, M.S.; DiDonato, A.; Lippard, S.J. X-ray Structure of a Hydroxylase Regulatory Protein Complex from a Hydrocarbon-Oxidizing Multicomponent Monooxygenase, *Pseudomonas* sp. OX1 Phenol Hydroxylase. *Biochemistry* **2006**, *45*, 15392–15404. [CrossRef]

131. Chauhan, S.; Barbieri, P.; Wood, T.K. Oxidation of trichloroethylene, 1,1-dichloroethylene, and chloroform by toluene/o-xylene monooxygenase from *Pseudomonas stutzeri* OX1. *Appl. Environ. Microbiol.* **1998**, *64*, 3023–3024. [CrossRef]

132. Mitchell, K.H.; Rogge, C.E.; Gierahn, T.; Fox, B.G. Insight into the mechanism of aromatic hydroxylation by toluene 4-monooxygenase by use of specifically deuterated toluene and p-xylene. *Proc. Natl. Acad. Sci. USA* **2003**, *100*, 3784–3789. [CrossRef] [PubMed]

133. Friedle, S.; Reisner, E.; Lippard, S.J. Current challenges of modeling diiron enzyme active sites for dioxygen activation by biomimetic synthetic complexes. *Chem. Soc. Rev.* **2010**, *39*, 2768–2779. [CrossRef]

134. Colby, J.; Stirling, D.I.; Dalton, H. The soluble methane mono-oxygenase of Methylococcus capsulatus (Bath). Its ability to oxygenate n-alkanes, n-alkenes, ethers, and alicyclic, aromatic and heterocyclic compounds. *Biochem. J.* **1977**, *165*, 395–402. [CrossRef]

135. Kovaleva, E.; Neibergall, M.; Chakrabarty, S.; Lipscomb, J.D. Finding intermediates in the O_2 activation pathways of non-heme iron oxygenases. *Acc. Chem. Res.* **2007**, *40*, 475–483. [CrossRef] [PubMed]

136. Tinberg, C.E.; Lippard, S.J. Revisiting the mechanism of dioxygen activation in soluble methane monooxygenase from M. capsulatus (Bath): Evidence for a multi-step, proton-dependent reaction pathway. *Biochemistry* **2009**, *48*, 12145–12158. [CrossRef]

137. Valentine, A.M.; Stahl, S.S.; Lippard, S.J. Mechanistic studies of the reaction of reduced methane monooxygenase hydroxylase with dioxygen and substrates. *J. Am. Chem. Soc.* **1999**, *121*, 3876–3887. [CrossRef]

138. Beauvais, L.G.; Lippard, S.J. Reactions of the peroxo intermediate of soluble methane monooxygenase hydroxylase with ethers. *J. Am. Chem. Soc.* **2005**, *127*, 7370–7378. [CrossRef]

139. Song, W.J.; Lippard, S.J. Mechanistic studies of reactions of peroxodiiron(III) intermediates in T201 variants of toluene/o-xylene monooxygenase hydroxylase. *Biochemistry* **2011**, *50*, 5391–5399. [CrossRef]

140. Murray, L.J.; Naik, S.G.; Ortillo, D.O.; García-Serres, R.; Lee, J.K.; Huynh, B.H.; Lippard, S.J. Characterization of the arene-oxidizing intermediate in ToMOH as a diiron(III) species. *J. Am. Chem. Soc.* **2007**, *129*, 14500–14510. [CrossRef]

141. Kappock, T.J.; Caradonna, J.P. Pterin-dependent amino acid hydroxylases. *Chem. Rev.* **1996**, *96*, 2659–2756. [CrossRef]

142. Flatmark, T.; Stevens, R.C. Structural insight into the aromatic amino acid hydroxylases and their disease-related mutant forms. *Chem. Rev.* **1999**, *99*, 2137–2160. [CrossRef] [PubMed]

143. Fitzpatrick, P.F. Tetrahydropterin-dependent amino acid hydroxylases. *Annu. Rev. Biochem.* **1999**, *68*, 355–381. [CrossRef] [PubMed]

144. Klinman, J.P. Life as aerobes: Are there simple rules for activation of dioxygen by enzymes? *J. Biol. Inorg. Chem.* **2001**, *6*, 1–13. [CrossRef]

145. Nagatsu, T.; Levitt, M.; Udenfriend, S. Tyrosine hydroxylase the initial step in norepinephrine biosynthesis. *J. Biol. Chem.* **1964**, *239*, 2910–2917. [CrossRef]

146. Davis, M.D.; Kaufman, S. Evidence for the formation of the 4a-carbinolamine during the tyrosine-dependent oxidation of tetrahydrobiopterin by rat liver phenylalanine hydroxylase. *J. Biol. Chem.* **1989**, *264*, 8585–8596. [CrossRef]

147. Francisco, W.A.; Tian, G.; Fitzpatrick, P.F.; Klinman, J.P. Oxygen-18 kinetic isotope effect studies of the tyrosine hydroxylase reaction: Evidence of rate limiting oxygen activation. *J. Am. Chem. Soc.* **1998**, *120*, 4057–4062. [CrossRef]

148. Bassan, A.; Blomberg, M.R.; Siegbahn, P.E. Mechanism of Dioxygen Cleavage in Tetrahydrobiopterin-Dependent Amino Acid Hydroxylases. *Chem. Eur. J.* **2003**, *9*, 106–115. [CrossRef]

149. Kemsley, J.N.; Wasinger, E.C.; Datta, S.; Mitić, N.; Acharya, T.; Hedman, B.; Caradonna, J.P.; Hodgson, K.O.; Solomon, E.I. Spectroscopic and Kinetic Studies of PKU Inducing Mutants of Phenylalanine Hydroxylase: Arg158Gln and Glu280Lys. *J. Am. Chem. Soc.* **2003**, *125*, 5677–5686. [CrossRef]

150. Dix, T.A.; Bollag, G.E.; Domanico, P.; Benkovic, S.J. Phenylalanine hydroxylase: Absolute configuration and source of oxygen of the 4a-hydroxytetrahydropterin species. *Biochemistry* **1985**, *24*, 2955–2958. [CrossRef]

151. Daly, J.; Levitt, M.; Guroff, G.; Udenfriend, S. Isotope studies on the mechanism of action of adrenal tyrosine hydroxylase. *Arch. Biochem. Biophys.* **1968**, *126*, 593–598. [CrossRef]

152. Siegmund, H.-U.; Kaufman, S. Hydroxylation of 4-methylphenylalanine by rat liver phenylalanine hydroxylase. *J. Biol. Chem.* **1991**, *266*, 2903–2910. [CrossRef] [PubMed]

153. Olsson, E.; Martinez, A.; Teigen, K.; Jensen, V.R. Formation of the Iron–Oxo Hydroxylating Species in the Catalytic Cycle of Aromatic Amino Acid Hydroxylases. *Chem. Eur. J.* **2011**, *17*, 3746–3758. [CrossRef]

154. Olsson, E.; Martinez, A.; Teigen, K.; Jensen, V.R. Substrate Hydroxylation by the Oxido–Iron Intermediate in Aromatic Amino Acid Hydroxylases: A DFT Mechanistic Study. *Eur. J. Inorg. Chem.* **2011**, *2011*, 2720–2732. [CrossRef]

155. Kal, S.; Xu, S.; Que, L., Jr. Bio-inspired Nonheme Iron Oxidation Catalysis: Involvement of Oxoiron(V) Oxidants in Cleaving Strong C–H Bonds. *Angew. Chem. Int. Ed.* **2020**, *59*, 7332–7349. [CrossRef] [PubMed]

156. Bryliakov, K.P.; Talsi, E.P. Active sites and mechanisms of bioinspired oxidation with H_2O_2, catalyzed by non-heme Fe and related Mn complexes. *Coord. Chem. Rev.* **2014**, *276*, 73–96. [CrossRef]

157. Oloo, W.N.; Que, L., Jr. Bioinspired Nonheme Iron Catalysts for C–H and C=C Bond Oxidation: Insights into the Nature of the Metal-Based Oxidants. *Acc. Chem. Res.* **2015**, *48*, 2612–2621. [CrossRef] [PubMed]

158. Olivo, G.; Cussó, O.; Costas, M. Biologically inspired C–H and C=C oxidations with hydrogen peroxide catalyzed by iron coordination complexes. *Chem. Asian J.* **2016**, *11*, 3148–3158. [CrossRef]

159. Olivo, G.; Cussó, O.; Borrell, M.; Costas, M. Oxidation of alkane and alkene moieties with biologically inspired nonheme iron catalysts and hydrogen peroxide: From free radicals to stereoselective transformations. *J. Biol. Inorg. Chem.* **2017**, *22*, 425–452. [CrossRef]

160. Lyakin, O.Y.; Bryliakov, K.P.; Talsi, E.P. Non-heme oxoiron(V) intermediates in chemo-, regio- and stereoselective oxidation of organic substrates. *Coord. Chem. Rev.* **2019**, *384*, 126–139. [CrossRef]

161. Kim, C.; Chen, K.; Kim, J.; Que, L. Stereospecific alkane hydroxylation with H_2O_2 catalyzed by an iron(II) –tris(2-pyridylmethyl)amine complex. *J. Am. Chem. Soc.* **1997**, *119*, 5964–5965. [CrossRef]

162. Chen, K.; Que, L. Stereospecific alkane hydroxylation by non-heme iron catalysts: Mechanistic evidence for an Fe^VO active species. *J. Am. Chem. Soc.* **2001**, *123*, 6327–6337. [CrossRef] [PubMed]

163. Aldrich-Wright, J.R.; Vagg, R.S.; Williams, P.A. Design of chiral picen-based metal complexes for molecular recognition of α-aminoacids and nucleic acids. *Coord. Chem. Rev.* **1997**, *166*, 361–389. [CrossRef]

164. Knof, U.; von Zelewsky, A. Predetermined chirality at metal centers. *Angew. Chem. Int. Ed.* **1999**, *38*, 302–322. [CrossRef]

165. Ng, C.; Sabat, M.; Fraser, C.L. Metal complexes with cis α topology from stereoselective quadridentate ligands with amine, pyridine, and quinoline donor groups. *Inorg. Chem.* **1999**, *38*, 5545–5556. [CrossRef]

166. Costas, M.; Que, J. Lawrence, Ligand topology tuning of iron-catalyzed hydrocarbon oxidations. *Angew. Chem. Int. Ed.* **2002**, *41*, 2179–2181. [CrossRef]

167. Lee, D.; Park, H. Ligand Taxonomy for Bioinorganic Modeling of Dioxygen-Activating Non-Heme Iron Enzymes. *Chem. Eur. J.* **2020**, *26*, 5916–5926.

168. Gamba, I.; Codolà, Z.; Lloret-Fillol, J.; Costas, M. Making and breaking of the O–O bond at iron complexes. *Coord. Chem. Rev.* **2017**, *334*, 2–24. [CrossRef]

169. Dantignana, V.; Company, A.; Costas, M. Oxoiron(V) Complexes of Relevance in Oxidation Catalysis of Organic Substrates. *Isr. J. Chem.* **2020**, *60*, 1004–1018. [CrossRef]

170. Borrell, M.; Costas, M. Mechanistically driven development of an iron catalyst for selective *syn*-dihydroxylation of alkenes with aqueous hydrogen peroxide. *J. Am. Chem. Soc.* **2017**, *139*, 12821–12829. [CrossRef]

171. Chen, K.; Costas, M.; Kim, J.; Tipton, A.K.; Que, L. Olefin cis-dihydroxylation versus epoxidation by non-heme iron catalysts: Two faces of an Fe^{III}–OOH coin. *J. Am. Chem. Soc.* **2002**, *124*, 3026–3035. [CrossRef]

172. Borrell, M.; Costas, M. Greening oxidation catalysis: Iron catalyzed alkene syn-dihydroxylation with aqueous hydrogen peroxide in green solvents. *ACS Sustain. Chem. Eng.* **2018**, *6*, 8410–8416. [CrossRef]

173. Prat, I.; Mathieson, J.S.; Güell, M.; Ribas, X.; Luis, J.M.; Cronin, L.; Costas, M. Observation of Fe(V)=O using variable-temperature mass spectrometry and its enzyme-like C–H and C=C oxidation reactions. *Nat. Chem.* **2011**, *3*, 788–793. [CrossRef] [PubMed]

174. Hitomi, Y.; Arakawa, K.; Funabiki, T.; Kodera, M. An Iron(III)–Monoamidate Complex Catalyst for Selective Hydroxylation of Alkane C–H Bonds with Hydrogen Peroxide. *Angew. Chem. Int. Ed.* **2012**, *51*, 3448–3452. [CrossRef]

175. Xu, S.; Veach, J.J.; Oloo, W.N.; Peters, K.C.; Wang, J.; Perry, R.H.; Que, L. Detection of a transient $Fe^V(O)(OH)$ species involved in olefin oxidation by a bio-inspired non-haem iron catalyst. *Chem. Commun.* **2018**, *54*, 8701–8704. [CrossRef] [PubMed]

176. Borrell, M.; Andris, E.; Navrátil, R.; Roithová, J.; Costas, M. Characterized *cis*-$Fe^V(O)(OH)$ intermediate mimics enzymatic oxidations in the gas phase. *Nat. Commun.* **2019**, *10*, 901. [CrossRef]

177. White, M.C.; Doyle, A.G.; Jacobsen, E.N. A synthetically useful, self-assembling MMO mimic system for catalytic alkene epoxidation with aqueous H_2O_2. *J. Am. Chem. Soc.* **2001**, *123*, 7194–7195. [CrossRef]

178. Chen, M.S.; White, M.C. A predictably selective aliphatic C–H oxidation reaction for complex molecule synthesis. *Science* **2007**, *318*, 783–787. [CrossRef]

179. Chen, M.S.; White, M.C. Combined effects on selectivity in Fe-catalyzed methylene oxidation. *Science* **2010**, *327*, 566–571. [CrossRef]

180. White, M.C. Adding aliphatic C–H bond oxidations to synthesis. *Science* **2012**, *335*, 807–809. [CrossRef]

181. Mas-Ballesté, R.; Que, L. Iron-catalyzed olefin epoxidation in the presence of acetic acid: Insights into the nature of the metal-based oxidant. *J. Am. Chem. Soc.* **2007**, *129*, 15964–15972. [CrossRef]

182. Lyakin, O.Y.; Talsi, E.P. Direct C–H Oxidation of Aromatic Substrates in the Presence of Biomimetic Iron Complexes. In *Frontiers of Green Catalytic Selective Oxidations*; Springer: Singapore, 2019; pp. 253–276.

183. Kitajima, N.; Ito, M.; Fukui, H.; Morooka, Y. A reaction mimic of tyrosine hydroxylase: Hydroxylation of a phenoxo ferric complex to a catecholato complex with *m*CPBA. *J. Am. Chem. Soc.* **1993**, *115*, 9335–9336. [CrossRef]

184. Ménage, S.; Galey, J.B.; Hussler, G.; Seité, M.; Fontecave, M. Aromatic Hydroxylation by H_2O_2 and O_2 Catalyzed by a μ-Oxo Diiron(III) Complex. *Angew. Chem. Int. Ed.* **1996**, *35*, 2353–2355. [CrossRef]

185. Ménage, S.; Galey, J.-B.; Dumats, J.; Hussler, G.; Seité, M.; Luneau, I.G.; Chottard, G.; Fontecave, M. O_2 activation and aromatic hydroxylation performed by diiron complexes. *J. Am. Chem. Soc.* **1998**, *120*, 13370–13382. [CrossRef]

186. Mekmouche, Y.; Ménage, S.; Toia-Duboc, C.; Fontecave, M.; Galey, J.B.; Lebrun, C.; Pécaut, J. H_2O_2-Dependent Fe-Catalyzed Oxidations: Control of the Active Species. *Angew. Chem. Int. Ed.* **2001**, *40*, 949–952. [CrossRef]

187. Lange, S.J.; Miyake, H.; Que, L. Evidence for a nonheme Fe(IV)=O species in the intramolecular hydroxylation of a phenyl moiety. *J. Am. Chem. Soc.* **1999**, *121*, 6330–6331. [CrossRef]

188. Jensen, M.P.; Mehn, M.P.; Que, L., Jr. Intramolecular Aromatic Amination through Iron-Mediated Nitrene Transfer. *Angew. Chem. Int. Ed.* **2003**, *42*, 4357–4360. [CrossRef]

189. Jensen, M.P.; Lange, S.J.; Mehn, M.P.; Que, E.L.; Que, L. Biomimetic Aryl Hydroxylation Derived from Alkyl Hydroperoxide at a Nonheme Iron Center. Evidence for an Fe^{IV}=O Oxidant. *J. Am. Chem. Soc.* **2003**, *125*, 2113–2128. [CrossRef] [PubMed]

190. Oh, N.Y.; Seo, M.S.; Lim, M.H.; Consugar, M.B.; Park, M.J.; Rohde, J.-U.; Han, J.; Kim, K.M.; Kim, J.; Que, L., Jr. Self-hydroxylation of perbenzoic acids at a nonheme iron(II) center. *Chem. Commun.* **2005**, 5644–5646. [CrossRef]

191. Taktak, S.; Flook, M.; Foxman, B.M.; Que, L., Jr.; Rybak-Akimova, E.V. *ortho*-Hydroxylation of benzoic acids with hydrogen peroxide at a non-heme iron center. *Chem. Commun.* **2005**, 5301–5303. [CrossRef]

192. Makhlynets, O.V.; Das, P.; Taktak, S.; Flook, M.; Mas-Ballesté, R.; Rybak-Akimova, E.V.; Que, L., Jr. Iron-Promoted ortho-and/or ipso-Hydroxylation of Benzoic Acids with H_2O_2. *Chem. Eur. J.* **2009**, *15*, 13171–13180. [CrossRef]

193. Makhlynets, O.V.; Rybak-Akimova, E.V. Aromatic Hydroxylation at a Non-Heme Iron Center: Observed Intermediates and Insights into the Nature of the Active Species. *Chem. Eur. J.* **2010**, *16*, 13995–14006. [CrossRef]

194. Makhlynets, O.V.; Oloo, W.N.; Moroz, Y.S.; Belaya, I.G.; Palluccio, T.D.; Filatov, A.S.; Müller, P.; Cranswick, M.A.; Que, L.; Rybak-Akimova, E.V. H_2O_2 activation with biomimetic non-haem iron complexes and AcOH: Connecting the g= 2.7 EPR signal with a visible chromophore. *Chem. Commun.* **2014**, *50*, 645–648. [CrossRef]

195. Ansari, A.; Kaushik, A.; Rajaraman, G. Mechanistic Insights on the ortho-Hydroxylation of Aromatic Compounds by Non-heme Iron Complex: A Computational Case Study on the Comparative Oxidative Ability of Ferric-Hydroperoxo and High-Valent Fe^{IV}=O and Fe^{V}=O Intermediates. *J. Am. Chem. Soc.* **2013**, *135*, 4235–4249. [CrossRef]

196. Ségaud, N.; Rebilly, J.-N.; Sénéchal-David, K.; Guillot, R.; Billon, L.; Baltaze, J.-P.; Farjon, J.; Reinaud, O.; Banse, F. Iron Coordination Chemistry with New Ligands Containing Triazole and Pyridine Moieties. Comparison of the Coordination Ability of the N-Donors. *Inorg. Chem.* **2013**, *52*, 691–700. [CrossRef]

197. Martinho, M.; Banse, F.; Bartoli, J.-F.; Mattioli, T.A.; Battioni, P.; Horner, O.; Bourcier, S.; Girerd, J.-J. New example of a non-heme mononuclear iron(IV) oxo complex. Spectroscopic data and oxidation activity. *Inorg. Chem.* **2005**, *44*, 9592–9596. [CrossRef]

198. Rebilly, J.N.; Zhang, W.; Herrero, C.; Dridi, H.; Sénéchal-David, K.; Guillot, R.; Banse, F. Hydroxylation of aromatics by H_2O_2 catalyzed by mononuclear non-heme iron complexes: Role of triazole hemilability in substrate-induced bifurcation of the H_2O_2 activation mechanism. *Chem. Eur. J.* **2020**, *26*, 659–668. [CrossRef]

199. de Visser, S.P.; Oh, K.; Han, A.-R.; Nam, W. Combined Experimental and Theoretical Study on Aromatic Hydroxylation by Mononuclear Nonheme Iron(IV)–Oxo Complexes. *Inorg. Chem.* **2007**, *46*, 4632–4641. [CrossRef]

200. Bartoli, J.-F.; Lambert, F.; Morgenstern-Badarau, I.; Battioni, P.; Mansuy, D. Unusual efficiency of a non-heme iron complex as catalyst for the hydroxylation of aromatic compounds by hydrogen peroxide: Comparison with iron porphyrins. *Comptes Rendus Chim.* **2002**, *5*, 263–266. [CrossRef]

201. Balland, V.; Mathieu, D.; Pons-Y-Moll, N.; Bartoli, J.F.; Banse, F.; Battioni, P.; Girerd, J.-J.; Mansuy, D. Non-heme iron polyazadentate complexes as catalysts for oxidations by H_2O_2: Particular efficiency in aromatic hydroxylations and beneficial effects of a reducing agent. *J. Mol. Catal. A Chem.* **2004**, *215*, 81–87. [CrossRef]

202. Thibon, A.; Bartoli, J.-F.; Guillot, R.; Sainton, J.; Martinho, M.; Mansuy, D.; Banse, F. Non-heme iron polyazadentate complexes as catalysts for aromatic hydroxylation by H_2O_2: Particular efficiency of tetrakis(2-pyridylmethyl)ethylenediamine–iron(II) complexes. *J. Mol. Catal. A* **2008**, *287*, 115–120. [CrossRef]

203. Bianchi, D.; Bortolo, R.; Tassinari, R.; Ricci, M.; Vignola, R. A novel iron-based catalyst for the biphasic oxidation of benzene to phenol with hydrogen peroxide. *Angew. Chem. Int. Ed.* **2000**, *39*, 4321–4323. [CrossRef]

204. Bianchi, D.; Bertoli, M.; Tassinari, R.; Ricci, M.; Vignola, R. Direct synthesis of phenols by iron-catalyzed biphasic oxidation of aromatic hydrocarbons with hydrogen peroxide. *J. Mol. Catal. A Chem.* **2003**, *200*, 111–116. [CrossRef]

205. Bianchi, D.; Bertoli, M.; Tassinari, R.; Ricci, M.; Vignola, R. Ligand effect on the iron-catalysed biphasic oxidation of aromatic hydrocarbons by hydrogen peroxide. *J. Mol. Catal. A Chem.* **2003**, *204*, 419–424. [CrossRef]

206. Kejriwal, A.; Bandyopadhyay, P.; Biswas, A.N. Aromatic hydroxylation using an oxo-bridged diiron(III) complex: A bio-inspired functional model of toluene monooxygenases. *Dalton Trans.* **2015**, *44*, 17261–17267. [CrossRef] [PubMed]

207. Raba, A.; Cokoja, M.; Herrmann, W.A.; Kühn, F.E. Catalytic hydroxylation of benzene and toluene by an iron complex bearing a chelating di-pyridyl-di-NHC ligand. *Chem. Commun.* **2014**, *50*, 11454–11457. [CrossRef]

208. Raba, A.; Cokoja, M.; Ewald, S.; Riener, K.; Herdtweck, E.; Pöthig, A.; Herrmann, W.A.; Kühn, F.E. Synthesis and Characterization of Novel Iron(II) Complexes with Tetradentate Bis(N-heterocyclic carbene)–Bis (pyridine)(NCCN) Ligands. *Organometallics* **2012**, *31*, 2793–2800. [CrossRef]

209. Rogers, M.M.; Stahl, S.S. N-Heterocyclic carbenes as ligands for high-oxidation-state metal complexes and oxidation catalysis. In *N-Heterocyclic Carbenes in Transition Metal Catalysis*; Springer: New York, NY, USA, 2006; pp. 21–46.

210. Strassner, T. The role of NHC ligands in oxidation catalysis. In *Organometallic Oxidation Catalysis*; Springer: Berlin/Heidelberg, Germany, 2006; pp. 125–148.

211. Lindhorst, A.C.; Schütz, J.; Netscher, T.; Bonrath, W.; Kühn, F.E. Catalytic oxidation of aromatic hydrocarbons by a molecular iron–NHC complex. *Catal. Sci. Technol.* **2017**, *7*, 1902–1911. [CrossRef]

212. Silva, G.C.; Carvalho, N.M.; Horn, A., Jr.; Lachter, E.R.; Antunes, O.A. Oxidation of aromatic compounds by hydrogen peroxide catalyzed by mononuclear iron(III) complexes. *J. Mol. Catal. A Chem.* **2017**, *426*, 564–571. [CrossRef]

213. Olivo, G.; Lanzalunga, O.; Di Stefano, S. Non-Heme Imine-Based Iron Complexes as Catalysts for Oxidative Processes. *Adv. Synth. Catal.* **2016**, *358*, 843–863. [CrossRef]

214. Capocasa, G.; Olivo, G.; Barbieri, A.; Lanzalunga, O.; Di Stefano, S. Direct hydroxylation of benzene and aromatics with H_2O_2 catalyzed by a self-assembled iron complex: Evidence for a metal-based mechanism. *Catal. Sci. Technol.* **2017**, *7*, 5677–5686. [CrossRef]

215. Ticconi, B.; Colcerasa, A.; Di Stefano, S.; Lanzalunga, O.; Lapi, A.; Mazzonna, M.; Olivo, G. Oxidative functionalization of aliphatic and aromatic amino acid derivatives with H_2O_2 catalyzed by a nonheme imine based iron complex. *RSC Adv.* **2018**, *8*, 19144–19151. [CrossRef]

216. Capocasa, G.; Di Berto Mancini, M.; Fratceloreto, F.; Lanzalunga, O.; Olivo, G.; Di Stefano, S. Easy Synthesis of a Self-Assembled Imine-Based Iron(II) Complex Endowed with Crown-Ether Receptors. *Eur. J. Org. Chem.* **2020**, *23*, 3390–3397. [CrossRef]

217. Olivo, G.; Arancio, G.; Mandolini, L.; Lanzalunga, O.; Di Stefano, S. Hydrocarbon oxidation catalyzed by a cheap nonheme imine-based iron(II) complex. *Catal. Sci. Technol.* **2014**, *4*, 2900–2903. [CrossRef]

218. Olivo, G.; Giosia, S.; Barbieri, A.; Lanzalunga, O.; Di Stefano, S. Alcohol oxidation with H_2O_2 catalyzed by a cheap and promptly available imine based iron complex. *Org. Biomol. Chem.* **2016**, *14*, 10630–10635. [CrossRef]

219. Ticconi, B.; Capocasa, G.; Cerrato, A.; Di Stefano, S.; Lapi, A.; Marincioni, B.; Olivo, G.; Lanzalunga, O. Insight into the chemoselective aromatic vs. side-chain hydroxylation of alkylaromatics with H_2O_2 catalyzed by a non-heme imine-based iron complex. *Catal. Sci. Technol.* **2021**, *11*, 171–178. [CrossRef]

220. Olivo, G.; Nardi, M.; Vìdal, D.; Barbieri, A.; Lapi, A.; Gómez, L.; Lanzalunga, O.; Costas, M.; Di Stefano, S. C–H Bond Oxidation Catalyzed by an Imine-Based Iron Complex: A Mechanistic Insight. *Inorg. Chem.* **2015**, *54*, 10141–10152. [CrossRef]

221. Lyakin, O.Y.; Zima, A.M.; Tkachenko, N.V.; Bryliakov, K.P.; Talsi, E.P. Direct Evaluation of the Reactivity of Nonheme Iron(V)–Oxo Intermediates toward Arenes. *ACS Catal.* **2018**, *8*, 5255–5260. [CrossRef]

222. Lyakin, O.Y.; Zima, A.M.; Samsonenko, D.G.; Bryliakov, K.P.; Talsi, E.P. EPR Spectroscopic Detection of the Elusive $Fe^V=O$ Intermediates in Selective Catalytic Oxofunctionalizations of Hydrocarbons Mediated by Biomimetic Ferric Complexes. *ACS Catal.* **2015**, *5*, 2702–2707. [CrossRef]

223. Zima, A.M.; Lyakin, O.Y.; Ottenbacher, R.V.; Bryliakov, K.P.; Talsi, E.P. Dramatic effect of carboxylic acid on the electronic structure of the active species in Fe(PDP)-catalyzed asymmetric epoxidation. *ACS Catal.* **2016**, *6*, 5399–5404. [CrossRef]

224. Zima, A.M.; Lyakin, O.Y.; Ottenbacher, R.V.; Bryliakov, K.P.; Talsi, E.P. Iron-catalyzed enantioselective epoxidations with various oxidants: Evidence for different active species and epoxidation mechanisms. *ACS Catal.* **2017**, *7*, 60–69. [CrossRef]

225. Zima, A.M.; Lyakin, O.Y.; Lubov, D.P.; Bryliakov, K.P.; Talsi, E.P. Aromatic C–H oxidation by non-heme iron(V)-oxo intermediates bearing aminopyridine ligands. *J. Mol. Catal.* **2020**, *483*, 110708. [CrossRef]

226. Van Heuvelen, K.M.; Fiedler, A.T.; Shan, X.; De Hont, R.F.; Meier, K.K.; Bominaar, E.L.; Münck, E.; Que, L. One-electron oxidation of an oxoiron(IV) complex to form an $[O=Fe^V=NR]^+$ center. *Proc. Natl. Acad. Sci. USA* **2012**, *109*, 11933–11938. [CrossRef]

227. Serrano-Plana, J.; Oloo, W.N.; Acosta-Rueda, L.; Meier, K.K.; Verdejo, B.; García-España, E.; Basallote, M.G.; Münck, E.; Que, L., Jr.; Company, A.; et al. Trapping a Highly Reactive Nonheme Iron Intermediate That Oxygenates Strong C–H Bonds with Stereoretention. *J. Am. Chem. Soc.* **2015**, *137*, 15833–15842. [CrossRef] [PubMed]

228. Tkachenko, N.V.; Ottenbacher, R.V.; Lyakin, O.Y.; Zima, A.M.; Samsonenko, D.G.; Talsi, E.P.; Bryliakov, K.P. Highly Efficient Aromatic C–H Oxidation with H_2O_2 in the Presence of Iron Complexes of the PDP Family. *ChemCatChem* **2018**, *10*, 4052–4057. [CrossRef]

229. Tkachenko, N.V.; Lyakin, O.Y.; Zima, A.M.; Talsi, E.P.; Bryliakov, K.P. Effect of different carboxylic acids on the aromatic hydroxylation with H_2O_2 in the presence of an iron aminopyridine complex. *J. Organomet. Chem.* **2018**, *871*, 130–134. [CrossRef]

230. Kal, S.; Draksharapu, A.; Que, L., Jr. Sc^{3+} (or $HClO_4$) Activation of a Nonheme Fe^{III}–OOH Intermediate for the Rapid Hydroxylation of Cyclohexane and Benzene. *J. Am. Chem. Soc.* **2018**, *140*, 5798–5804. [CrossRef] [PubMed]

231. Li, F.; Van Heuvelen, K.M.; Meier, K.K.; Münck, E.; Que, L., Jr. Sc^{3+}-triggered oxoiron(IV) formation from O_2 and its non-heme iron(II) precursor via a Sc^{3+}–peroxo–Fe^{3+} intermediate. *J. Am. Chem. Soc.* **2013**, *135*, 10198–10201. [CrossRef] [PubMed]

232. Lee, Y.-M.; Bang, S.; Kim, Y.M.; Cho, J.; Hong, S.; Nomura, T.; Ogura, T.; Troeppner, O.; Ivanović-Burmazović, I.; Sarangi, R. A mononuclear nonheme iron(III)–peroxo complex binding redox-inactive metal ions. *Chem. Sci.* **2013**, *4*, 3917–3923. [CrossRef]

233. Zhang, J.; Wei, W.-J.; Lu, X.; Yang, H.; Chen, Z.; Liao, R.-Z.; Yin, G. Nonredox metal ions promoted olefin epoxidation by iron(II) complexes with H_2O_2: DFT calculations reveal multiple channels for oxygen transfer. *Inorg. Chem.* **2017**, *56*, 15138–15149. [CrossRef]

234. Nodzewska, A.; Watkinson, M. Remarkable increase in the rate of the catalytic epoxidation of electron deficient styrenes through the addition of $Sc(OTf)_3$ to the MnTMTACN catalyst. *Chem. Commun.* **2018**, *54*, 1461–1464. [CrossRef]

235. Chatterjee, S.; Paine, T.K. Olefin *cis*-Dihydroxylation and Aliphatic C–H Bond Oxygenation by a Dioxygen-Derived Electrophilic Iron–Oxygen Oxidant. *Angew. Chem. Int. Ed.* **2015**, *54*, 9338–9342. [CrossRef] [PubMed]

236. Kal, S.; Que, L., Jr. Activation of a Non-Heme Fe^{III}-OOH by a Second Fe^{III} to Hydroxylate Strong C–H Bonds: Possible Implications for Soluble Methane Monooxygenase. *Angew. Chem. Int. Ed.* **2019**, *58*, 8484–8488. [CrossRef] [PubMed]

237. Cheng, L.; Wang, H.; Cai, H.; Zhang, J.; Gong, X.; Han, W. Iron-catalyzed arene C–H hydroxylation. *Science* **2021**, *374*, 77–81. [CrossRef] [PubMed]

238. Klinman, J.P. Mechanisms whereby mononuclear copper proteins functionalize organic substrates. *Chem. Rev.* **1996**, *96*, 2541–2562. [CrossRef]

239. Fontecave, M.; Pierre, J.-L. Oxidations by copper metalloenzymes and some biomimetic approaches. *Coord. Chem. Rev.* **1998**, *170*, 125–140. [CrossRef]

240. Klabunde, T.; Eicken, C.; Sacchettini, J.C.; Krebs, B. Crystal structure of a plant catechol oxidase containing a dicopper center. *Nat. Struct. Mol. Biol.* **1998**, *5*, 1084–1090. [CrossRef]

241. Solomon, E.I.; Sundaram, U.M.; Machonkin, T.E. Multicopper oxidases and oxygenases. *Chem. Rev.* **1996**, *96*, 2563–2606. [CrossRef]

242. Rolff, M.; Schottenheim, J.; Decker, H.; Tuczek, F. Copper–O$_2$ reactivity of tyrosinase models towards external monophenolic substrates: Molecular mechanism and comparison with the enzyme. *Chem. Soc. Rev.* **2011**, *40*, 4077–4098. [CrossRef]

243. Decker, H.; Schweikardt, T.; Tuczek, F. The first crystal structure of tyrosinase: All questions answered? *Angew. Chem. Int. Ed.* **2006**, *45*, 4546–4550. [CrossRef]

244. Matoba, Y.; Kumagai, T.; Yamamoto, A.; Yoshitsu, H.; Sugiyama, M. Crystallographic evidence that the dinuclear copper center of tyrosinase is flexible during catalysis. *J. Biol. Chem.* **2006**, *281*, 8981–8990. [CrossRef]

245. Serrano-Plana, J.; Garcia-Bosch, I.; Company, A.; Costas, M. Structural and reactivity models for copper oxygenases: Cooperative effects and novel reactivities. *Acc. Chem. Res.* **2015**, *48*, 2397–2406. [CrossRef] [PubMed]

246. Karlin, K.D.; Hayes, J.C.; Gultneh, Y.; Cruse, R.W.; McKown, J.W.; Hutchinson, J.P.; Zubieta, J. Copper-mediated hydroxylation of an arene: Model system for the action of copper monooxygenases. Structures of a binuclear copper(I) complex and its oxygenated product. *J. Am. Chem. Soc.* **1984**, *106*, 2121–2128. [CrossRef]

247. Karlin, K.D.; Nasir, M.S.; Cohen, B.I.; Cruse, R.W.; Kaderli, S.; Zuberbuehler, A.D. Reversible dioxygen binding and aromatic hydroxylation in O$_2$-reactions with substituted xylyl dinuclear copper(I) complexes: Syntheses and low-temperature kinetic/thermodynamic and spectroscopic investigations of a copper monooxygenase model system. *J. Am. Chem. Soc.* **1994**, *116*, 1324–1336. [CrossRef]

248. Pidcock, E.; Obias, H.V.; Zhang, C.X.; Karlin, K.D.; Solomon, E.I. Investigation of the reactive oxygen intermediate in an arene hydroxylation reaction performed by xylyl-bridged binuclear copper complexes. *J. Am. Chem. Soc.* **1998**, *120*, 7841–7847. [CrossRef]

249. Becker, M.; Schindler, S.; Karlin, K.D.; Kaden, T.A.; Kaderli, S.; Palanché, T.; Zuberbühler, A.D. Intramolecular ligand hydroxylation: Mechanistic high-pressure studies on the reaction of a dinuclear copper(I) complex with dioxygen. *Inorg. Chem.* **1999**, *38*, 1989–1995. [CrossRef]

250. Maiti, D.; Fry, H.C.; Woertink, J.S.; Vance, M.A.; Solomon, E.I.; Karlin, K.D. A 1: 1 copper–dioxygen adduct is an end-on bound superoxo copper(II) complex which undergoes oxygenation reactions with phenols. *J. Am. Chem. Soc.* **2007**, *129*, 264–265. [CrossRef]

251. Maiti, D.; Lee, D.H.; Gaoutchenova, K.; Würtele, C.; Holthausen, M.C.; Narducci Sarjeant, A.A.; Sundermeyer, J.; Schindler, S.; Karlin, K.D. Reactions of a Copper(II) Superoxo Complex Lead to C–H and O–H Substrate Oxygenation: Modeling Copper-Monooxygenase C–H Hydroxylation. *Angew. Chem. Int. Ed.* **2008**, *47*, 82–85. [CrossRef]

252. Karlin, K.D.; Zhang, C.X.; Rheingold, A.L.; Galliker, B.; Kaderli, S.; Zuberbühler, A.D. Reversible dioxygen binding and arene hydroxylation reactions: Kinetic and thermodynamic studies involving ligand electronic and structural variations. *Inorg. Chim. Acta* **2012**, *389*, 138–150. [CrossRef]

253. Lee, J.Y.; Peterson, R.L.; Ohkubo, K.; Garcia-Bosch, I.; Himes, R.A.; Woertink, J.; Moore, C.D.; Solomon, E.I.; Fukuzumi, S.; Karlin, K.D. Mechanistic insights into the oxidation of substituted phenols via hydrogen atom abstraction by a cupric–superoxo complex. *J. Am. Chem. Soc.* **2014**, *136*, 9925–9937. [CrossRef]

254. Kim, S.; Lee, J.Y.; Cowley, R.E.; Ginsbach, J.W.; Siegler, M.A.; Solomon, E.I.; Karlin, K.D. A N$_3$S(thioether)-ligated Cu^{II}-superoxo with enhanced reactivity. *J. Am. Chem. Soc.* **2015**, *137*, 2796–2799. [CrossRef]

255. Mahapatra, S.; Kaderli, S.; Llobet, A.; Neuhold, Y.-M.; Palanché, T.; Halfen, J.A.; Young, V.G.; Kaden, T.A.; Que, L.; Zuberbühler, A.D.; et al. Binucleating ligand structural effects on (μ-peroxo)-and bis(μ-oxo) dicopper complex formation and decay: Competition between arene hydroxylation and aliphatic C–H bond activation. *Inorg. Chem.* **1997**, *36*, 6343–6356. [CrossRef]

256. Sander, O.; Henß, A.; Näther, C.; Würtele, C.; Holthausen, M.C.; Schindler, S.; Tuczek, F. Aromatic Hydroxylation in a Copper Bis(imine) Complex Mediated by a μ-η^2:η^2 Peroxo Dicopper Core: A Mechanistic Scenario. *Chem. Eur. J.* **2008**, *14*, 9714–9729. [CrossRef] [PubMed]

257. Menif, R.; Martell, A.E.; Squattrito, P.J.; Clearfield, A. New hexaaza macrocyclic binucleating ligands. Oxygen insertion with a dicopper(I) Schiff base macrocyclic complex. *Inorg. Chem.* **1990**, *29*, 4723–4729. [CrossRef]

258. Santagostini, L.; Gullotti, M.; Monzani, E.; Casella, L.; Dillinger, R.; Tuczek, F. Reversible dioxygen binding and phenol oxygenation in a tyrosinase model system. *Chem. Eur. J.* **2000**, *6*, 519–522. [CrossRef]

259. Palavicini, S.; Granata, A.; Monzani, E.; Casella, L. Hydroxylation of phenolic compounds by a peroxodicopper(II) complex: Further insight into the mechanism of tyrosinase. *J. Am. Chem. Soc.* **2005**, *127*, 18031–18036. [CrossRef]

260. Itoh, S.; Kumei, H.; Taki, M.; Nagatomo, S.; Kitagawa, T.; Fukuzumi, S. Oxygenation of phenols to catechols by a (μ-η^2:η^2-peroxo) dicopper(II) complex: Mechanistic insight into the phenolase activity of tyrosinase. *J. Am. Chem. Soc.* **2001**, *123*, 6708–6709. [CrossRef]

261. Battaini, G.; De Carolis, M.; Monzani, E.; Tuczek, F.; Casella, L. The phenol *ortho*-oxygenation by mononuclear copper(I) complexes requires a dinuclear μ-η^2:η^2-peroxodicopper(II) complex rather than mononuclear CuO$_2$ species. *Chem. Commun.* **2003**, 726–727. [CrossRef]

262. Citek, C.; Lyons, C.T.; Wasinger, E.C.; Stack, T.D.P. Self-assembly of the oxy-tyrosinase core and the fundamental components of phenolic hydroxylation. *Nat. Chem.* **2012**, *4*, 317–322. [CrossRef]

263. Company, A.; Palavicini, S.; Garcia-Bosch, I.; Mas-Ballesté, R.; Que, L., Jr.; Rybak-Akimova, E.V.; Casella, L.; Ribas, X.; Costas, M. Tyrosinase-Like Reactivity in a Cu$^{III}_2$(μ-O)$_2$ Species. *Chem. Eur. J.* **2008**, *14*, 3535–3538. [CrossRef]

264. Tachi, Y.; Aita, K.; Teramae, S.; Tani, F.; Naruta, Y.; Fukuzumi, S.; Itoh, S. Dicopper–Dioxygen Complex Supported by Asymmetric Pentapyridine Dinucleating Ligand. *Inorg. Chem.* **2004**, *43*, 4558–4560. [CrossRef]

265. Garcia-Bosch, I.; Company, A.; Frisch, J.R.; Torrent-Sucarrat, M.; Cardellach, M.; Gamba, I.; Güell, M.; Casella, L.; Que, L., Jr.; Ribas, X.; et al. O_2 Activation and Selective Phenolate ortho Hydroxylation by an Unsymmetric Dicopper μ-η^1:η^1-Peroxido Complex. *Angew. Chem. Int. Ed.* **2010**, *49*, 2406–2409. [CrossRef] [PubMed]

266. Matsumoto, T.; Furutachi, H.; Kobino, M.; Tomii, M.; Nagatomo, S.; Tosha, T.; Osako, T.; Fujinami, S.; Itoh, S.; Kitagawa, T.; et al. Intramolecular arene hydroxylation versus intermolecular olefin epoxidation by (μ-η^2:η^2-peroxo)dicopper(II) complex supported by dinucleating ligand. *J. Am. Chem. Soc.* **2006**, *128*, 3874–3875. [CrossRef] [PubMed]

267. Mirica, L.M.; Vance, M.; Rudd, D.J.; Hedman, B.; Hodgson, K.O.; Solomon, E.I.; Stack, T. A Stabilized μ-η^2:η^2 Peroxodicopper(II) Complex with a Secondary Diamine Ligand and Its Tyrosinase-like Reactivity. *J. Am. Chem. Soc.* **2002**, *124*, 9332–9333. [CrossRef] [PubMed]

268. Mirica, L.M.; Rudd, D.J.; Vance, M.A.; Solomon, E.I.; Hodgson, K.O.; Hedman, B.; Stack, T.D.P. μ-η^2:η^2-Peroxodicopper(II) complex with a secondary diamine ligand: A functional model of tyrosinase. *J. Am. Chem. Soc.* **2006**, *128*, 2654–2665. [CrossRef] [PubMed]

269. Mirica, L.M.; Vance, M.; Rudd, D.J.; Hedman, B.; Hodgson, K.O.; Solomon, E.I.; Stack, T.D.P. Tyrosinase reactivity in a model complex: An alternative hydroxylation mechanism. *Science* **2005**, *308*, 1890–1892. [CrossRef]

270. Hamann, J.N.; Tuczek, F. New catalytic model systems of tyrosinase: Fine tuning of the reactivity with pyrazole-based N-donor ligands. *Chem. Commun.* **2014**, *50*, 2298–2300. [CrossRef]

271. Mirica, L.M.; Ottenwaelder, X.; Stack, T.D.P. Structure and spectroscopy of copper–dioxygen complexes. *Chem. Rev.* **2004**, *104*, 1013–1046. [CrossRef]

272. Lewis, E.A.; Tolman, W.B. Reactivity of dioxygen–copper systems. *Chem. Rev.* **2004**, *104*, 1047–1076. [CrossRef]

273. Halfen, J.A.; Mahapatra, S.; Wilkinson, E.C.; Kaderli, S.; Young, V.G., Jr.; Que, L., Jr.; Zuberbühler, A.D.; Tolman, W.B. Reversible cleavage and formation of the dioxygen O–O bond within a dicopper complex. *Science* **1996**, *271*, 1397–1400. [CrossRef]

274. Tolman, W.B. Making and breaking the dioxygen O–O bond: New insights from studies of synthetic copper complexes. *Acc. Chem. Res.* **1997**, *30*, 227–237. [CrossRef]

275. Op't Holt, B.T.; Vance, M.A.; Mirica, L.M.; Heppner, D.E.; Stack, T.D.P.; Solomon, E.I. Reaction coordinate of a functional model of tyrosinase: Spectroscopic and computational characterization. *J. Am. Chem. Soc.* **2009**, *131*, 6421–6438. [CrossRef] [PubMed]

276. Holland, P.L.; Rodgers, K.R.; Tolman, W.B. Is the Bis(μ-oxo)dicopper Core Capable of Hydroxylating an Arene? *Angew. Chem. Int. Ed.* **1999**, *38*, 1139–1142. [CrossRef]

277. Herres-Pawlis, S.; Verma, P.; Haase, R.; Kang, P.; Lyons, C.T.; Wasinger, E.C.; Flörke, U.; Henkel, G.; Stack, T.D.P. Phenolate hydroxylation in a bis(μ-oxo)dicopper(III) complex: Lessons from the guanidine/amine series. *J. Am. Chem. Soc.* **2009**, *131*, 1154–1169. [CrossRef] [PubMed]

278. Itoh, S. Developing mononuclear copper–active-oxygen complexes relevant to reactive intermediates of biological oxidation reactions. *Acc. Chem. Res.* **2015**, *48*, 2066–2074. [CrossRef]

279. Kunishita, A.; Teraoka, J.; Scanlon, J.D.; Matsumoto, T.; Suzuki, M.; Cramer, C.J.; Itoh, S. Aromatic Hydroxylation Reactivity of a Mononuclear Cu(II) –Alkylperoxo Complex. *J. Am. Chem. Soc.* **2007**, *129*, 7248–7249. [CrossRef]

280. Kunishita, A.; Scanlon, J.D.; Ishimaru, H.; Honda, K.; Ogura, T.; Suzuki, M.; Cramer, C.J.; Itoh, S. Reactions of copper(II)-H_2O_2 adducts supported by tridentate bis(2-pyridylmethyl)amine ligands: Sensitivity to solvent and variations in ligand substitution. *Inorg. Chem.* **2008**, *47*, 8222–8232. [CrossRef]

281. Würtele, C.; Gaoutchenova, E.; Harms, K.; Holthausen, M.C.; Sundermeyer, J.; Schindler, S. Crystallographic characterization of a synthetic 1:1 end-on copper dioxygen adduct complex. *Angew. Chem. Int. Ed.* **2006**, *45*, 3867–3869. [CrossRef]

282. Conde, A.; Diaz-Requejo, M.M.; Pérez, P.J. Direct, copper-catalyzed oxidation of aromatic C–H bonds with hydrogen peroxide under acid-free conditions. *Chem. Commun.* **2011**, *47*, 8154–8156. [CrossRef]

283. Vilella, L.; Conde, A.; Balcells, D.; Díaz-Requejo, M.M.; Lledós, A.; Pérez, P.J. A competing, dual mechanism for catalytic direct benzene hydroxylation from combined experimental-DFT studies. *Chem. Sci.* **2017**, *8*, 8373–8383. [CrossRef]

284. Wu, L.; Zhong, W.; Xu, B.; Wei, Z.; Liu, X. Synthesis and characterization of copper(II) complexes with multidentate ligands as catalysts for the direct hydroxylation of benzene to phenol. *Dalton Trans.* **2015**, *44*, 8013–8020. [CrossRef]

285. Tsuji, T.; Zaoputra, A.A.; Hitomi, Y.; Mieda, K.; Ogura, T.; Shiota, Y.; Yoshizawa, K.; Sato, H.; Kodera, M. Specific enhancement of catalytic activity by a dicopper core: Selective hydroxylation of benzene to phenol with hydrogen peroxide. *Angew. Chem. Int. Ed.* **2017**, *56*, 7779–7782. [CrossRef] [PubMed]

286. Muthuramalingam, S.; Anandababu, K.; Velusamy, M.; Mayilmurugan, R. Benzene Hydroxylation by Bioinspired Copper(II) Complexes: Coordination Geometry versus Reactivity. *Inorg. Chem.* **2020**, *59*, 5918–5928. [CrossRef] [PubMed]

287. Yamada, M.; Karlin, K.D.; Fukuzumi, S. One-step selective hydroxylation of benzene to phenol with hydrogen peroxide catalysed by copper complexes incorporated into mesoporous silica–alumina. *Chem. Sci.* **2016**, *7*, 2856–2863. [CrossRef] [PubMed]

288. Kumari, S.; Muthuramalingam, S.; Dhara, A.K.; Singh, U.; Mayilmurugan, R.; Ghosh, K. Cu(I) complexes obtained via spontaneous reduction of Cu(II) complexes supported by designed bidentate ligands: Bioinspired Cu(I) based catalysts for aromatic hydroxylation. *Dalton Trans.* **2020**, *49*, 13829–13839. [CrossRef] [PubMed]

289. Boer, J.L.; Mulrooney, S.B.; Hausinger, R.P. Nickel-dependent metalloenzymes. *Arch. Biochem. Biophys.* **2014**, *544*, 142–152. [CrossRef]

290. Corona, T.; Company, A. Spectroscopically characterized synthetic mononuclear nickel–oxygen species. *Chem. Eur. J.* **2016**, *22*, 13422–13429. [CrossRef]

291. Kimura, E.; Machida, R. A mono-ozygenase model for selective aromatic hydroxylation with nickel(II)-macrocyclic polyamines. *J. Chem. Soc. Chem. Commun.* **1984**, 499–500. [CrossRef]

292. Honda, K.; Cho, J.; Matsumoto, T.; Roh, J.; Furutachi, H.; Tosha, T.; Kubo, M.; Fujinami, S.; Ogura, T.; Kitagawa, T.; et al. Oxidation Reactivity of Bis(μ-oxo) Dinickel(III) Complexes: Arene Hydroxylation of the Supporting Ligand. *Angew. Chem. Int. Ed.* **2009**, *48*, 3304–3307. [CrossRef]

293. Kunishita, A.; Doi, Y.; Kubo, M.; Ogura, T.; Sugimoto, H.; Itoh, S. Ni(II)/H_2O_2 reactivity in bis[(pyridin-2-yl)methyl]amine tridentate ligand system. Aromatic hydroxylation reaction by bis(μ-oxo)dinickel(III) complex. *Inorg. Chem.* **2009**, *48*, 4997–5004. [CrossRef]

294. Tano, T.; Doi, Y.; Inosako, M.; Kunishita, A.; Kubo, M.; Ishimaru, H.; Ogura, T.; Sugimoto, H.; Itoh, S. Nickel(II) Complexes of tpa Ligands with 6-Phenyl Substituents (Phntpa). Structure and H_2O_2-Reactivity. *Bull. Chem. Soc. Jpn.* **2010**, *83*, 530–538. [CrossRef]

295. Hikichi, S.; Yoshizawa, M.; Sasakura, Y.; Akita, M.; Moro-oka, Y. First Synthesis and Structural Characterization of Dinuclear M(III) Bis(μ-oxo) Complexes of Nickel and Cobalt with Hydrotris(pyrazolyl)borate Ligand. *J. Am. Chem. Soc.* **1998**, *120*, 10567–10568. [CrossRef]

296. Itoh, S.; Bandoh, H.; Nagatomo, S.; Kitagawa, T.; Fukuzumi, S. Aliphatic hydroxylation by a bis(μ-oxo)dinickel(III) complex. *J. Am. Chem. Soc.* **1999**, *121*, 8945–8946. [CrossRef]

297. Shiren, K.; Ogo, S.; Fujinami, S.; Hayashi, H.; Suzuki, M.; Uehara, A.; Watanabe, Y.; Moro-oka, Y. Synthesis, Structures, and Properties of Bis(μ-oxo)nickel(III) and Bis(μ-superoxo)nickel(II) Complexes: An Unusual Conversion of a $Ni^{III}_2(\mu-O)_2$ Core into a $Ni^{II}_2(\mu-OO)_2$ Core by H_2O_2 and Oxygenation of Ligand. *J. Am. Chem. Soc.* **2000**, *122*, 254–262. [CrossRef]

298. Mandimutsira, B.S.; Yamarik, J.L.; Brunold, T.C.; Gu, W.; Cramer, S.P.; Riordan, C.G. Dioxygen activation by a nickel thioether complex: Characterization of a $Ni^{III}_2(\mu-O)_2$ Core. *J. Am. Chem. Soc.* **2001**, *123*, 9194–9195. [CrossRef] [PubMed]

299. Itoh, S.; Bandoh, H.; Nakagawa, M.; Nagatomo, S.; Kitagawa, T.; Karlin, K.D.; Fukuzumi, S. Formation, Characterization, and Reactivity of Bis(μ-oxo)dinickel(III) Complexes Supported by A Series of Bis[2-(2-pyridyl)ethyl]amine Ligands. *J. Am. Chem. Soc.* **2001**, *123*, 11168–11178. [CrossRef]

300. Schenker, R.; Mandimutsira, B.S.; Riordan, C.G.; Brunold, T.C. Spectroscopic and Computational Studies on [(PhTttBu)$_2$Ni$_2$(μ-O)$_2$]: Nature of the Bis-μ-oxo (Ni^{3+})$_2$ "Diamond" Core. *J. Am. Chem. Soc.* **2002**, *124*, 13842–13855. [CrossRef]

301. Morimoto, Y.; Bunno, S.; Fujieda, N.; Sugimoto, H.; Itoh, S. Direct hydroxylation of benzene to phenol using hydrogen peroxide catalyzed by nickel complexes supported by pyridylalkylamine ligands. *J. Am. Chem. Soc.* **2015**, *137*, 5867–5870. [CrossRef]

302. Morimoto, Y.; Takagi, Y.; Saito, T.; Ohta, T.; Ogura, T.; Tohnai, N.; Nakano, M.; Itoh, S. A Bis(μ-oxido)dinickel(III) Complex with a Triplet Ground State. *Angew. Chem. Int. Ed.* **2018**, *57*, 7640–7643. [CrossRef]

303. Masferrer-Rius, E.; Hopman, R.M.; van der Kleij, J.; Lutz, M.; Klein Gebbink, R.J.M. On the Ability of Nickel Complexes Derived from Tripodal Aminopyridine Ligands to Catalyze Arene Hydroxylations. *Chimia* **2020**, *74*, 489–494. [CrossRef]

304. Muthuramalingam, S.; Anandababu, K.; Velusamy, M.; Mayilmurugan, R. One step phenol synthesis from benzene catalysed by nickel(II) complexes. *Catal. Sci. Technol.* **2019**, *9*, 5991–6001. [CrossRef]

305. McEvoy, J.P.; Brudvig, G.W. Water-splitting chemistry of photosystem II. *Chem. Rev.* **2006**, *106*, 4455–4483. [CrossRef] [PubMed]

306. Cady, C.W.; Crabtree, R.H.; Brudvig, G.W. Functional models for the oxygen-evolving complex of photosystem II. *Coord. Chem. Rev.* **2008**, *252*, 444–455. [CrossRef] [PubMed]

307. Umena, Y.; Kawakami, K.; Shen, J.-R.; Kamiya, N. Crystal structure of oxygen-evolving photosystem II at a resolution of 1.9 Å. *Nature* **2011**, *473*, 55–60. [CrossRef] [PubMed]

308. Cinco, R.M.; McFarlane Holman, K.L.; Robblee, J.H.; Yano, J.; Pizarro, S.A.; Bellacchio, E.; Sauer, K.; Yachandra, V.K. Calcium EXAFS establishes the Mn-Ca cluster in the oxygen-evolving complex of photosystem II. *Biochemistry* **2002**, *41*, 12928–12933. [CrossRef] [PubMed]

309. Cahiez, G.; Duplais, C.; Buendia, J. Chemistry of organomanganese(II) compounds. *Chem. Rev.* **2009**, *109*, 1434–1476. [CrossRef] [PubMed]

310. Carney, J.R.; Dillon, B.R.; Thomas, S.P. Recent advances of manganese catalysis for organic synthesis. *Eur. J. Org. Chem.* **2016**, *2016*, 3912–3929. [CrossRef]

311. Philip, R.M.; Radhika, S.; Abdulla, C.A.; Anilkumar, G. Recent Trends and Prospects in Homogeneous Manganese-Catalysed Epoxidation. *Adv. Synth. Catal.* **2021**, *363*, 1272–1289. [CrossRef]

312. Chen, J.; Jiang, Z.; Fukuzumi, S.; Nam, W.; Wang, B. Artificial nonheme iron and manganese oxygenases for enantioselective olefin epoxidation and alkane hydroxylation reactions. *Coord. Chem. Rev.* **2020**, *421*, 213443. [CrossRef]

313. Sun, W.; Sun, Q. Bioinspired manganese and iron complexes for enantioselective oxidation reactions: Ligand design, catalytic activity, and beyond. *Acc. Chem. Res.* **2019**, *52*, 2370–2381. [CrossRef]

314. Wu, X.; Seo, M.S.; Davis, K.M.; Lee, Y.-M.; Chen, J.; Cho, K.-B.; Pushkar, Y.N.; Nam, W. A highly reactive mononuclear non-heme manganese(IV)–Oxo complex that can activate the strong C–H bonds of alkanes. *J. Am. Chem. Soc.* **2011**, *133*, 20088–20091. [CrossRef]

315. Aratani, Y.; Yamada, Y.; Fukuzumi, S. Selective hydroxylation of benzene derivatives and alkanes with hydrogen peroxide catalysed by a manganese complex incorporated into mesoporous silica–alumina. *Chem. Commun.* **2015**, *51*, 4662–4665. [CrossRef] [PubMed]
316. Masferrer-Rius, E.; Borrell, M.; Lutz, M.; Costas, M.; Klein Gebbink, R.J.M. Aromatic C H Hydroxylation Reactions with Hydrogen Peroxide Catalyzed by Bulky Manganese Complexes. *Adv. Synth. Catal.* **2021**, *363*, 3785–3795. [CrossRef]